공학박사학위논문

A study on the fluorescence property and the solubility of the perylene derivatives and their application on the LCD color filter

액정 디스플레이 컬러필터용 퍼릴렌 유도체의 형광 거동과 용해도에 대한 연구

2017년 6월

서울대학교 대학원

재료공학부

김 정 윤

Abstract

A study on the fluorescence property and the solubility of the perylene derivatives and their application on the LCD color filter

Jeong Yun Kim

Department of Materials Science and Engineering

The Graduate School

Seoul National University

Liquid crystal displays (LCDs) have captured a larger portion of the display market than other types of displays. The LCD module consists of a backlight unit that radiates white light and a liquid crystal panel for producing imagery. One of the most essential component of LCD

modules is the color filter, which converts the white backlight into red (R), green (G), and blue (B) colored lights. The LCDs operate by using liquid crystals and polarizers to control and assemble these colored lights into the correct patterns to produce images. Numerous studies have reported improvements to the performance of LCDs by enhancing the optical properties of the color filters. Traditional color filters use pigments which lead to light scatting and cause a small amount of light to leak into the full-black state due to their large particle size. This problem can be resolved by using dyes of smaller particle size. In general, dyes with smaller particle sizes have superior color purity and transmittance. Dyes to be used in LCD color filters should have sufficient thermal stability to withstand the color filter manufacturing process, be soluble in the relevant organic industrial solvents, and possess superior spectral properties.

In this study, several substituents were introduced at terminal- and bay-positions of the perylene molecule to develop red dyes that can be used as colorants in LCD color filters. The feasibility of the newly synthesized dyes for use in LCD color filters was evaluated based on the spectral properties, thermal stability, and solubility of dyes. In addition,

the relationship between the chemical structure of the dyes and their properties was analyzed using density functional theory (DFT) calculations.

Perylene-based dyes generally exhibit strong fluorescence. Fluorescence of the dyes increases both the maximum and the minimum brightness of color filters, although the latter is more affected. Therefore, color filters containing highly fluorescent dyes exhibit a lower contrast ratio than those with dyes that are less fluorescent. The fluorescence properties of the color filters fabricated with the synthesized dyes showed same results. The fluorescence increased the minimum brightness of the color filters, and as a result, their contrast ratio decreased. To resolve this low-contrast ratio problem, new perylene-based dyes with high solubility and low fluorescence were developed. Accordingly, the color filters fabricated with these low-fluorescence dyes exhibited lower minimum brightness levels and improved contrast ratios compared to the color filters made with high-fluorescence dyes.

Perylene-based dyes with methoxy groups at various positions and orientations were synthesized to understand the effect of methoxy groups on dye fluorescence. It was found that methoxy groups of terminal-

substituents had a lesser effect on fluorescence quenching than methoxy groups of bay-substituents. Moreover, only the methoxy groups at the *para*-position of the bay-substituents showed fluorescence quenching ability. These results are interpreted to show that fluorescence quenching is greatly influenced when the methoxy groups are involved in the main conjugation systems, which are majorly attributed by the main body of the perylene molecule. The relationship between the positions and orientations of the methoxy groups and the molecular conjugation systems were further analyzed by molecular orbital modeling obtained by time-dependent density functional theory (TD-DFT) simulations, and the substituents containing methoxy groups are presumed to inhibit the fluorescence of dyes due to their the electron-donating effect.

KEYWORDS: Liquid crystal display, Color filter, Perylene, Solubility, Fluorescence, Intermolecular interaction, Contrast ratio

Student Number: 2010-23182

Contents

Chapter 3. The Effect of Fluorescence of Perylene Red Dyes on the Contrast Ratio of LCD Color Filters

Chapter 4. Synthesis of High-soluble and Non-fluorescent Perylene Derivatives and Their Effect on the Contrast Ratio of LCD Color Filters

List of Tables

List of Schemes

List of Figures

Chapter 1

Introduction

1.1 Basis for LCDs and LCD color filters

Displays are becoming one of the most critical components of electronic devices. Starting in the late 20th century, many flat-panel displays have been invented and widely used, however, LCD modules have maintained a dominant presence in the market [1-7]. There is a need to develop next-generation display technologies so to have large formats and low power consumption screens. To this end, developing a highly efficient color filter is critical for developing high-performance LCDs [5-11]. Color filters use optical materials to convert white light into RGB colored lights. The fundamental structures of an LCD and an LCD color filter are shown in **Fig. 1.1** and **Fig. 1.2**, respectively. Briefly, an LCD consists of a backlight unit, two polarizing films, liquid crystals, and color filters. An LCD color filter consists of a glass substrate, a black matrix, a color filter layer with RGB colors, and an indium tin oxide (ITO)

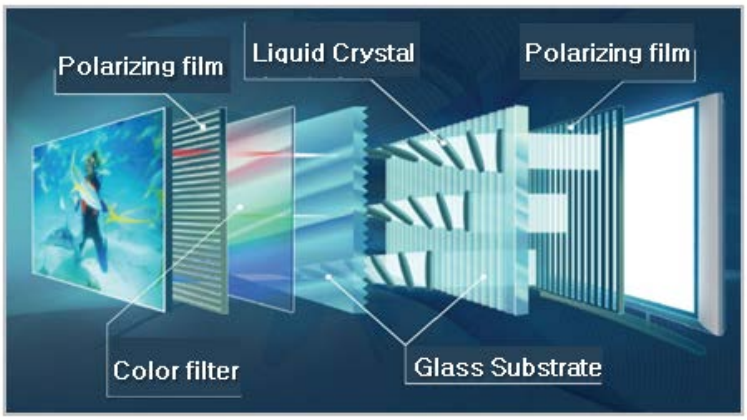

Fig. 1.1 The fundamental structures of LCD

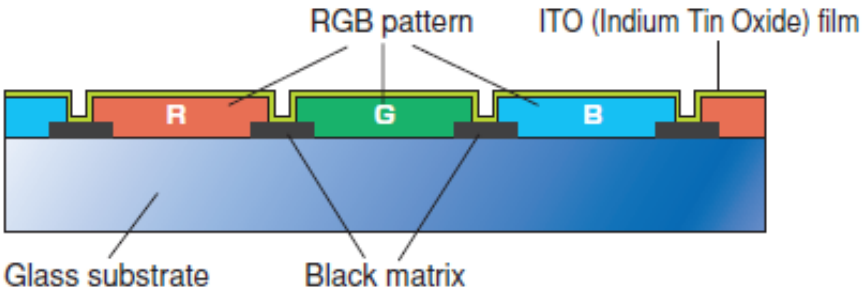

Fig. 1.2 The fundamental structures of LCD color filter

film. A schematic diagram of the operation mechanism of an LCD and its color filter is shown in **Fig. 1.3**, and the manufacturing process of a color filter using the photolithographic method is shown in **Fig. 1.4**.

The desirable properties of color filters were evaluated based on their color purity, contrast ratio, and brightness [10, 11]. Of these three criteria, high-contrast ratio was the most important factor for manufacturing displays with superior optical properties. Contrast ratio is the ratio of maximum brightness to minimum brightness. To obtain a high contrast ratio, light should not be transmitted when the polarizers are closed to produce a dark image (full-black state) [5-7, 10, 11].

1.2 Dye-based LCD color filters

Traditional LCD color filters are usually manufactured by using pigments as their colorants. Pigments are widely used as coloring materials owing to their high tinctorial strength, high stability, and competitive pricing. However, pigment-based color filters have some drawbacks also such as low contrast ratio and low brightness owing to their large particle size after heat treatment in the manufacturing process

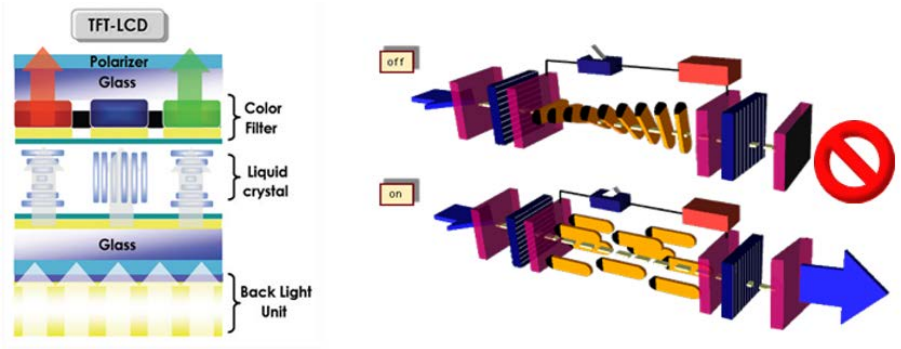

Fig. 1.3 A schematic diagram of LCD and the operation mechanism of LCD color filter

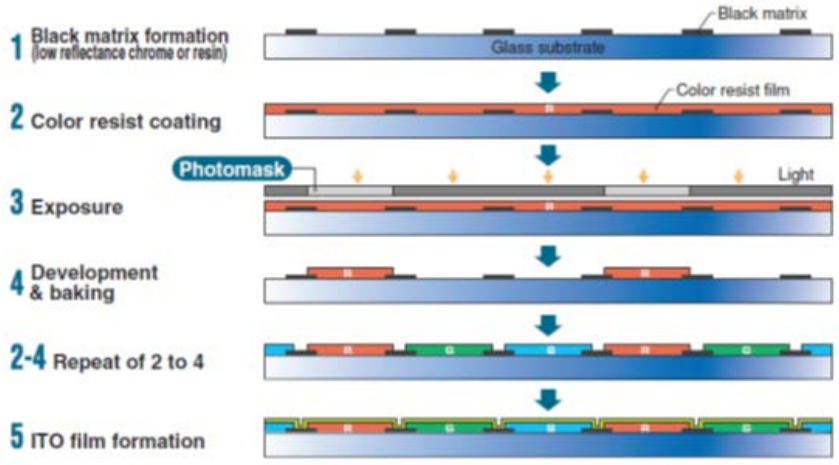

Fig. 1.4 Color filter manufacturing process by the photolithographic method

[2]. These problems can be resolved by using dyes with smaller particles. Dye-based color filters and displays exhibit superior transmittance compared to those using pigments and pigment-based color filters. This advantage stems from the ability of dyes to scatter less light than pigments due to the small particle size in the film state. Therefore, many researches and developments have been oriented toward dye-based and pigment-dye hybrid color filters to develop displays that exhibit superior optical properties [12, 13]. Optical performance of pigment-based and dye-based color filter are figured in **Fig. 1.5**.

For these proposes, dyes need to possess properties such as: (1) high solubility in organic industrial solvents such as propylene glycol monomethyl ether acetate (PGMEA), (2) appropriate absorption-transmittance spectra, and (3) sufficient thermal stability at industrial processing temperatures.

1.3 Perylene derivatives for dye-based color filters

Perylene derivatives are widely used as colorants in optical devices due to their characteristic spectral properties and sufficient thermal, light,

and chemicals stabilities [12, 14, 15]. Perylene is a planar molecule and consists of five parallel benzene rings and an evident π-π electron cloud over the plane of perylene main body. Therefore, perylene derivatives exhibit excellent thermal stability, originating from their very high resonance stabilization energy and π-π interactions, with a very strong and sharp absorption peak at approximately 530 nm [2].

However, perylene derivatives are not typically soluble in organic industrial solvents such as PGMEA and cyclohexanone, commonly used in the manufacturing process of LCDs. Specifically, the solubility of perylene-based dyes need to be greater than 5 wt% in industrial solvents to be used as colorants in color filters [9, 10]. Typically, bulky substituents such as benzene derivatives are introduced at the terminal- and bay-positions of the perylene molecule to reduce planarity and intermolecular interactions, and to increase the steric hindrance of the perylene-based dyes. A general strategy for developing perylene derivatives for use as colorants in dye-based LCD color filters is shown in **Fig. 1.6**.

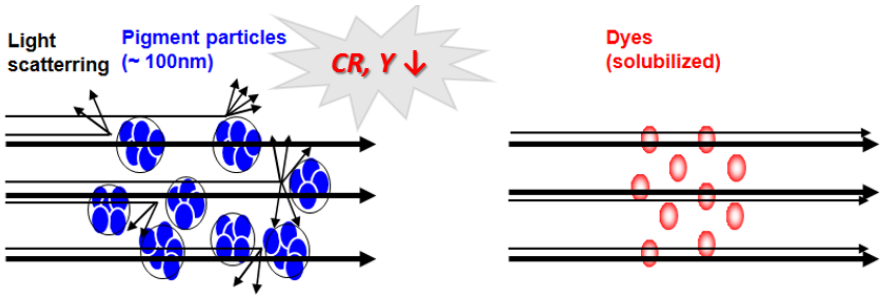

Fig. 1.5 Optical performance of pigment-based and dye-based color filter

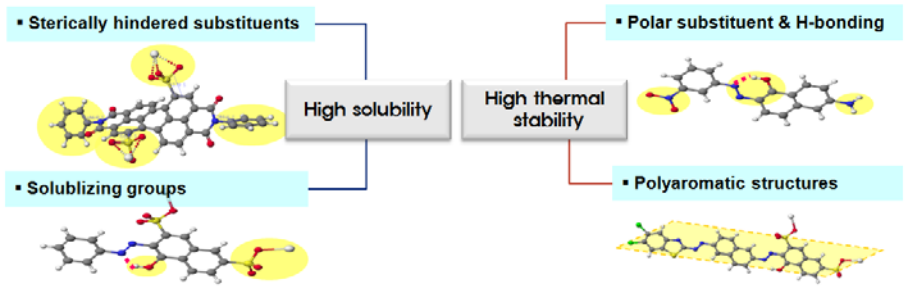

Fig. 1.6 General strategy and purpose for developing perylene derivatives for dye-based LCD color filters

1.4 Previous researches and research purpose

The color filter is an essential component for superior optical performance of LCDs. Therefore, much work has been done in the past several decades on LCDs and LCD color filters. Our research group (Prof. J. P. Kim) has reported various novel organic molecules for use in dye-based LCD color filters [1-11, 16, 17]. For example, water-soluble perylene-based dyes were successfully applied to ink-jet printed color filters. In addition, thermally stable and optically favorable coronene, benzocorrole, and phthalocyanine dyes were also developed, and their spectral and physical properties were characterized. However, manufacturing technologies using mill bases for pigment-based color filters have been improved quickly to have smaller particle sizes for color filters and to improve the optical performance of LCDs. On this account, most of the reported dye-based color filter techniques are not accepted in the real display industries.

In this study, various series of perylene derivatives were designed and synthesized, and were found to be soluble in organic solvents and had suitable color properties. Substituents were introduced at the terminal-

and bay-position of the perylene molecule to enhance their performances for LCD color filters. These perylene derivatives were evaluated based on their physical properties, including spectral properties and molecular geometry and whether these derivatives could be successfully used in dye- and pigment-dye hybrid color filters. The relationship between the fluorescence of the synthesized dyes and the contrast ratio of the color filters using those dyes was investigated. The negative effects resulting from the strong fluorescence of perylene-based dyes were also investigated. Moreover, the perylene-based dyes with high solubility and low fluorescence were designed and synthesized. The dyes gave superior contrast ratios in color filters than the dyes with high fluorescence. Finally, the fluorescence properties of the perylene derivatives and the effects of electron-donating groups on fluorescence quenching were analyzed.

1.5 Reference

[1] Kim YD, Kim JP, Kwon OS, Cho IH, Dyes Pigm., 2009, **81**, 45-52

[2] Choi J, Sakong C, Choi JH, Yoon C, Kim JP, Dyes Pigm., 2011, **90**,

82-88

[3] Kim YD, Cho JH, Park CR, Choi JH, Yoon C, Kim JP, Dyes Pigm., 2011, **89**, 1-8

[4] Sakong C, Kim YD, Choi JH, Yoon C, Kim JP, Dyes Pigm., 2011, **88**, 166-173

[5] Choi J, Lee W, Sakong C, Yuk SB, Park JS, Kim JP, Dyes Pigm., 2012, **94**, 34-39

[6] Choi J, Lee W, Namgoong JW, Kim TM, Kim JP, Dyes Pigm., 2013, **99**, 357-365

[7] Choi J, Kim SH, Lee W, Chang JB, Namgoong JW, Kim YH, Dyes Pigm., 2014, **101**, 186-195

[8] Kim SH, Choi J, Sakong C, Namgoong JW, Lee W, Kim DH, Dyes Pigm., 2015, **113**, 390-401

[9] Kim JY, Choi J, Namgoong JW, Kim SH, Sakong C, Yuk SB, J. Inclusion Phenom. Macrocyclic. Chem., 2015, **82**, 203-212

[10] Kim JY, Sakong C, Choi S, Jang H, Kim SH, Chang KS, Dyes Pigm., 2016, **131**, 293-300

[11] Kim JY, Hwang TG, Kim SH, Namgoong JW, Kim JE, Sakong C, Dyes Pigm., 2017, **136**, 836-845

[12] Huang C, Barlow S, Marder SR, J. Org. Chem., 2011, **76**, 2386-2407

[13] Stolarski R, Fiksinski KJ, Dyes Pigm., 1994, **24**, 295-303

[14] Dincalp H, Askar Z, Zafer C, Icli S, Dyes Pigm., 2011, **91**, 182-191

[15] Reghu RR, Bisoyi HK, Grazulevicius JV, Anjukandi P, Gaidelis V, Jankauskas V, J. Mater. Chem., 2011, **21**, 7811

[16] Kim SH, Namgoong JW, Yuk SB, Kim JY, Lee W, Yoon C, J. Inclusion Phenom. Macrocyclic. Chem., 2015, **82**, 195-202

[17] Yuk SB, Lee W, Namgoong JW, Choi J, Chang JB, Kim SH, J. Inclusion Phenom. Macrocyclic. Chem., 2015, **82**, 187-194

Chapter 2

Synthesis and Characterization of Novel Perylene Dyes with New Substituents at Terminal-position as Colorants for LCD Color Filter

2.1 Introduction

Displays are becoming the most essential component of electronic devices. Since the late 20th century, various types of flat-panel displays have been invented and widely used, but LCD (liquid crystal display) modules are the most popular and have a great market share [1, 2].

A highly efficient color filter is critical in the development of the high-performance LCDs [3, 4]. Notably, dye-based color filters have particular technical advantages in regard to their optical properties owing to reduced light scattering due to the small particle size in the film state; this causes color filters and displays to exhibit superior transmittance to pigment-based one [5]. As such, dye-based color filters and dye-pigment

hybrid color filters have recently garnered significant attention.

Dyes should possess suitable properties in order to be applied in dye-based color filters [5]. The most important properties include: (1) high solubility in organic industrial solvents such as PGMEA (propylene glycol monomethyl ether acetate), (2) appropriate absorption-transmittance spectra, and (3) sufficient thermal stability at industrial processing temperatures.

In previous studies [1-3, 5-8], we investigated dye-based color filters with some novel perylene-based red dyes. Perylene-based dyes are advantageous as optical materials in that they have high color strength and stability. Moreover, their structures can easily be modified via the introduction of various substituents under moderate conditions.

In this study, six novel perylene-based red dyes were additionally synthesized by introducing substituents in the bay- and terminal-positions. They were designed to examine the relationship between their structures and physical properties. The geometries of some of the synthesized dyes were also analyzed for the same purpose. The properties of the synthesized dyes were examined to evaluate the viability of the dyes in dye-based LCD color filters. The absorption

spectra, TGA (thermogravimetric analyzer), and solubility of the dyes were also examined. Afterward, mill bases and spin-coated color filters were fabricated using the synthesized dyes, and the transmittance and chromaticity of the prepared color filters were investigated. All of the measured properties were described in relation to the analyzed geometry structures.

2.2 Experimental

2.2.1 Materials and instrumentations

Perylene-3,4,9,10-tetracarboxylic dianhydride, 4-*tert*-octylphenol, iodine, sulfuric acid, bromine and acetic acid purchased from Sigma-Aldrich, 2,6-diisopropylaniline, 2-methoxy-6-methylaniline, 2,4,6-trimethylphenol and 2-allylphenol purchased from TCI, K_2CO_3 anhydrous, methylene chloride and other chemical solvent purchased from SAMCHUN pure chemical were used without any accessional purification. Transparent glass substrates were purchased from Paul Marienfeld GmbH & CO. KG. and acrylic binder of LC20160 was

supplied by SAMSUNG Cheil industries Inc.

^{1}H and ^{13}C NMR spectra were recorded by a Bruker Avance 500 spectrometer at 500 MHz using chloroform-d and TMS as the solvent and internal standard. Matrix Assisted Laser Desorption/Ionization Time Of Flight (MALDI-TOF) mass spectra were recorded by a Voyager-DE STR Biospectrometry Workstation with α-cyano-4-hydroxycinnamic acid (CHCA) as the matrix. Absorption and transmittance spectra were measured using a Perkin Elmer Lambda 25 UV/Vis spectrophotometer. Thermogravimetric analysis (TGA) was conducted under nitrogen atmosphere at a heating rate of 10 ℃ min^{-1} using a TA Instruments Thermogravimetric Analyzer 2050. And chromatic characteristics of the color filters were analyzed on a Scinco color spectrophotometer. Lastly, optimized geometry calculation of dyes was analyzed using the Gaussian 09 program.

2.2.2 Synthesis

2.2.2.1 1,(7)-dibromoperylene-3,4,9,10-tetracarboxydiimide (1,2) : Bromination

Perylene-3,4,9,10-tetracarboxylic dianhydride (32.0 g, 81.4 mmol), iodine (0.78 g, 3.04 mmol) and sulfuric acid (98 %, 450 mL) were mixed and stirred 2 h at room temperature. The temperature of the mixture was raised to 80 ℃, bromine (7.5 mL, 146.65 mmol) was added dropwise over 1 h. In this condition, the mixture was reacted for 16 h. After, cooled to room temperature and excess bromine gas was displaced by nitrogen gas. The mixture was poured in 3 L of ice-water slowly, to obtain precipitate and the precipitate collected by suction filtration in crude product form. The crude produce was washed with distilled water several times. Then, crude product was dried at 100 ℃ under reduced pressure and used for the next step without further purification. The crude contain both **1** and **2**, there were separated in next step, after importing derivatives in terminal-position to get more solubility that able to purifying by column chromatography.

2.2.2.2 N,N'-Bis(R_1)-1,(7)-dibromoperylene-3,4,9,10-tetracarboxydiimide (3,4) : Terminal-position Substitution

The crude 1,(7)-dibromoperylene-3,4,9,10-tetracarboxydiimide (8.0

g, 14.5 mmol), R_1-NH_2 (46.7 mmol), acetic acid (4.6 mL) and N-Methyl-2-pyrrolidone (NMP) (100 mL) were mixed and heated at 120 ℃ under the nitrogen atmosphere for 96 h. The precipitate obtained after adding water to the mixture was collected by suction filtration. The crude product was washed with water and dried. And the crude product purified by column chromatography on silica gel using CH_2Cl_2 as the eluent. The first reddish band containing tribrominated diimide could be separated [9]. Second reddish band containing dibrominated diimide and third one containing monobrominated diimide could be collected. To obtain **PI-series**, using 2,6-diisopropylaniline as R_1-NH_2 and to **PM-series**, 2-methoxy-6-methylaniline used.

2.2.2.3 N,N'-Bis(2,6-diisopropylphenyl)-1,7-bis(o-allylphenoxy)-perylene-3,4,9,10-tetracarboxydiimide (PI2-AP) : Bay-position Substitution

N,N''-Bis(2,6-diisopropylphenyl)-1,7-dibromoperylene-3,4,9,10-tetracarboxydiimide (one of form **4**) (0.50 g, 0.575 mmol) was mixed with potassium carbonate anhydrous (0.35 g), 2-allylphenol (0.20 g ,

1.50 mmol) and NMP (50 mL). The mixture was heated to 40 ℃ under nitrogen atmosphere and was stirred at this temperature for 1.5 h. The mixture was cooled to room temperature and poured into 5 % HCl aqueous solution (400 mL). The precipitate was filtered, repeatedly washed with water, and dried in a vacuum at 75 ℃. The crude product was purified by column chromatography on silica gel using CH_2Cl_2 as the eluent to obtain **PI2-AP** as red solid.

Yield 68.9 %; ^{1}H NMR ($CDCl_3$, ppm): 9.73 (d,2H), 8.67 (d,2H), 7.41 (t,2H), 7.35 (d,2H), 7.30 (m,10H), 6.98 (t,2H), 6.06 (septet,2H), 5.10 (d,2H), 5.06 (d,2H), 3.58 (d,4H), 2.71 (septet,4H), 1.15 (d,24H); ^{13}C NMR (126 MHz, $CDCl_3$): δ = 24.18, 24.22, 29.38, 34.60, 116.82, 119.51, 122.50, 123.95, 124.23, 125.78, 125.95, 128.68, 129.32, 129.82, 129.91, 130.65, 130.86, 131.72, 131.96, 133.96, 136.41, 145.80, 152.96, 155.71, 163.10, 163.68; MALDI-TOF MS: m/z 975.69 (100 %, [M+2K-H]-)

2.2.2.4 N,N'-Bis(2,6-diisopropylphenyl)-1,7-bis(2,4,6-trimethyl phenoxy)-perylene-3,4,9,10-tetracarboxydiimide (PI2-TMP)

PI2-TMP was synthesized in the same manner with **PI2-AP** using

N,N'-Bis(2,6-diisopropylphenyl)-1,7-dibromoperylene-3,4,9,10-tetracarboxydiimide (one of form **4**) (0.50 g, 0.575 mmol), potassium carbonate anhydrous (0.35 g) and 2,4,6-trimethylphenol (0.21 g, 1.50 mmol). The reaction temperature was set at 60 ℃ for 2 h.

Yield 77.2 %; ^{1}H NMR ($CDCl_3$, ppm): 9.91 (d,2H), 8.73 (d,2H), 7.36 (t,2H), 7.30 (m,6H), 7.03 (s,4H), 2.74 (septet,4H), 2.35 (s,6H), 2.18 (m,12H), 1.20 (d,24H); ^{13}C NMR (126 MHz, $CDCl_3$): δ = 16.62, 24.15, 24.21, 24.26, 29.34, 29.36, 120.16, 122.10, 122.73, 124.15, 124.22, 124.90, 125.08, 125.25, 128.16, 129.16, 129.28, 129.50, 129.99, 130.14, 130.35, 130.40, 130.49, 130.57, 130.71, 130.76, 133.61, 133.91, 136.46, 138.65, 145.80, 145.83, 147.76, 162.96, 163.12, 163.47, 163.57; MALDI-TOF MS: m/z 980.56 (100 %, [M+2K-H]-)

2.2.2.5 N,N'-Bis(2,6-diisopropylphenyl)-1,7-bis(p-tert-octylphenoxy)-perylene-3,4,9,10-tetracarboxydiimide (PI2-S2)

PI2-S2 was synthesized in the same manner with **PI2-AP** using N,N'-Bis(2,6-diisopropylphenyl)-1,7-dibromoperylene-3,4,9,10-tetracarboxydiimide (one of form **4**) (0.50 g, 0.575 mmol), potassium

carbonate anhydrous (0.35 g) and 4-*tert*-octylphenol (0.31 g, 1.50 mmol).

Yield 75.6 %; ^{1}H NMR ($CDCl_3$, ppm): 9.67 (d,2H), 8.70 (d,2H), 8.42 (d,4H), 7.34 (m,6H), 7.26 (s,2H), 7.10 (d,4H), 2.72 (septet,4H), 1.40 (s,4H), 1.16 (d,24H), 0.75 (s,18H), 0.73 (s,12H); ^{13}C NMR (126 MHz, $CDCl_3$): δ = 24.18, 24.22, 29.38, 31.72, 31.99, 32.61, 38.64, 57.36, 118.88, 119.01, 122.46, 123.34, 124.11, 124.19, 124.27, 124.57, 124.75, 125.98, 128.18, 128.44, 129.25, 129.83, 129.90, 130.69, 130.90, 131.99, 133.96, 145.82, 147.44, 147.57, 152.63, 152.75, 155.72, 156.79, 163.10, 163.70; MALDI-TOF MS: m/z 1120.63 (100 %, [M+2K-H]-)

2.2.2.6 N,N'-Bis(2-methoxy-6-methylphenyl)-1,7-bis(o-allylphenoxy)-perylene-3,4,9,10-tetracarboxydiimide (PM-AP)

PM-AP was synthesized in the same manner with **PI2-AP** using N,N'-Bis(2-methoxy-6-methylphenyl)-1,7-dibromoperylene-3,4,9,10-tetracarboxydiimide (one of form **4**) (0.50 g, 0.634 mmol), potassium carbonate anhydrous (0.35 g) and 2-allylphenol (0.21 g, 1.60 mmol).

Yield 71.1 %; ^{1}H NMR ($CDCl_3$, ppm): 9.71 (d,2H), 8.74 (d,2H), 7.42 (d,2H), 7.40 (t,2H), 7.26 (m,6H), 6.98 (m,6H), 6.04 (sextet,2H), 5.12

(d,2H), 5.09 (d,2H), 3.74 (s,6H), 3.54 (d,4H), 2.16 (d,6H); ^{13}C NMR (126 MHz, $CDCl_3$): δ = 17.76, 17.80, 29.14, 29.91, 30.65, 34.65, 109.40, 109.48, 116.85, 120.10, 120.25, 121.89, 122.67, 122.83, 122.87, 123.16, 123.25, 123.60, 123.83, 124.29, 125.90, 125.92, 126.03, 128.12, 128.74, 129.24, 129.91, 129.97, 130.59, 131.73, 131.86, 131.98, 132.05, 133.96, 134.05, 136.29, 136.35, 155.82, 156.90, 162.67, 163.05, 163.34; MALDI-TOF MS: m/z 895.48 (100 %, [M+2K-H]-)

2.2.2.7 N,N'-Bis(2-methoxy-6-methylphenyl)-1,7-bis(2,4,6-trimethyl phenoxy)-perylene-3,4,9,10-tetracarboxydiimide (PM-TMP)

PM-TMP was synthesized in the same manner with **PI2-AP** using N,N'-Bis(2-methoxy-6-methylphenyl)-1,7-dibromoperylene-3,4,9,10-tetracarboxydiimide (one of form **4**) (0.50 g, 0.634 mmol), potassium carbonate anhydrous (0.35 g) and 2,4,6-trimethylphenol (0.22 g, 1.60 mmol). The reaction temperature was set at 60 ℃ for 2 h.

Yield 73.2 %; ^{1}H NMR ($CDCl_3$, ppm): 9.91 (d,2H), 8.73 (d,2H), 7.36 (s,2H), 6.95 (m,10H), 3.74 (s,6H), 2.33 (s,6H), 2.16 (m,18H); ^{13}C NMR (126 MHz, $CDCl_3$): δ = 16.58, 17.83, 21.04, 29.92, 109.10, 109.31,

109.50, 117.53, 119.05, 121.62, 122.24, 122.30, 122.67, 122.78, 122.88, 123.21, 124.16, 125.33, 128.13, 129.44, 129.90, 130.17, 130.26, 130.63, 130.66, 131.75, 134.42, 136.21, 137.55, 148.03, 148.08, 155.04, 156.17, 157.31, 162.97, 163.13; MALDI-TOF MS: m/z 899.41 (100 %, [M+2K-H]-)

2.2.2.8 N,N'-Bis(2-methoxy-6-methylphenyl)-1,7-bis(p-tert-octylphenoxy)-perylene-3,4,9,10-tetracarboxydiimide (PM-S2)

PM-S2 was synthesized in the same manner with **PI2-AP** using N,N'-Bis(2-methoxy-6-methylphenyl)-1,7-dibromoperylene-3,4,9,10-tetracarboxydiimide (one of form **4**) (0.50 g, 0.575 mmol), potassium carbonate anhydrous (0.35 g) and 4-*tert*-octylphenol (0.32 g, 1.60 mmol).

Yield 77.1 %; ^{1}H NMR ($CDCl_3$, ppm): 9.68 (d,2H), 8.77 (d,2H), 8.40 (d,4H), 7.32 (m,6H), 7.22 (s,2H), 7.10 (d,4H), 2.78 (m,4H), 1.44 (s,4H), 1.17 (d,12H), 1.01 (s,2H), 0.78 (s,12H), 0.73 (s,12H); ^{13}C NMR (126 MHz, $CDCl_3$): δ = 17.82, 31.69, 31.73, 31.89, 31.96, 32.05, 109.45, 114.70, 119.09, 119.22, 122.62, 122.86, 123.22, 124.15, 124.23, 125.94, 127.42, 128.08, 128.41, 129.16, 129.90, 129.97, 130.66, 133.94, 137.58,

147.59, 152.52, 155.04, 155.69, 162.67, 163.08; MALDI-TOF MS: m/z 1039.03 (100 %, [M+2K-H]-)

2.2.3 Preparation of dye-based inks and color filters

The red ink for a color filter was composed of the synthesized dye (0.01 g), propylene glycol methyl ether acetate (PGMEA) (0.1 g) and LC20160 (0.8 g) as a binder based on acrylate [5]. The prepared dye-based inks were coated on a transparent glass substrate using a MIDAS System SPIN-1200D spin coater. The coating speed was initially 100 rpm for 10 s, which was then increased to 500 rpm and kept constant for 20 s. The wet dye-coated color filters were dried at 80 ℃ for 20 min, pre-baked at 150 ℃ for 10 min and post-baked at 200 ℃ for 1 h. After each step, the coordinate values of the color filters were measured. All spin-coated dye-based color filters were 1.6 μm thick.

2.2.4 Geometry optimization of the synthesized dyes

The difference of thermal stability and solubility due to the structural

differences in the dyes were analyzed by optimizing the dye structures using the Gaussian 09 program and examining the core twist angles that affect the intermolecular interaction. The optimized geometries of the dye structures were calculated with DFT on the B3LYP/6-31+G (d,p) level.

2.2.5 Investigation of solubility

The solubility of the synthesized dyes in CH_2Cl_2 and PGMEA were examined to determine the effects of substituents at the terminal- and bay-position. The prepared dyes were added to the solvents at various concentrations, and the solutions were sonicated for 5 min using an ultrasonic cleaner ME6500E. The solutions were left to stand for 48 h at 20 ℃ and checked for precipitation to determine the solubility of the dyes.

2.2.6 Measurement of spectral and chromatic properties

Absorption spectra of the synthesized dyes and the transmittance

spectra of fabricated dye-based color filters were measured using a UV-Vis spectrophotometer. The chromatic values were recorded on a color spectrophotometer.

2.2.7 Measurement of thermal stability

The thermal stability of the synthesized dyes was evaluated by thermogravimetric analyzer (TGA). The prepared dyes were heated to 110 ℃ and held at that temperature for 10 min to remove the residual water and solvents. The dye was then, heated to 220 ℃ and held at that temperature for 30 min to simulate the processing thermal conditions of color filter manufacturing. The dyes were finally heated to 400 ℃ to determine their degradation temperature. The heating was carried out at the rate of 10 ℃ min^{-1} under nitrogen atmosphere.

To check the thermal stability of the dyes in color filters, the fabricated color filters were heated to 200 ℃ for 1 h in a forced convention oven (OF-02GW Jeiotech CO., Ltd.). The color difference values (ΔE_{ab}) before and after heating were measured on a color spectrophotometer in CIE $L^*a^*b^*$ mode [5].

2.3 Results and Discussion

2.3.1 Design and synthesis of dyes

In previous studies [5, 7, 8], some limitative substituents were adopted in the terminal- and bay-position of perylene-based dyes. However, in this study, we introduced new substituents in the terminal position to synthesize two series of dyes. On each terminal-substituted dye, three kinds of substituents were additionally introduced in the bay position. The synthesized dyes were intentionally designed to analyze the change of physical properties with the type of substituents introduced.

The introduction of substituents in the terminal position disturbs the intermolecular interaction between dyes [5, 7], and crystal packing density of the dyes will decrease due to the steric restriction caused by the adopted substituents [10]. However, as mentioned in our previous report [2, 5, 7], conjugation between the perylene main body and the substituents is not affected. Therefore, bulky aromatic groups could be introduced in the terminal position without a concomitant such as bathochromic shift of the synthesized dyes.

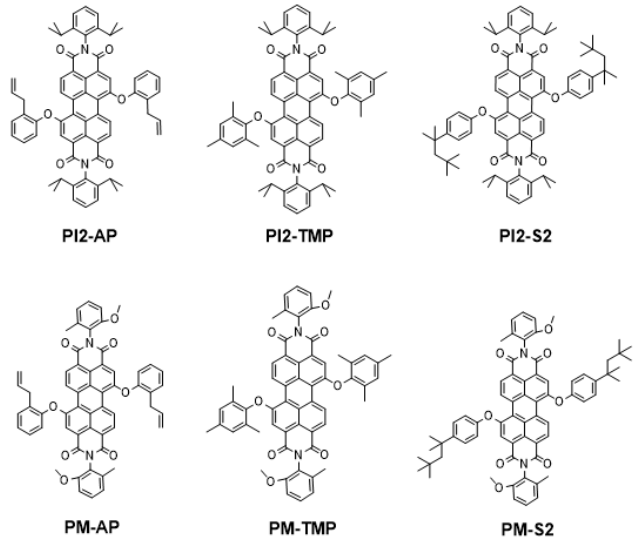

Fig. 2.1 The Structures of synthesized dyes

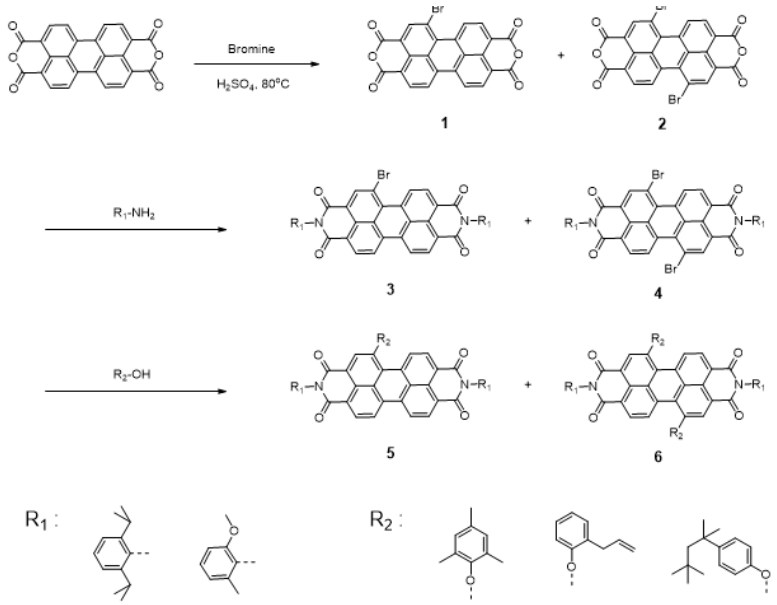

Scheme 2.1 Synthetic routes of the designed dyes

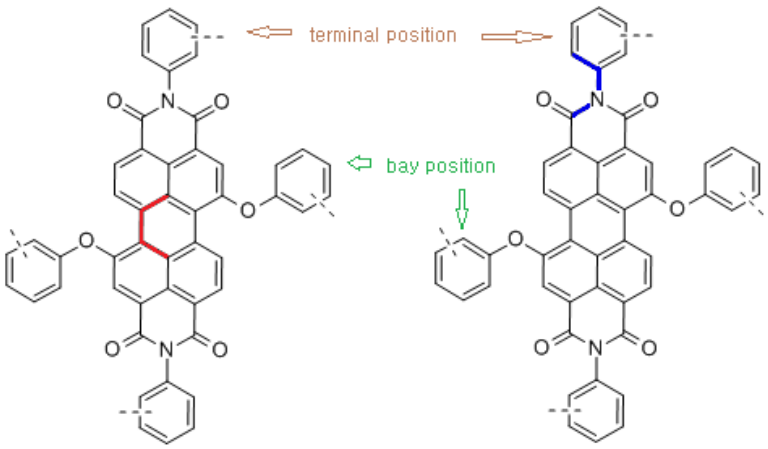

Fig. 2.2 The position of dihedral angle of perylene main body (left, red) and dihedral angle of terminal-substituent (right, blue)

Table 2.1 Reaction yield of **PI2-S2** upon reaction time (%)

Product	0.5 h	1 h	1.5 h	2 h	2.5 h	3 h	3.5 h	4 h
1,7-di(subsitituted)	57	66	75	75	74	74	70	66
mono-subsitituted	12	7	0	0	0	0	0	0

The introduction of substituents in the bay position also increases steric restriction within dye structures [5], and the planarity of dyes will be decreased [11]. However, the substituents in the bay position were attached to the main body via an ether linkage, so that the substituents had significant influence on the spectral properties of the dyes [12].

In many perylene-based dye synthesis [5, 8], substituents were usually introduced into the bay position at temperatures greater than 120 ℃. However, in this study, we optimized the reaction conditions and found that the introduction of substituents was possible at much lower temperature (40–60 ℃) and in a shorter reaction time (under 2 hours). **Table 2.1** show that the reaction yield reached its maximum within 2 hours of the bay position substitution reaction for **PI2-S2** dye.

2.3.2 Determination of optimized geometries of the dyes

The molecular geometries of **PI2-AP**, **PI2-TMP**, and **PM-AP** were optimized using the Gaussian 09 program. The molecular geometries of the three dyes are shown in **Fig. 2.3 – Fig. 2.5** and the molecular twisting angles of specific parts of the dyes are indicated in **Table 2.2**. As shown

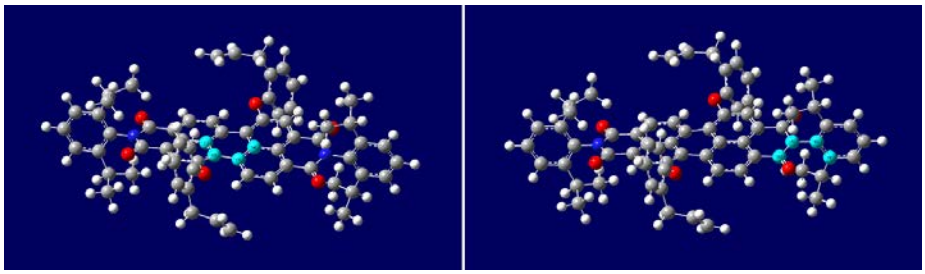

Fig. 2.3 Geometry-optimized structures of dye **PI2-AP**

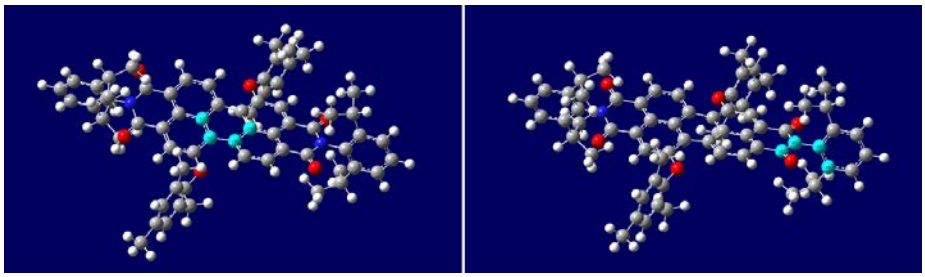

Fig. 2.4 Geometry-optimized structures of dye **PI2-TMP**

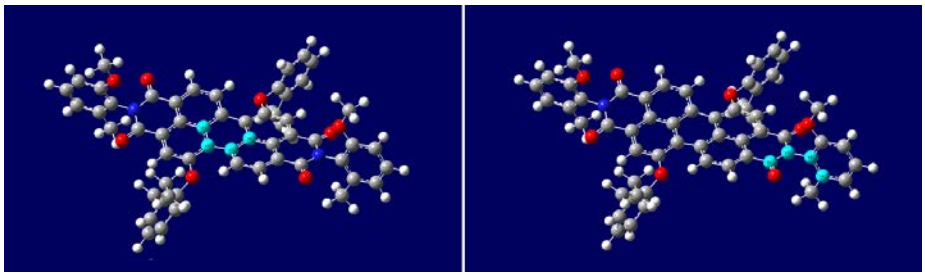

Fig. 2.5 Geometry-optimized structures of dye **PM-AP**

Table 2.2 Dihedral angle of the highlighted parts

Synthesized dye	Dihedral angles of the perylene main body (displayed at left figure)	Dihedral angles of the terminal-substituent (displayed at right figure)
PI2-AP	11.72818	86.79419
PI2-TMP	12.85749	88.94329
PM-AP	12.51582	89.85623

Table 2.3 Calculated lengths of terminal position substituent

Synthesized dye	Lengths (Å)
PI2-AP	8.39537
PI2-TMP	8.39624
PM-AP	7.78934

in **Fig. 2.2**, the dihedral angle of the perylene main body affects the planarity of the aromatic rings that compose the perylene main body. And the dihedral angle of the terminal-substituent indicates the twisting angle between the perylene main body and the substituents in the terminal position. Generally, many perylene-based derivatives exhibit a dihedral angle between 9–20° for the perylene main body, and between 85–90° for the terminal-substituent [5].

As shown in **Table 2.2**, the differences in the dihedral angles of the perylene main body of the synthesized dyes were very small to relate the influences of the planarity of perylene main body on any physical properties of them. This also means that the effect of bay position substituents used in this study on dihedral angle of the perylene main body is minimal. However, the freedom of rotation of the aromatic ring in the bay position substituents would affect the planarity and aggregation of the synthesized dyes owing to the change of intermolecular interaction.

The calculated lengths of terminal position substituents were indicated in **Table 2.3**. All of the substituents introduced in the terminal position exhibited dihedral angles of about 90°. Therefore, the dyes with

bulky terminal position substituents would have lower crystal packing densities, and this would affect the physical properties of the synthesize dyes such as solubilities and thermal stabilities.

2.3.3 Properties of the synthesized dyes

Generally, un-substituted perylene dyes are not soluble in organic industrial solvents, such as PGMEA or cyclohexanone. The synthesized dyes exhibited acceptable solubility in organic solvents to be used in dye-based LCD color filters. Their solubilities in CH_2Cl_2 and PGMEA are listed in **Table 2.4**.

In terms of terminal position substituents, the **PI-** substituent (1,3-diisopropylbenzene) had a larger effect on solubility than the **PM-** substituent (1-methoxy-3-methylbenzene). This is because, as shown in **Table 2.3**, the diisopropyl- group is bulkier than the methoxy-methyl- group in the **PM-** substituent, which decreases intermolecular interactions between the dyes [13].

With regard to the substituents introduced in the bay position, the effects of substituents for increasing solubility are in the order of **-TMP**

(2,4,6-trimethylbenzene) > **-S2** (4-*tert*-octylbenzene) > **-AP** (2-allylbenzene). The two methyl groups attached to ortho-position of the aromatic ring in **-TMP** substituent prevent free rotation of the substituent attached to the perylene main body. Therefore, it would prevent planar arrangement of the dyes. Consequently, without reference to the bulkiness of the substituents, the **-TMP** substituent will increase the solubility of the dyes in organic industrial solvents. The **-AP** substituent and the **-S2** substituent can rotate more freely than the **-TMP** substituent on an axis of ether-linkage. Among them, the **-S2** substituent is bulkier than the **-AP** substituent, which will increase the steric hindrance between dye molecules. Therefore, the dyes with **-S2** substituent exhibited higher solubility then the dyes with **-AP** substituent.

To be used in red color filters, dyes should have absorption maxima below 560 nm and strong transmittances above 600 nm [5, 8]. As shown in **Fig. 2.6**, the synthesized perylene dyes showed bathochromic shift in their absorption, as compared to the un-substituted perylene dianhydride (λ_{max} = 526 nm). Except **PI2-TMP** dye, all of the synthesized dyes exhibited similar absorption maxima, because substituents introduced in bay positions had similar effects on the conjugation system. The

bathochromic shift occurred in absorption spectra of **PI2-TMP** dye could be attributed to the distortion of perylene main body caused by the bay position substituents [14-16].

Synthesized dyes should have suitable thermal stabilities at industrial process temperatures to be used as color filter colorants. It has been found that dye aggregation has a significant effect on the thermal stabilities of dyes [17]. Dye aggregation primarily occurs due to (1) π-π stacking interactions between aromatic rings, (2) packing of molecules with planar structures, (3) intermolecular interactions, such as Van der Waals and dipole-dipole interactions between large molecules or those containing polar substituents, and (4) intermolecular hydrogen bonding. As mentioned in previous studies [5, 17], perylene dyes have many aromatic rings and form flat molecular structures, which contributes to strong intermolecular interactions.

As shown in **Fig. 2.7**, all of the synthesized dyes suffered little weight losses in isothermal process at 220 ℃; the weight losses of the dyes are listed in **Table 2.6**. Generally, the thermal stability show inverse relationship with solubility, because the intermolecular interactions increase the thermal stability and decrease the solubility. However, the

Table 2.4 Solubility of the synthesis dyes at 20 ℃ in CH_2Cl_2 and PGMEA

(wt%)

Synthesis dye	CH_2Cl_2	PGMEA
PI2-AP	5	4.5
PI2-TMP	8.5	8
PI2-S2	6	6
PM-AP	5	4
PM-TMP	6	5.5
PM-S2	5.5	5.5

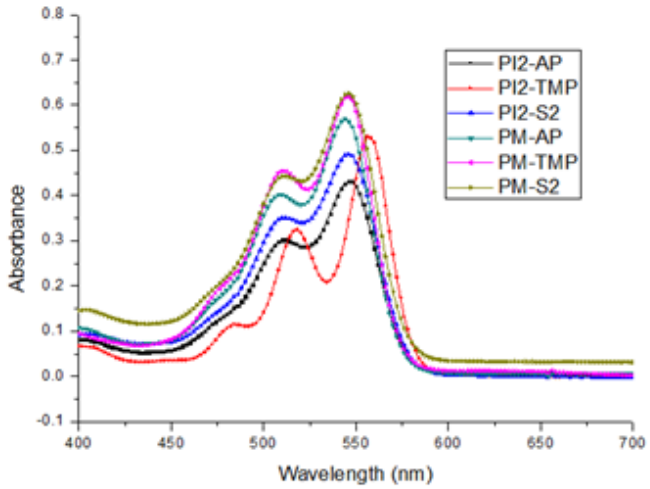

Fig. 2.6 Absorption spectra of synthesized dyes in CH_2Cl_2

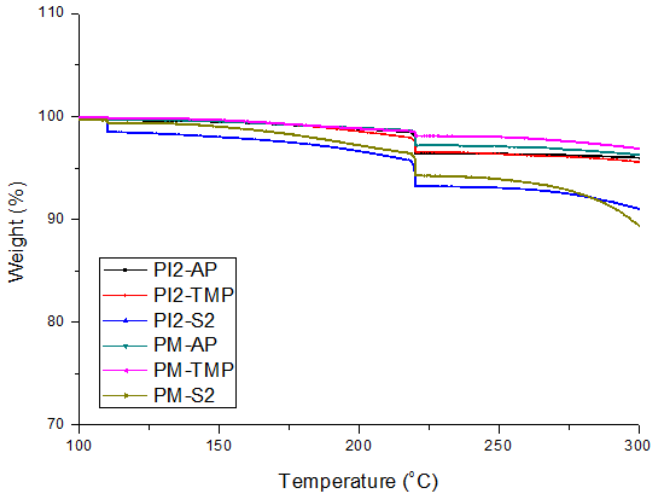

Fig. 2.7 Thermogravimetric analysis of the synthesized dyes

Table 2.5 Absorption spectra of the synthesized dyes in CH_2Cl_2

Synthesis dye	λ_{max} (nm)	ε_{max} (L mol^{-1} cm^{-1})
PI2-AP	546	43180
PI2-TMP	556	53000
PI2-S2	546	49090
PM-AP	544	56960
PM-TMP	546	61900
PM-S2	544	62630

Table 2.6 Weight loss of synthesized dyes in 220 ℃, 30 min isothermal process

Synthesized dye	Weight loss (%)
PI2-AP	1.82
PI2-TMP	1.54
PI2-S2	2.66
PM-AP	1.92
PM-TMP	0.54
PM-S2	2.80

dyes with **-TMP** substituents exhibited the least weight loss despite they had the highest solubility among the synthesized dyes. And, the dyes with **-S2** substituents showed the lowest thermal stability. These results are considered coming from the degradation of the synthesized dyes in alkyl chains attached to substituents, not in the perylene main body of the dyes. Consequently, the lengths of the alkyl chains attached to substituents have influenced on the thermal stabilities of the synthesized dyes.

2.3.4 Properties of the fabricated color filters

Transmittances of the dye-based color filters fabricated using the synthesized dyes are shown in **Fig. 2.8** and **Table 2.7**. As illustrated in **Fig. 2.8**, a widely used pigment-based color filter showed 94.6 % transmittance at 650 nm [5] and color filters fabricated with the synthesized dyes exhibited 96–99 % transmittances at the same wavelength. The decreased light scattering due to the smaller particle size of the dye-based color filters may have resulted in the superior transmittances. All of the fabricated color filters showed rapid rises of

transmittances from 550 nm, which was suitable for use in dye-based color filters.

There were unwanted transmittances in 400–500 nm for all of the fabricated dye-based color filters and yellow color compensating dyes would be needed to cut off these unwanted transmittances [5]. Also, the color filter fabricated with **PI2-AP** dye showed undesirable transmittance within 500–550 nm. This resulted the poor solubility of **PI2-AP** in PGMEA which led to the insufficient color content in the color filter.

The coordinate values of the color filters fabricated with the synthesized dyes are shown in **Table 2.8**. All color filters showed increased brightness and decreased x and y values after the post-baking process as compared to those after the pre-baking process. In the post-baking process, (1) dyes could be degraded due to the applied heat and (2) dyes could aggregate due to the mobility in film state caused by the applied heat. As mentioned before, the degradations of perylene-based dyes are considered mainly occurring in alkyl chains of substituents without any subsidiary color differences. Therefore, the color differences of perylene-based dyes would depend on the intensity of intermolecular

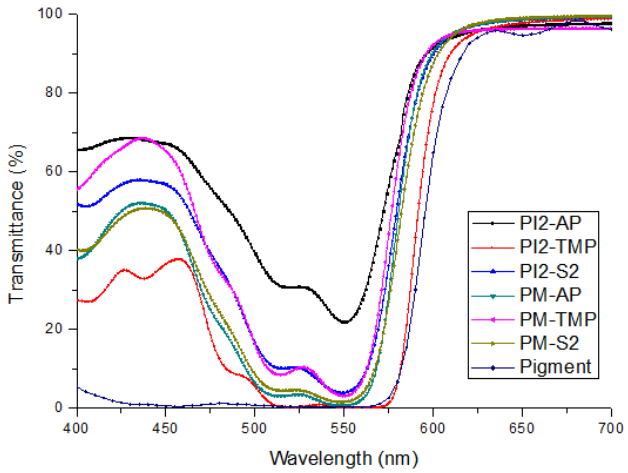

Fig. 2.8 Transmittance spectra of the fabricated dye-based color filters

Table 2.7 Transmittance of the fabricated dye-based color filters at 650 nm

Color filter	Transmittance at 650 nm (%)
PI2-AP	97.191
PI2-TMP	97.764
PI2-S2	98.617
PM-AP	98.657
PM-TMP	96.330
PM-S2	99.026
Pigment-based	94.600

Table 2.8 The coordinate values corresponding to the CIE 1931 chromaticity diagram and the color difference values of the dye-based color filters

Color filter		Y	x	y	ΔE_{ab}
PI2-AP	Prebaked	37.0545	0.4637	0.2733	3.491
	Postbaked	39.3698	0.4530	0.2683	
PI2-TMP	Prebaked	27.5083	0.5835	0.2351	0.546
	Postbaked	27.6950	0.5826	0.2345	
PI2-S2	Prebaked	29.2612	0.5968	0.2571	8.121
	Postbaked	34.5622	0.5851	0.2529	
PM-AP	Prebaked	37.6701	0.5655	0.2554	2.338
	Postbaked	38.4842	0.5636	0.2527	
PM-TMP	Prebaked	26.8823	0.6093	0.2596	2.005
	Postbaked	27.1275	0.6011	0.2533	
PM-S2	Prebaked	34.2552	0.6419	0.3170	7.532
	Postbaked	37.3227	0.6325	0.3064	

interactions and miscibility between dyes and binders.

Dyes with **-TMP** substituents exhibited the smallest ΔE_{ab}, meaning the aggregations of the dyes were not active than those of the other synthesized dyes. As mentioned before, the **-TMP** substituent had the greatest effect on preventing intermolecular interactions, which would lead to lower dye aggregation. Dyes with **-S2** substituents showed the largest $\Delta E_{ab,}$ meaning poor miscibility between the substituent and binders used. However, with the limited information on the binders used, further analysis on the aggregation of dyes within binder system was difficult.

2.4 Conclusion

In this study, six novel perylene-based dyes were synthesized in moderate condition. Five of the synthesized dyes exhibited acceptable spectral properties as colorants for red color filters. Also, most of the synthesized dyes showed appropriate solubilities in organic industrial solvents and sufficient thermal stabilities in the temperatures for color filter manufacturing.

The effects of substituents that introduced in bay- and terminal-positions were demonstrated by optimizing geometries of the synthesized dyes. The substituents introduced in bay- and terminal-positions had significant effects on the physical properties of the perylene-based dyes. The introduced substituents decreased intermolecular interactions of the synthesized dyes and increased their solubilities. The substituents in the terminal positions were introduced perpendicularly to the perylene main body, and the size of the substituents had a more significant influence than the dihedral angle with perylene main body. The substituents introduced in bay positions also make differences to their properties, such as solubilities, absorption-transmittance spectra, and thermal stabilities.

Color filters fabricated with the synthesized dyes showed the dye aggregation after the post-baking process. The color differences of the fabricated color filters were mainly influenced by the dye aggregation which varied depending on the intensity of intermolecular interactions and miscibility between dyes and binders.

2.5 References

[1] Choi J, Kim SH, Lee W, Chang JB, Namgoong JW, Kim YH, Han SH, Kim JP, Dyes Pigm., 2014, **101**, 186-195

[2] Choi J, Lee W, Namgoong JW, Kim TM, Kim JP, Dyes Pigm., 2013, **99**, 357-365

[3] Choi J, Lee W, Sakong C, Yuk SB, Park JS, Kim JP, Dyes Pigm., 2012, **94**, 34-39

[4] Hwang YJ, Shin DM, Mol. Cryst. Liq. Cryst., 2007, **472**, 25/[415]-32/[422]

[5] Choi J, Sakong C, Choi JH, Yoon C, Kim JP, Dyes Pigm., 2011, **90**, 82-88

[6] Kim YD, Cho JH, Park CR, Choi JH, Yoon C, Kim JP, Dyes Pigm., 2011, **89**, 1-8

[7] Kim YD, Kim JP, Kwon OS, Cho IH, Dyes Pigm., 2009, **81**, 45-52

[8] Sakong C, Kim YD, Choi JH, Yoon C, Kim JP, Dyes Pigm., 2011, **88**, 166-173

[9] Wei ZJ, Xu YW, Zhang L, Luo MM, Chin. Chem. Lett., 2014, **25**, 1367-1370

[10] Lynch DE, Byriel KA, Cryst. Eng., 1999, **2**, 225-239

[11] Zhang X, Pang S, Zhang Z, Ding X, Zhang S, He S, Zhan C,

Tetrahedron Lett., 2012, **53**, 1094-1097

[12] Chen J, Shi MM, Hu XL, Wang M, Chen, HZ, Polymer, 2010, **51**, 2897-2902

[13] Kufazvinei C, Ruether M, Wang J, Blau W, Org. Electron., 2009, **10**, 674-680

[14] Hutchings MG, Dyes Pigm., 1991, **17**, 227-240

[15] Durbeej B, Eriksson LA, Chem. Phys. Lett., 2003, **375**, 30-38

[16] Reghu RR, Bisoyi HK, Grazulevicius JV, Anjukandi P, Gaidelis V, Jankauskas V, J. Mater. Chem., 2011, **21**, 7811

[17] Tsai HY, Chen KY, J. Lumin., 2014, **149**, 103-111

Chapter 3

The Effect of Fluorescence of Perylene Red Dyes on the Contrast Ratio of LCD Color Filters

3.1 Introduction

Color filters are essential components of liquid crystal displays (LCDs) [1-8]. The desirable properties of color filters are color purity, contrast ratio, and brightness [9-12]. High-contrast color filters are the most important components in the manufacture of displays with superior optical properties [9, 10].

Contrast ratio is the proportion of maximum brightness to minimum brightness [6, 9, 10]. To obtain a high contrast ratio, light should not be transmitted when the polarizers are closed to produce a dark image (full-black state) [9]. In traditional pigment-based color filters, a small amount of light is transmitted in the full-black state due to light scattering [5, 6, 10]. The problem, which is caused by the large size of the pigments, can

be resolved by replacing pigments with dyes of smaller particle size [2, 4, 10]. However, many dyes that are used as colorants in LCD color filters exhibit fluorescence, which significantly brightens the full-black state of the device due to their emission. Consequently, dye-based color filters may exhibit a lower contrast ratio than expected.

Perylene-based dyes are suitable colorants for LCD color filters due to their strong color strengths and high thermal stabilities [2-4, 10, 12]. However, perylene derivatives with bulky substituents commonly exhibit strong fluorescence, because these groups can prevent intermolecular interactions and irradiative energy transfers that are the most important mechanisms of fluorescence quenching [13-15].

This paper will discuss the effect of fluorescence on the contrast ratio of dye-based and pigment-dye hybrid color filters. Perylene-based red dyes were synthesized with bulky substituents at terminal- and bay-positions to improve their solubilities in industrial solvents [2, 10]. Color filters were prepared with low color content to minimize the effect of aggregation on optical properties for the obvious investigation about the influence of the fluorescence on the contrast ratio. The fluorescence of the synthesized dyes in solution and the fabricated dye-based and

pigment-dye hybrid color filters were measured and compared. The maximum brightness and the contrast ratio of the color filters were measured, and the minimum brightness was calculated from the results. Finally, the correlation between fluorescence and optical properties of the color filters was analyzed.

3.2 Experimental

3.2.1 Materials and instrumentations

Perylene-3,4,9,10-tetracarboxylic dianhydride, 4-tert-octylphenol, iodine, sulfuric acid, bromine and acetic acid purchased from Sigma-Aldrich, 2,6-diisopropylaniline, 2,4,6-trimethylphenol and 2-allylphenol purchased from TCI, K_2CO_3 anhydrous, methylene chloride and other chemical solvents purchased from SAMCHUN pure chemical were used without any additional purification. Transparent glass substrates were purchased from Paul Marienfeld GmbH & CO. KG.

^{1}H and ^{13}C NMR spectra were recorded by a Bruker Avance 500 spectrometer at 500 MHz using chloroform-d and TMS as the solvent

and internal standard. Matrix Assisted Laser Desorption/Ionization Time Of Flight (MALDI-TOF) mass spectra were recorded by a Voyager-DESTR Biospectrometry Workstation with α-cyano-4-hydroxycinnamic acid (CHCA) as the matrix. Elemental analysis (EA) was completed on a CE Instrument EA1112. Absorption spectra were measured using a Perkin Elmer Lambda 25 UV/Vis spectrophotometer. Fluorescence spectra were measured using a Perkin Elmer LS 55 Fluorescence spectrometer. Contrast ratio and brightness of color filters were measured using a CT-1 of TSUBOSAKA and MC-3700: 28C of OTSUKA ELECTRONICS. The thickness of the spin-coated film was measured using a Nano System Nanoview E-1000.

3.2.2 Synthesis

The dyes **PI2-AP**, **PI2-TMP**, **PI2-S2**, and **PI1-S2** were already reported in our previous study [2, 10]. The syntheses of these dyes are detailed in this paper.

3.2.2.1 1,(7)-(di)bromoperylene-3,4,9,10-tetracarboxydiimide (1,2) :

Bromination

Perylene-3,4,9,10-tetracarboxylic dianhydride (32.0 g, 81.4 mmol), iodine (0.78 g, 3.04 mmol), and sulfuric acid (98 %, 450 mL) were mixed and stirred for 2 h at room temperature. The temperature of the mixture was raised to 80 ℃, bromine (7.5 mL, 146.65 mmol) was added dropwisely for 1 h. The mixture was reacted for 16 h. Then, it was cooled to room temperature and bromine gas was displaced by nitrogen gas. The mixture was slowly poured into 3 L of ice-water, producing precipitate collected by suction filtration in crude product form. The crude product was washed with distilled water several times. Then, the crude product was dried at 100 ℃ under reduced pressure and used in the next step without further purification. The crude containing both **1** and **2** was separated by column chromatography in next step, after importing derivatives in terminal-position to increase solubility.

3.2.2.2 N,N'-Bis(2,6-diisopropylphenyl)-1,(7)-(di)bromoperylene-3,4,9,10-tetracarboxydiimide (3,4) : Terminal-position Substitution

The crude 1,(7)-(di)bromoperylene-3,4,9,10-tetracarboxydiimide (8.0 g, 14.5 mmol), 2,6-diisopropylaniline (8.28 g, 46.7 mmol), acetic acid (4.6 mL), and N-Methyl-2-pyrrolidone (NMP) (100 mL) were mixed and heated at 120 ℃ under the nitrogen atmosphere for 96 h. The precipitate was obtained by adding water to the mixture and be collected by suction filtration. The crude product was washed with water and dried. The crude product was purified by column chromatography in silica gel using CH_2Cl_2 as the eluent. The first reddish band containing tribrominated diimide could be separated. Second reddish band containing dibrominated diimide and third one containing monobrominated diimide could be collected. Detailed structure analysis was done after next step.

3.2.2.3 N,N'-Bis(2,6-diisopropylphenyl)-1,7-bis(o-allylphenoxy)-perylene-3,4,9,10-tetracarboxydiimide (PI2-AP) : Bay-position Substitution

N,N'-Bis(2,6-diisopropylphenyl)-1,7-dibromoperylene-3,4,9,10-tetracarboxydiimide (0.50 g, 0.575 mmol) was mixed with potassium

carbonate anhydrous (0.35 g), 2-allylphenol (0.20 g , 1.50 mmol) and NMP (50 mL). The mixture was heated at 40 ℃ under nitrogen atmosphere and was stirred at for 1.5 h. The mixture was cooled to room temperature, and then poured into 400 mL of 5 % HCl aqueous solution. The precipitate was filtered, washed with water, and dried in vacuum at 80 ℃. The crude product was purified by column chromatography in silica gel using CH_2Cl_2 as the eluent to obtain **PI2-AP** as red solid.

Yield 71.5 %; ^{1}H NMR ($CDCl_3$, ppm): 9.72 (d,2H), 8.67 (d,2H), 7.46 (t,2H), 7.35 (d,2H), 7.30 (m,10H), 6.97 (t,2H), 6.06 (septet,2H), 5.14 (d,2H), 5.07 (d,2H), 3.59 (d,4H), 2.71 (septet,4H), 1.14 (d,24H); ^{13}C NMR (126 MHz, $CDCl_3$): δ= 24.18, 24.22, 29.40, 34.61, 116.82, 119.54, 122.53, 123.94, 124.24, 125.80, 125.96, 128.70, 129.33, 129.83, 129.93, 130.68, 130.86, 131.75, 131.98, 133.98, 136.42, 145.83, 152.98, 155.74, 163.12, 163.69; MALDI-TOF MS: m/z 976.3 (100 %, [M+2K]+); EA Found (%): C, 81.51; H, 6.14; N, 2.80; O, 9.56. Calc. (%) for $C_{66}H_{58}N_2O_6$: C, 81.29; H, 5.99; N, 2.87; O, 9.84.

3.2.2.4 N,N'-Bis(2,6-diisopropylphenyl)-1,7-bis(2,4,6-trimethyl phenoxy)-perylene-3,4,9,10-tetracarboxydiimide (PI2-TMP)

PI2-TMP was synthesized in the same manner with **PI2-AP** using N,N'-Bis(2,6-diisopropylphenyl)-1,7-dibromoperylene-3,4,9,10-tetracarboxydiimide (0.50 g, 0.575 mmol), potassium carbonate anhydrous (0.35 g) and 2,4,6-trimethylphenol (0.21 g, 1.50 mmol). The reaction temperature was set at 60 ℃ for 2 h.

Yield 78.0 %; ^{1}H NMR ($CDCl_3$, ppm): 9.69 (m,2H), 8.72 (d,2H), 7.48 (t,2H), 7.32 (m,6H), 7.03 (s,4H), 2.74 (septet,4H), 2.34 (s,6H), 2.18 (m,12H), 1.19 (m,24H); ^{13}C NMR (126 MHz, $CDCl_3$): δ= 16.62, 24.15, 24.21, 24.26, 29.38, 29.48, 120.17, 122.13, 122.76, 124.16, 124.21, 124.92, 125.27, 128.17, 129.17, 129.30, 129.50, 129.98, 130.15, 130.24, 130.41, 130.50, 130.54, 130.72, 130.77, 133.62, 133.93, 136.46, 138.65, 145.83, 147.79, 162.97, 163.12; MALDI-TOF MS: m/z 980.3 (100 %, [M +2K]+); EA Found (%): C, 80.96; H, 6.14; N, 2.98; O, 9.91. Calc. (%) for $C_{66}H_{62}N_2O_6$: C, 80.95; H, 6.38; N, 2.86; O, 9.80.

3.2.2.5 N,N'-Bis(2,6-diisopropylphenyl)-1,7-bis(p-tert-octylphenoxy)-perylene-3,4,9,10-tetracarboxydiimide (PI2-S2)

PI2-S2 was synthesized in the same manner with **PI2-AP** using N,N'-

Bis(2,6-diisopropylphenyl)-1,7-dibromoperylene-3,4,9,10-tetracarboxydiimide (0.50 g, 0.575 mmol), potassium carbonate anhydrous (0.35 g) and 4-tert-octylphenol (0.31 g, 1.50 mmol).

Yield 76.9 %; ^{1}H NMR ($CDCl_3$, ppm): 9.66 (d,2H), 8.69 (d,2H), 8.38 (d,4H), 7.45 (m,2H), 7.32 (m,4H), 7.25 (s,2H), 7.10 (d,4H), 2.72 (septet,4H), 1.39 (s,4H), 1.16 (d,24H), 0.75 (s,18H), 0.73 (s,12H); ^{13}C NMR (126 MHz, $CDCl_3$): δ= 24.18, 24.22, 29.39, 31.72, 32.00, 32.63, 38.66, 57.38, 118.89, 119.02, 122.49, 123.34, 124.12, 124.20, 124.26, 124.58, 124.75, 126.00, 128.18, 128.45, 129.25, 129.83, 129.92, 130.73, 130.90, 131.98, 133.97, 145.88, 147.47, 147.59, 152.78, 155.71, 162.94, 163.10, 163.71; MALDI-TOF MS: m/z 1120.5 (100 %, [M+2K]+); EA Found (%): C, 81.76; H, 7.41; N, 2.47; O, 8.35. Calc. (%) for $C_{76}H_{82}N_2O_6$: C, 81.54; H, 7.38; N, 2.50; O, 8.58.

3.2.2.6 N,N'-Bis(2,6-diisopropylphenyl)-1-o-allylphenoxy-perylene-3,4,9,10-tetracarboxydiimide (PI1-AP)

PI1-AP was synthesized in the same manner with **PI2-AP** using N,N'-Bis(2,6-diisopropylphenyl)-1-bromoperylene-3,4,9,10-

tetracarboxydiimide (0.50 g, 0.575 mmol), potassium carbonate anhydrous (0.21 g) and 2-allylphenol (0.15 g , 1.13 mmol).

Yield 73.4 %; ^{1}H NMR ($CDCl_3$, ppm): 9.71 (d,2H), 8.83 (d,2H), 8.75 (t,2H), 8.26 (s,1H), 7.48 (t,2H), 7.34 (m,8H), 6.06 (septet,2H), 5.12 (d,1H), 3.56 (d,2H), 2.77 (septet,4H), 1.19 (d,24H); ^{13}C NMR (126 MHz, $CDCl_3$): δ= 24.18, 24.22, 28.71, 29.44, 34.55, 116.87, 119.84, 122.79, 122.85, 123.19, 123.40, 124.15, 124.27, 124.30, 124.38, 124.62, 124.75, 126.08, 126.46, 127.65, 128.77, 129.06, 129.26, 129.38, 129.87, 130.09, 130.51, 130.84, 131.73, 131.86, 132.06, 132.85, 134.50, 135.06, 135.27, 136.34, 145.81, 145.89, 146.41, 152.60, 156.72, 162.90, 163.70, 163.94; MALDI-TOF MS: m/z 844.2 (100 %, [M+2K]+); EA Found (%): C, 81.21; H, 5.95; N, 3.57; O, 9.27. Calc. (%) for $C_{57}H_{50}N_2O_5$: C, 81.21; H, 5.98; N, 3.32; O, 9.49.

3.2.2.7 N,N'-Bis(2,6-diisopropylphenyl)-1-2,4,6-trimethylphenoxy-perylene-3,4,9,10-tetracarboxydiimide (PI1-TMP)

PI1-TMP was synthesized in the same manner with **PI2-AP** using N,N'-Bis(2,6-diisopropylphenyl)-1-bromoperylene-3,4,9,10-

tetracarboxydiimide (0.50 g, 0.575 mmol), potassium carbonate anhydrous (0.21 g) and 2,4,6-trimethylphenol (0.16 g, 1.13 mmol). The reaction temperature was set at 60 ℃ for 2 h.

Yield 77.3 %; ^{1}H NMR ($CDCl_3$, ppm): 9.89 (d,2H), 8.83 (t,2H), 8.05 (s,1H), 7.50 (m,2H), 7.34 (d,4H), 7.04 (s,4H), 3.03 (s,1H), 2.78 (septet,4H), 2.35 (s,2H), 2.18 (s,6H), 1.19 (m,24H); ^{13}C NMR (126 MHz, $CDCl_3$): δ= 16.49, 21.05, 23.09, 23.46, 24.13, 28.38, 28.71, 29.36, 29.44, 120.02, 121.01, 122.40, 122.63, 123.18, 123.25, 123.37, 124.29, 124.39, 124.73, 125.81, 127.66, 127.77, 129.49, 129.95, 130.16, 130.66, 130.75, 130.90, 131.66, 131.86, 132.93, 134.91, 135.07, 135.45, 145.81, 147.81, 157.28, 163.03, 163.76, 164.01; MALDI-TOF MS: m/z 846.3 (100 %, [M+2K]+); EA Found (%): C, 81.22; H, 6.07; N, 3.42; O, 9.29. Calc. (%) for $C_{57}H_{52}N_2O_5$: C, 81.02; H, 6.20; N, 3.32; O, 9.47.

3.2.2.8 N,N'-Bis(2,6-diisopropylphenyl)-1-p-tert-octylphenoxy-perylene-3,4,9,10-tetracarboxydiimide (PI1-S2)

PI1-S2 was synthesized in the same manner with **PI2-AP** using N,N'-Bis(2,6-diisopropylphenyl)-1-bromoperylene-3,4,9,10-

tetracarboxydiimide (0.50 g, 0.575 mmol), potassium carbonate anhydrous (0.21 g) and 4-tert-octylphenol (0.23 g, 1.12 mmol).

Yield 79.2 %; ^{1}H NMR ($CDCl_3$, ppm): 9.68 (d,2H), 8.82 (d,2H), 8.76 (d,4H), 8.39 (s,1H), 7.49 (m,4H), 7.34 (m,4H), 2.78 (septet,4H), 1.40 (s,2H), 1.18 (d,24H), 0.74 (s,15H); ^{13}C NMR (126 MHz, $CDCl_3$): δ= 24.22, 29.42, 29.45, 31.72, 32.00, 32.64, 57.40, 119.12, 122.75, 122.81, 123.38, 124.08, 124.31, 124.61, 125.37, 126.56, 127.66, 128.54, 129.08, 129.24, 129.85, 130.06, 130.51, 130.86, 131.70, 132.91, 134.51, 135.07, 135.28, 147.82, 152.43, 156.80, 162.89, 163.70, 163.95; MALDI-TOF MS: m/z 916.3 (100 %, [M+2K]+); EA Found (%): C, 81.40; H, 6.85; N, 3.00; O, 8.74. Calc. (%) for $C_{62}H_{62}N_2O_5$: C, 81.37; H, 6.83; N, 3.06; O, 8.74.

3.2.3 Fabrication of dye-based color filters

The red inks for dye-based color filters composed of the synthesized dye (0.01 g), propylene glycol methyl ether acetate (PGMEA) (0.1 g), and acrylic binder (0.8 g). The prepared dye-based inks were coated on a transparent glass substrate using a MIDAS System SPIN-1200D spin

coater. The rotating speed was initially set at 100 rpm for 10 s, and then increased to 500 rpm for 20 s. The dye-coated color filters were dried at 80 ℃ for 20 min, pre-baked at 150 ℃ for 10 min and post-baked at 200 ℃ for 1 h. All spin-coated dye-based color filters were 1.6 μm thick.

3.2.4 Fabrication of pigment-dye hybrid color filters

The red inks for pigment-dye hybrid color filters were composed of the pigment red 177 (13–15 %), acrylic polymer dispersant (3–5 %), acrylic polymer (3–5 %), propylene glycol methyl ether acetate (PGMEA) (75–80 %), and synthesized dyes (0.5 wt% or 1.0 wt% compared with pigment red 177). The concentrations of color content were adjusted to show appropriate color coordination as red color filters. The prepared inks were coated on a transparent glass substrate using a spin coater. The spin-coated color filters were pre-baked at 80 ℃ for 10 min and post-baked at 230 ℃ for 30 min. The contrast ratio of the color filters were measured by CT-1 instrument of TSUBOSAKA and the brightness of them were measured by MC-3700: 28C of OTSUKA ELECTRONICS.

3.3 Results and discussion

3.3.1 Design concept and synthesis of the dyes

Perylene-based dyes have many advantages as colorants in optical devices including high color strength and thermal stability [2, 4, 10, 12]. However, their applications are limited by low solubility in industrial solvents due to their planar molecular structures [10, 12].

The synthetic routes and molecular structures of the synthesized dyes are shown in **Scheme 3.1** and **Fig. 3.1**. All dyes are designed to have increased solubility in organic solvents. Un-substituted perylene dyes are not soluble in industrial solvents such as PGMEA and cyclohexanone [2, 10, 12]. Introduction of substituents at their terminal- and bay-positions increases the solubility of the dyes in organic solvents. The substituents introduced on perylene-based dyes effectively decrease the intermolecular interactions and planarities of the dyes [2, 10]. Solubilities of the synthesized dyes are listed in **Table 3.1**. Dyes should have solubilities greater than 5 wt% in industrial solvents to be used as colorants in color filters [2, 10, 12]. As indicated in **Table 3.1**, most of

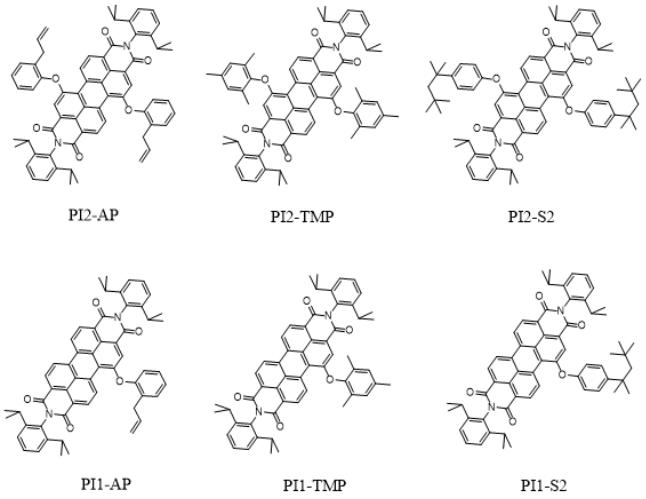

Fig. 3.1 Structure of the synthesized dyes

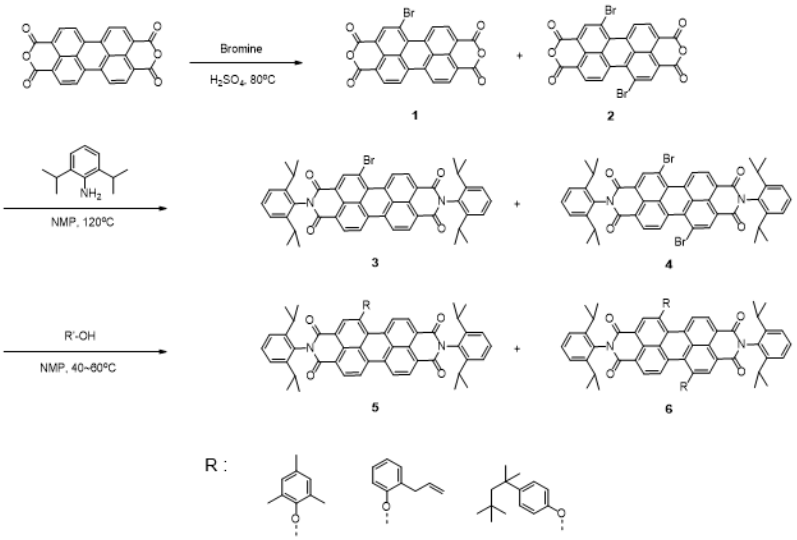

Scheme 3.1 Synthetic routes of the designed dyes

Table 3.1 Solubility of the synthesized dyes at 20 ℃ (wt%)

Dye	PI2-AP	PI2-TMP	PI2-S2	PI1-AP	PI1-TMP	PI1-S2
CH_2Cl_2	5.1	8.5	6.2	6.0	8.9	6.7
PGMEA	4.4	7.8	5.7	5.0	7.9	6.1

the synthesized dyes showed suitable solubility in industrial organic solvents.

Bromination and substitution reactions at terminal-positions were carried out by well-known procedures [1, 2, 4, 16-18]. Bay-position substitution reactions were performed at a lower temperature and for a shorter time than the standard method by the procedure reported in our previous study [10]. The reaction yields of all bay-position substitution reactions exceeded 70 %.

3.3.2 Spectral properties of the synthesized dyes

All dyes were designed to have a similar length of conjugation. Therefore, they exhibited similar absorption spectra as shown in **Fig. 3.2** [19, 20]. Consequently, the spectral properties of the synthesized dyes rarely affected the optical properties of the color filters. However, the varied size and shape of the substituents affected the planarity and crystal packing structure of the dyes. Therefore, the synthesized dyes exhibited different fluorescence properties depending on their molecular structures [21].

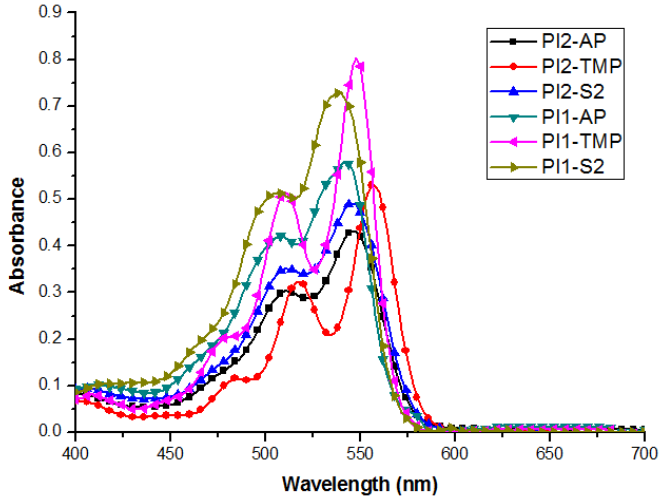

Fig. 3.2 Absorption spectra of synthesized dyes in chloroform (10^{-5} mol/L)

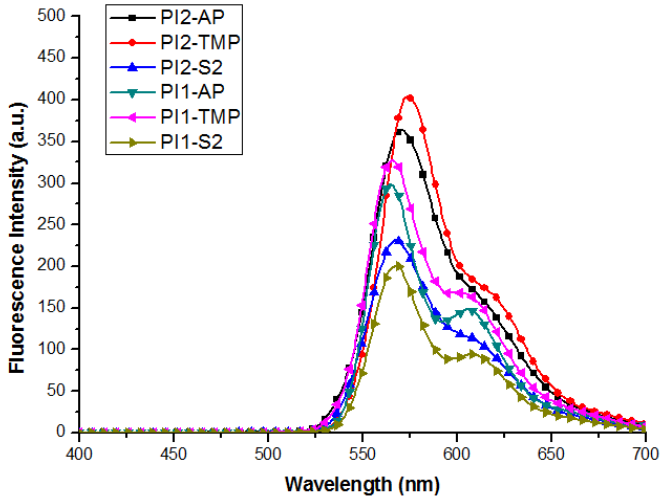

Fig. 3.3 Fluorescence of synthesized dyes in chloroform (10^{-8} mol/L)

Table 3.2 Spectral and fluorescence properties of the synthesized dyes

Dye	PI2-AP	PI2-TMP	PI2-S2	PI1-AP	PI1-TMP	PI1-S2
λ_{em} [a]	571	574.5	567.5	565	566	568
Max. Emission Intensity	363.74	403.16	231.50	298.16	327.48	200.29
Σ(emission) [b]	45751.41	47443.33	29065.89	32892.27	39489.99	22455.93
λ_{abs} [c]	546	556	546	542	548	538
Δss [d]	25	18.5	21.5	23	18	30

a. λ_{em} : maximum emission wavelength (nm).

b. Σ(emission) : integral of fluorescence intensity in visible-ray region, total emission intensity.

c. λ_{abs} : maximum absorption wavelength (nm).

d. Δss : stokes shift.

As shown in **Fig. 3.3**, the synthesized perylene dyes exhibited strong fluorescence over 500–700 nm [16, 22-24]. Fluorescence was measured at an excitation wavelength corresponding to the wavelength of maximum absorption, respectively. The emission spectra of synthesized dyes exhibited different maximum wavelengths and intensities depending on their molecular structures. The bay-substituted dyes with three methyl groups at ortho- and para-positions exhibited the highest fluorescence intensity than other dyes. Furthermore, di-bay-substituted dyes showed stronger fluorescence than mono-bay-substituted dyes. This behavior evidently results from the difference in conjugation length and crystal packing of the dyes [13, 15, 25, 26]. All emission maxima are shifted bathochromically from the wavelength of maximum absorption by 18–30 nm. The intensity at the wavelength of maximum emission and the total emission intensity within the visible region (400–700 nm) are listed in **Table 3.2**. The total emission intensity of the most strongly fluorescent dye (**PI2-TMP**) was about twice as large as that of the most weakly fluorescent dye (**PI1-S2**).

3.3.3 Optical properties of the fabricated dye-based color filters

Dye-based color filters were prepared with low color content concentrations to minimize the effect of dye aggregation on optical properties of the color filters. As shown in **Fig. 3.4**, the fabricated color filters exhibited strong fluorescence in the visible region despite their low color content. The total emission of the color filters in the visible region correlates with the emission of the dyes in solution as listed in **Table 3.2**. Thus, the fluorescence properties of the dyes in solution would be maintained in the film state with similar tendency.

The optical properties of the fabricated dye-based color filters are shown in **Table 3.3**. The contrast ratios are very small, because the inks for the color filters have low color content concentrations. The value of RY (Max. Y) is the maximum brightness of the color filter with the polarizer entirely open. Min. Y is the brightness in the full-black state, which is calculated from the maximum brightness and contrast ratio. The minimum brightness shows the same behavior in pre- and post-baked color filters. This phenomenon suggests that the influence of heat treatment on optical properties was minimized by the low color contents [6, 10]. Moreover, the sequence of increasing minimum brightness of the fabricated color filters is identical to that of the total emission intensity

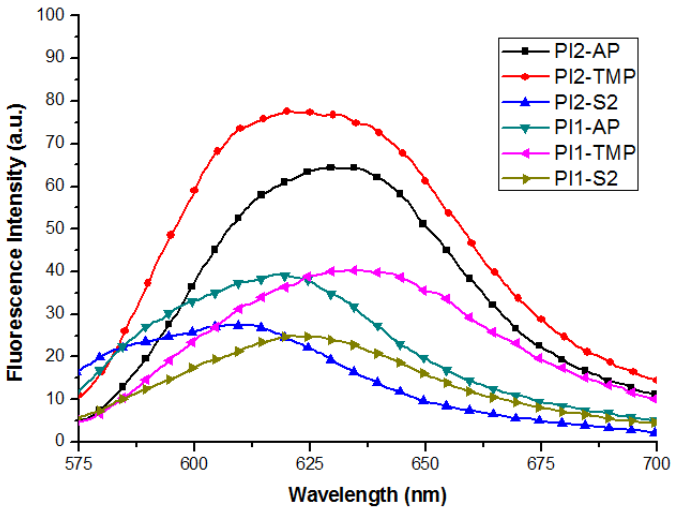

Fig. 3.4 Fluorescence of fabricated dye-based color filters

Table 3.3 Optical properties of the fabricated dye-based color filter [a]

Dye		PI2-AP	PI2-TMP	PI2-S2	PI1-AP	PI1-TMP	PI1-S2
Pre-baked	**Rx**	0.37828	0.35346	0.40584	0.39646	0.39021	0.36881
	Ry	0.23125	0.21607	0.25125	0.26480	0.23116	0.23712
	RY (Max. Y) [b]	37.294	37.022	38.776	40.451	37.263	38.776
	C/R [c]	38	33	57	54.5	47.5	87.5
	Min. Y [d]	**0.9814**	**1.1219**	**0.6803**	**0.7422**	**0.7845**	**0.4432**
Post-baked	**Rx**	0.37487	0.35348	0.40381	0.39449	0.39130	0.37452
	Ry	0.23423	0.21973	0.25306	0.24776	0.23216	0.23564
	RY (Max. Y)	39.093	36.704	39.606	40.480	37.427	39.151
	C/R	45	35	58	57.5	47	85.5
	Min. Y	**0.8687**	**1.0487**	**0.6829**	**0.7040**	**0.7963**	**0.4579**

a. The inks for dye-based color filters composed of the synthesized dye (0.01 g), propylene glycol methyl ether acetate (PGMEA) (0.1 g), and acrylic binder (0.8 g).

b. RY (Max. Y) : measured maximum brightness.

c. C/R : contrast ratio.

d. Min. Y : calculated brightness of full-black state.

of the dyes within the visible region. Therefore, it could be argued that the total emission intensity within visible region of the dyes significantly influences the minimum brightness of the fabricated color filters.

3.3.4 Optical properties of the fabricated pigment-dye hybrid color filters

Pigment-dye hybrid color filters were prepared by adding 0.5 or 1.0 wt% of the synthesized dyes in proportion to Pigment Red 177. The perylene-based dyes are well-known that they would easily exhibit H-aggregation and quench the fluorescence. Therefore, dye concentrations were carefully restricted lower than what is used in industry. FE-SEM images and average particle size were shown in **Fig. 3.5** and **Table 3.4**. The fabricated pigment-based and pigment-dye hybrid color filters have similar particle size within the difference of 6–7 nm. Transmittance spectra of the prepared color filters were illustrated in **Fig. 3.6** and **Table 3.5**. The transmittance spectra of the hybrid color filters were match up with the spectra of the pigment-based color filter within the whole visible region. By these results, it could be regarded that the added dyes would

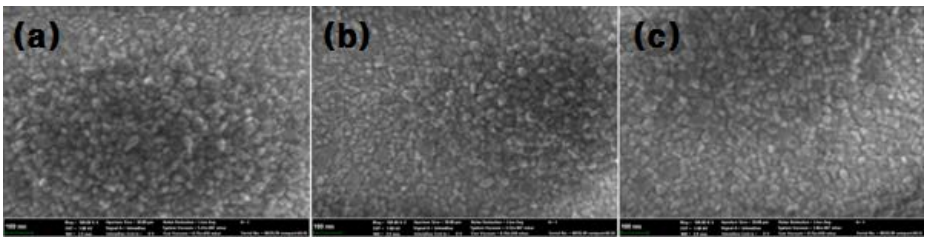

Fig. 3.5 FE-SEM images of pigment-based and pigment-dye hybrid color filters fabricated with **PI2-TMP** ((a) pigment-based, (b) 0.5 wt% dye added, (c) 1.0 wt% dye added color filter)

Table 3.4 Average particle size in FE-SEM images

Color Filter	**Pigment-based**	**0.5 wt% dye added**	**1.0 wt% dye added**
Average size (nm)	39.667	33.522	34.524

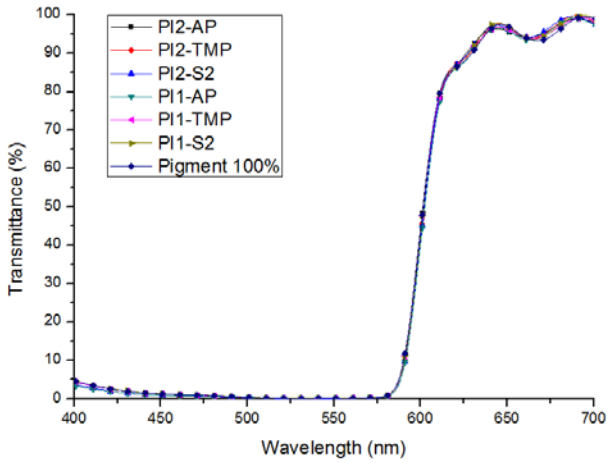

Fig. 3.6 Transmittance of pigment-based and pigment-dye hybrid color filters

Table 3.5 Transmittance of fabricated pigment-based and pigment-dye hybrid color filters at 645 and 650 nm

Dye	PI2-AP	PI2-TMP	PI2-S2	PI1-AP	PI1-TMP	PI1-S2	Pigment-based
at 645 nm (%)	96.41	97.62	97.33	96.70	96.81	97.90	97.46
at 650 nm (%)	95.72	97.02	96.48	95.99	96.34	97.03	97.56

have very limited effect on the aggregation behavior or optical performance of the color filters.

The fluorescence spectra of the fabricated pigment-dye hybrid color filters are illustrated in **Fig. 3.7**. The fluorescence of all hybrid color filters was measured with an excitation wavelength of 530 nm [27]. Therefore, the fabricated hybrid color filters have similar maximum emission peaks. All fabricated pigment-dye hybrid color filters exhibited an absorption maximum at 530 nm, because they consisted primarily of Pigment Red 177. However, the fluorescence properties of the color filters differed as shown in **Fig. 3.7**. These properties exhibited tendencies similar to those of dyes in solution and dye-based color filters. Color filters with 1.0 wt% dye showed stronger fluorescence than those with 0.5 wt%. These observations demonstrate that the fluorescence features of the dyes are retained in dye-based color filters and pigment-dye hybrid color filters.

The optical properties of the fabricated pigment-dye hybrid color filters are listed in **Table 3.6**. All hybrid color filters showed greater Min. Y values than pigment-based color filter (STD; Pigment Red 177, 100 %). This result indicates that the minimum brightness of pigment-dye hybrid

color filters was increased by the emission of the added dyes. In addition, the sequence of minimum brightness of the hybrid color filters was the same as that of dye-based ones. As mentioned before, added dyes have limited effect on the aggregation and optical properties of the fabricated color filters. Therefore, the minimum brightness and contrast ratio of pigment-dye hybrid color filters also were affected by the total emission within the visible region. Thus, color filters with strongly emitting dyes would exhibit a high minimum brightness and low contrast ratio.

The fluorescence of a dye could increase maximum brightness. However, as listed in **Table 3.6**, maximum brightness of the fabricated pigment-dye hybrid color filters were maintained in every case. There is no increase of maximum brightness from the added dyes. On the contrary to this result, the minimum brightness of the fabricated hybrid color filters were increased in all cases. Even though the increases in figures were small, they raised the minimum brightness considerably in proportion, which lowered contrast ratio values accordingly.

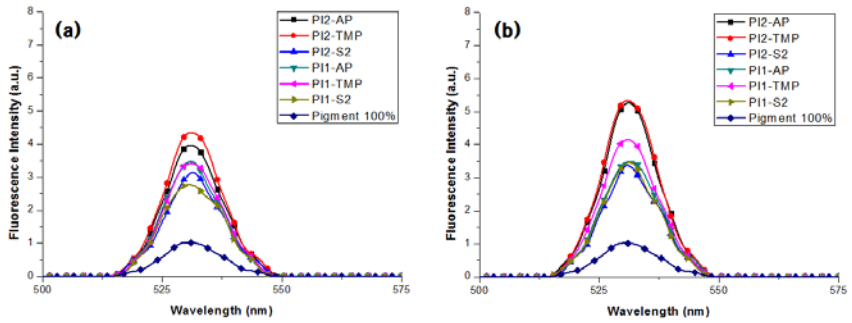

Fig. 3.7 Fluorescence of fabricated pigment-based and pigment-dye hybrid color filters (dye contents (a) 0.5 wt%, (b) 1.0 wt%)

Table 3.6 Optical properties of the fabricated pigment-dye hybrid color filters

Dye		PI2-AP	PI2-TMP	PI2-S2	PI1-AP	PI1-TMP	PI1-S2
0.5 wt %	Rx	0.656	0.656	0.656	0.656	0.656	0.656
	Ry	0.30311	0.30314	0.30362	0.30310	0.30312	0.30283
	RY (Max. Y) [a]	13.187	13.132	13.234	13.110	13.133	13.316
	C/R [b]	11294	11130	11824	11568	11428	11849
	Min. Y [c]	**0.00117**	**0.00118**	**0.00112**	**0.00113**	**0.00115**	**0.00112**
1.0 wt %	Rx	0.656	0.656	0.656	0.656	0.656	0.656
	Ry	0.30392	0.30375	0.30381	0.30394	0.30940	0.30384
	RY (Max. Y)	13.337	13.416	13.351	13.403	13.420	13.445
	C/R	10238	9234	11325	11124	11070	11727
	Min. Y	**0.00130**	**0.00145**	**0.00118**	**0.00120**	**0.00121**	**0.00115**
STD (pigment 100%) [d]		**Rx : 0.656, Ry : 0.30391, RY : 13.492, C/R : 12304, Min. Y : 0.00110**					

a. RY (Max. Y) : measured maximum brightness.

b. C/R : contrast ratio.

c. Min. Y : calculated brightness of full-black state.

d. STD : pigment-based color filter (Pigment Red 177, 100%).

3.4 Conclusion

To investigate the effect of fluorescence on the contrast ratio of color filters, six perylene-based dyes were synthesized, and dye-based and pigment-dye hybrid color filters were prepared from them. The fluorescence properties of the synthesized dyes in solution and the fabricated color filters were measured and compared to one another. The total visible-range emission intensity of the synthesized dyes in solution and the prepared color filters showed the same trend regardless of their states. The minimum brightness of the color filters calculated from the maximum brightness and contrast ratio showed a similar trend to the total emission intensity. Therefore, it is concluded that the total emission in the visible region is a key factor in determining the minimum brightness and contrast ratio of color filters. Consequently, color filters fabricated with strongly fluorescent dyes will exhibit high minimum brightness and low contrast ratio.

3.5 References

[1] Kim YD, Kim JP, Kwon OS, Cho IH, Dyes Pigm., 2009, **81**, 45-52

[2] Choi J, Sakong C, Choi JH, Yoon C, Kim JP, Dyes Pigm., 2011, **90**, 82-88

[3] Kim YD, Cho JH, Park CR, Choi JH, Yoon C, Kim JP, Dyes Pigm., 2011, **89**, 1-8

[4] Sakong C, Kim YD, Choi JH, Yoon C, Kim JP, Dyes Pigm., 2011, **88**, 166-173

[5] Choi J, Lee W, Sakong C, Yuk SB, Park JS, Kim JP, Dyes Pigm., 2012, **94**, 34-39

[6] Choi J, Lee W, Namgoong JW, Kim TM, Kim JP, Dyes Pigm., 2013, **99**, 357-365

[7] Choi J, Kim SH, Lee W, Chang JB, Namgoong JW, Kim YH, Han SH, Kim JP, Dyes Pigm., 2014, **101**, 186-195

[8] Lakshmi PP, Ojha DP, J. Mol. Liq., 2014, **197**, 106-113

[9] Yoon C, Choi Jh, Dyes Pigm., 2014, **101**, 344-350

[10] Kim JY, Choi J, Namgoong JW, Kim SH, Sakong C, Yuk SB, Choi S, Lee W, Kim JP, J. Incl. Phenom. Macrocycl. Chem., 2015, **82**, 203-212

[11] Kim SH, Namgoong JW, Yuk SB, Kim JY, Lee W, Yoon C, Kim

JP, J. Incl. Phenom. Macrocycl. Chem., 2015, **82**, 195-202

[12] Yuk SB, Lee W, Namgoong JW, Choi J, Chang JB, Kim SH, Kim JY, Kim JP, J. Incl. Phenom. Macrocycl. Chem., 2015, **82**, 187-194

[13] Langhals H, Ismael R, Yuruk O, Tetrahedron, 2000, **56**, 5435-5441

[14] Pu S, Fan C, Miao W, Liu G, Dyes Pigm., 2010, **84**, 25-35

[15] Chakraborty S, Debnath P, Dey D, Bhattacharjee D, Hussain SA, J. Photochem. Photobiol. A, 2014, **293**, 57-64

[16] Tsai HY, Chen KY, J. Lumin., 2014, **149**, 103-111

[17] Wei ZJ, Xu YW, Zhang L, Luo MM, Chin. Chem. Lett., 2014, **25**, 1367-1370

[18] Qiao Y, Chen J, Yi X, Duan W, Gao B, Wu Y, Tetrahedron Lett., 2015, **56**, 2749-2753

[19] Hutchings MG, Dyes Pigm., 1991, **17**, 227-240

[20] Durbeej B, Eriksson LA, Chem. Phys. Lett., 2003, **375**, 30-38

[21] Lynch DE, Byriel KA, Cryst. Eng., 1999, **2**, 225-239

[22] Reghu RR, Bisoyi HK, Grazulevicius JV, Anjukandi P, Gaidelis V, Jankauskas V, J. Mater. Chem., 2011, **21**, 7811

[23] Lee IL, Li SR, Chen KF, Ku PJ, Singh AS, Kuo HT, Eur. J. Org. Chem., 2012, **15**, 2906-2915

[24] Mazurak Z, Wanic A, Karolczak J, Czaja M, J. Lumin., 2015, **158**, 103-109

[25] Langhals H, Krotz O, Polborn K, Mayer P, Angew. Chem. Int. Ed. 2005, **44**, 2427-2428

[26] Biedermann F, Elmalem E, Ghosh I, Nau WM, Scherman OA, Angew. Chem. Int. Ed. 2012, **51**, 7739-7743

[27] Masuko M, Ohuchi S, Sode K, Ohtani H, Shimadzu A, Nucleic. Acids Res., 2000, **28**, e34-e

Chapter 4

Synthesis of High-soluble and Non-fluorescent Perylene Derivatives and Their Effect on the Contrast Ratio of LCD Color Filters

4.1 Introduction

Liquid crystal displays (LCDs) have captured a larger portion of the display market share than other types of displays [1-4]. Research into high-performance LCD devices is very important in order to exploit next-generation display industries such as large format and low power consumption screens [5, 6]. LCDs with traditional pigment-based color filters have some advantages in mass production and price competitiveness. However, pigment-based color filters have draw backs with respect to contrast ratio and brightness owing to their large particle size after heat treatment in the manufacturing process [7-9]. Therefore, research and development toward dye-based and pigment-dye hybrid

color filters has been in demand in order to develop displays that exhibit superior optical properties.

Perylene-based dyes have many merits for use as colorants in dye-based color filters due to their strong color strengths and thermal stabilities [10-13]. However, perylene-based dyes show powerful fluorescence likewise the other dyes that are commonly used for LCD color filters [14, 15]. Generally, in almost every report, bulky substituents were introduced to increase the solubilities of the dyes [5, 6, 16-18]. These bulky substituents usually make the fluorescence of the dyes stronger by broadening the intermolecular distance [19-23]. Therefore, the fluorescence of produced perylene derivatives that have bulky substituents would be naturally increased [24-28]. As mentioned in our previous study [3, 9], the fluorescence of the dyes can enhance the brightness of the color filters, meanwhile, that is a key factor of contrast ratio decrease by the unexpected increment of minimum brightness.

In this study, we designed and synthesized perylene-based dyes exhibiting sufficient solubilities in organic industrial solvents as well as significantly inhibited fluorescence. Dye-based color filters using the synthesized dyes were fabricated, and the influence of dye fluorescence

on optical performance of the prepared color filters was investigated. Dyes have to be soluble at least 4–5 wt% in organic industrial solvents to be used for LCD color filters [5, 6, 8, 9]. Therefore, we introduced bulky substituents at the terminal- and bay-positions of the perylene moiety. These substituents could enhance their solubilities by molecular distortion and intermolecular steric hindrance [29, 30]. However, the fluorescence of the synthesized dyes could be increased due to the bulky substituents which prevent dye aggregations and intermolecular interactions [21, 24-26]. Therefore, we designed the dyes to have substituents containing methoxy groups to reduce the fluorescence of the dyes [31]. Moreover, dyes with strong fluorescence and similar molecular structures to the fluorescence quenched dyes were also synthesized to clearly compare and analyze the effect of fluorescence on the optical properties. The dye-based color filters were fabricated in 1–3 wt% color content concentration to accurately investigate the relationship between the fluorescence of the dyes and the optical properties of the prepared color filters.

4.2 Experimental

4.2.1 Materials and instrumentation

Perylene-3,4,9,10-tetracarboxylic dianhydride, iodine, sulfuric acid, bromine, and acetic acid were purchased from Sigma-Aldrich; 2,6-diisopropylaniline, 2-methoxy-6-methylaniline, 4-methoxyphenol, and 4-ethylphenol were purchased from TCI; potassium carbonate anhydrous, methylene chloride, and other chemical solvents were purchased from Samchun Pure Chemical. All chemicals were used without any additional purification.

Elemental Analysis (EA) was completed on a CE Instruments EA1112 analyzer. ^{1}H and ^{13}C Nuclear Magnetic Resonance (NMR) spectra were recorded on a Bruker Avance 500 spectrometer running at 500 MHz using chloroform-d as a solvent with TMS as an internal standard. Matrix Assisted Laser Desorption/Ionization Time of Flight (MALDI-TOF) mass spectra were recorded on an Applied Biosystems Voyager-DESTR Biospectrometry Workstation using α-cyano-4-hydroxycinnamic acid (CHCA) as a matrix.

Absorption spectra were measured using a Perkin Elmer Lambda 25 UV/Vis spectrophotometer. Fluorescence spectra and quantum yield

were measured on a Perkin Elmer LS 55 and a PTI Quanta Master 40 fluorescence spectrometer, respectively. A Becker & Hickel SPC-150 equipped with a Time-Correlated Single Photon Counting (TCSPC) board was used to measure the time-resolved fluorescence decay with a time channel of 17.1 ps. Contrast ratio and brightness of color filters were measured by CT-1 of Tsubosaka and MC-3700: 28C of Otsuka Electronics.

4.2.2 Syntheses of the dyes

All synthetic procedures were carried out by following our previous reports [8, 9]. We had reported previously that bay-position substitution is possible at much lower temperature and in a shorter reaction time than the widely known method.

4.2.2.1 1,7-Dibromoperylene-3,4,9,10-tetracarboxydiimide : Bromination

Perylene-3,4,9,10-tetracarboxylic dianhydride (32.00 g, 81.40 mmol),

iodine (0.78 g, 3.04 mmol) and sulfuric acid (98 %, 450 mL) were mixed and stirred for 2 h at room temperature. The temperature of the mixture was raised to 80 ℃ and bromine (8.33 mL, 162.80 mmol) was added dropwise over 1 h. The resulting mixture allowed to react for 16 h, upon which time, it was cooled to room temperature and the remaining bromine gas was displaced by nitrogen gas. The mixture was slowly poured into 3 L of ice water and the crude precipitate formed was collected by suction filtration followed by washing several times with distilled water. The crude product was dried at 80 ℃ under reduced pressure and used in the next step without further purification. The crude product containing both mono- and di-bromoperylene derivatives was separated by column chromatography in next step, after introducing bulky substituents in the terminal-position to increase their solubilities.

4.2.2.2 N,N'-bis(R_1)-1,7-dibromoperylene-3,4,9,10-tetracarboxydiimide : Terminal-position substitution

Crude 1,7-dibromoperylene-3,4,9,10-tetracarboxydiimide (8.00 g, 14.55 mmol), R_1-NH_2 (45.00 mmol), acetic acid (4.60 mL) and N-

methyl-2-pyrrolidone (NMP; 100 mL) were mixed and heated to 120 °C under nitrogen atmosphere for 96 h. Water was added to the mixture and the resulting precipitate was collected by suction filtration. The crude product was washed with water and dried under reduced pressure. The crude product was purified by column chromatography in silica gel using CH_2Cl_2 as an eluent. Three bands were collected. The first band contained a small amount of tribrominated diimide, the second band contained the dibrominated diimide, and the third contained the monobrominated diimide. Detailed structural analysis was conducted after the next step. To obtain the **PI-series**, 2,6-diisopropylaniline was used as R_1-NH_2 and to obtain **PM-series**, 2-methoxy-6-methylaniline was used.

4.2.2.3 N,N'-Bis(R_1)-1,7-bis(R_2)-perylene-3,4,9,10-tetracarboxydiimide : Bay-position substitution

N,N'-bis(R_1)-1,7-dibromoperylene-3,4,9,10-tetracarboxydiimide (0.58 mmol) was mixed with anhydrous potassium carbonate (0.35 g, 2.54 mmol), R_2-OH (1.60 mmol) and NMP (60 mL). The mixture was

heated at 40 ℃ under nitrogen and was stirred for 1.5 h. The mixture was cooled to room temperature, and then poured into HCl (400 mL, 5 % aqueous). The precipitate was collected by suction filtration, washed with water and dried under vacuum at 80 ℃. The crude product was purified by column chromatography in silica gel using CH_2Cl_2 as an eluent to obtain the products as red solids.

4.2.2.4 Structural analysis

PI-4EP, Yield 73.2 %; ^{1}H NMR ($CDCl_3$, ppm): 9.66 (d,2H), 8.69 (d,2H), 8.42 (d,4H), 7.46 (m,4H), 7.34 (m,4H), 2.71 (septet,4H), 1.55 (s,2H), 1.25 (d,24H), 1.12 (s,12H); ^{13}C NMR (126 MHz, $CDCl_3$): δ= 24.20, 24.22, 28.44, 29.37, 31.16, 76.97, 77.22, 77.48, 119.36, 119.67, 122.49, 123.52, 124.22, 124.70, 124.89, 126.05, 128.13, 129.19, 129.82, 129.91, 130.09, 130.65, 130.97, 132.01, 133.98, 141.34, 145.80, 153.14, 155.64, 162.98, 163.13, 163.69; MALDI-TOF MS: m/z 953.4 (100 %, [M+2K]+); EA Found (%): C, 80.36; H, 6.30; N, 2.98; O, 10.33 Calc. (%) for $C_{64}H_{58}N_2O_5$: C, 80.82; H, 6.15; N, 2.95; O, 10.09.

PI-4ME, Yield 66.0 %; ^{1}H NMR ($CDCl_3$, ppm): 9.68 (d,2H), 8.70

(d,2H), 8.38 (m,4H), 7.46 (m,4H), 7.31 (m,4H), 2.72 (septet,4H), 2.17 (m,2H), 1.53 (m,20H), 1.16 (m,12H); ^{13}C NMR (126 MHz, $CDCl_3$): δ= 24.22, 29.37, 55.97, 76.97, 77.23, 77.48, 115.84, 121.02, 121.16, 122.43, 123.99, 124.14, 124.18, 124.22, 125.84, 129.21, 129.80, 129.92, 130.66, 130.66, 130.85, 134.00, 145.80, 148.80, 149.53, 156.26, 157.26, 163.14, 163.70; MALDI-TOF MS: m/z 957.3 (100 %, [M+2K]+); EA Found (%): C, 77.76; H, 5.83; N, 2.92; O, 13.44 Calc. (%) for $C_{62}H_{54}N_2O_8$: C, 77.97; H, 5.70; N, 2.93; O, 13.40.

PM-4EP, Yield 70.0 %; ^{1}H NMR ($CDCl_3$, ppm): 9.67 (d,2H), 8.74 (d,2H), 8.35 (m,4H), 7.55 (m,4H), 3.71 (m,4H), 2.13 (s,2H), 1.26 (d,16H), 0.88 (s,8H); ^{13}C NMR (126 MHz, $CDCl_3$): δ= 14.35, 15.87, 17.79, 19.39, 19.77, 23.20, 26.97, 28.46, 28.80, 29.46, 31.15, 33.30, 36.68, 36.78, 56.09, 66.11, 66.42, 77.48, 109.30, 109.38, 119.86, 119.98, 122.67, 122.83, 123.18, 124.10, 124.22, 125.95, 128.02, 129.04, 129.10, 129.94, 130.10, 130.67, 131.12, 131.76, 133.98, 137.55, 141.51, 141.64, 152.85, 152.98, 155.01, 155.88, 156.95, 162.48, 162.69, 163.04; MALDI-TOF MS: m/z 873.3 (100 %, [M+2K]+); EA Found (%): C, 76.83; H, 5.04; N, 3.00; O, 15.00 Calc. (%) for $C_{56}H_{42}N_2O_8$: C, 77.23; H, 4.86; N, 3.22; O, 14.70.

PM-4ME, Yield 74.9 %; ^{1}H NMR ($CDCl_3$, ppm): 9.68 (d,2H), 8.69 (d,2H), 8.36 (m,4H), 8.26 (s,2H), 3.75 (m,4H), 2.18 (s,2H), 1.55 (d,14H), 1.25 (s,8H); ^{13}C NMR (126 MHz, $CDCl_3$): δ= 17.79, 29.92, 55.97, 56.09, 77.22, 77.48, 109.37, 109.47, 115.87, 121.41, 121.52, 122.04, 122.61, 122.82, 123.18, 123.45, 123.77, 124.16, 125.78, 128.00, 129.13, 129.89, 129.94, 130.59, 131.75, 134.01, 137.5,, 148.39, 155.02, 156.45, 157.33, 157.53, 162.72, 163.06; MALDI-TOF MS: m/z 877.2 (100 %, [M+2K]+); EA Found (%): C, 73.84; H, 4.56; N, 2.98; O, 18.55 Calc. (%) for $C_{54}H_{39}N_2O_{10}$: C, 74.13; H, 4.38; N, 3.20; O, 18.29.

4.2.3 Geometry optimization of the dyes

Density functional theory (DFT) calculations were carried out with the Gaussian 09 package. We used the 6-311++G(d,p) Pople basis set for all elements and the conventional B3LYP exchange-correlation function. The intermolecular interactions were analyzed by examining the core twist angles and the size of substituents. Dihedral angles of perylene main body were calculated by measuring the distortion angle of benzene ring in the center of perylene main body. Calculated lengths of bay-

substituents were indicated by measuring the lineal distance from oxygen atom of ether linkage to farthest atom in the substituents. And, calculated lengths of terminal-substituents were indicated by measuring the longest lineal distance in the substituents.

4.2.4 Preparation of dye-based inks and color filters

The red inks for the dye-based color filters were composed of propylene glycol methyl ether acetate (PGMEA; 0.1 g), acrylic binder (0.8 g) and synthesized dye (1, 2 or 3 wt% of the acrylic binder). The prepared dye-based inks were coated on a transparent glass substrate using a MIDAS Systems SPIN-1200D spin coater. The rotation speed was initially set at 100 rpm for 10 s, and then increased to 500 rpm for 20 s. The dye-coated color filters were dried at 80 ℃ for 20 min, pre-baked at 150 ℃ for 10 min and post-baked at 200 ℃ for 1 h.

4.3 Results and discussion

4.3.1 Design concept of the synthesized dyes

Synthetic routes and molecular structures of the synthesized dyes are shown in **Scheme 4.1** and **Fig. 4.1**. Generally, perylene-based dyes have strong color strengths and thermal stabilities due to their high degree of planarity [10, 11, 15, 32]. However, they usually show inferior solubility in organic industrial solvents such as propylene glycol methyl ether acetate (PGMEA), a commonly used organic solvent in the LCD manufacturing process [5, 8, 30]. Bulky substituents containing a benzene ring were introduced in the terminal- and bay-positions of the perylene main body in order to reduce planarity and intermolecular interactions, as well as to increase the steric hindrance of the synthesized dyes [33-35]. The solubilities of the synthesized dyes in some organic solvents are listed in **Table 4.1**. All the dyes show sufficient solubilities as colorants for LCD color filters due to the contribution of the introduced bulky substituents.

All of the dyes were designed to have similar conjugation length. Therefore, it can be regarded that they would exhibit similar spectral properties [9, 36-40]. Hence, the effect of the spectral properties of the dyes on the optical performance of fabricated color filters would be minimized. The size and structure of the introduced substituents are also

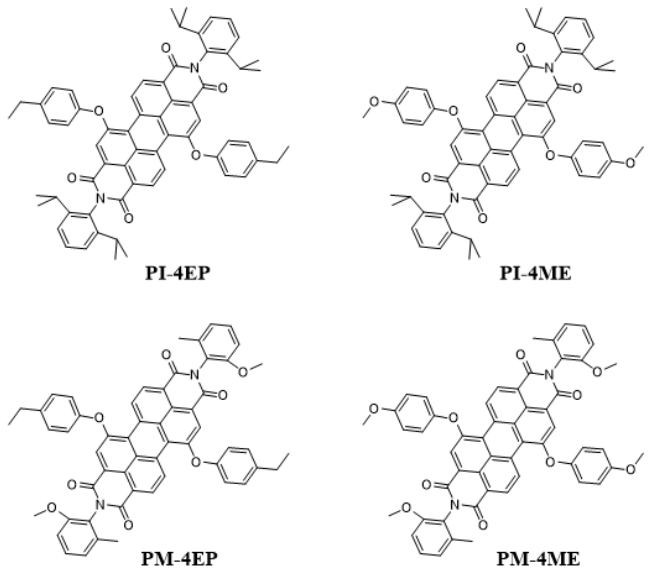

Fig. 4.1 Structure of the synthesized dyes

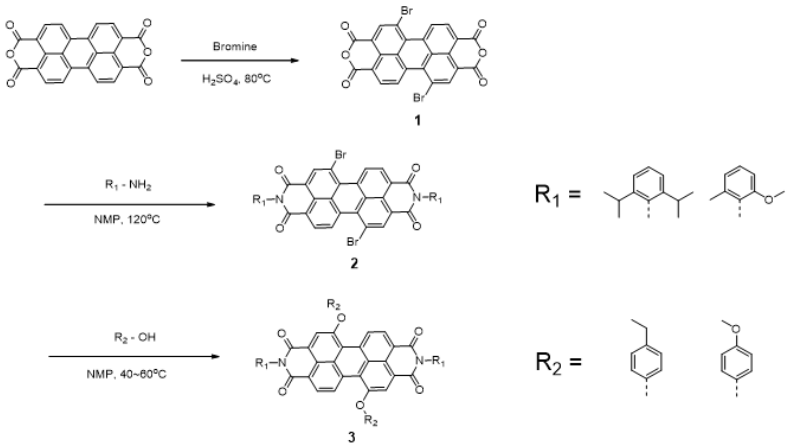

Scheme 4.1 Synthetic routes of the designed dyes

Table 4.1 Solubility of the synthesized dyes at 20 ℃ (wt%)

Dye	PI-4EP	PI-4ME	PM-4EP	PM-4ME
CH_2Cl_2	5.8	5.9	5.2	5.1
$CHCl_3$	6.0	6.0	5.7	5.8
PGMEA	5.0	5.1	4.7	4.8

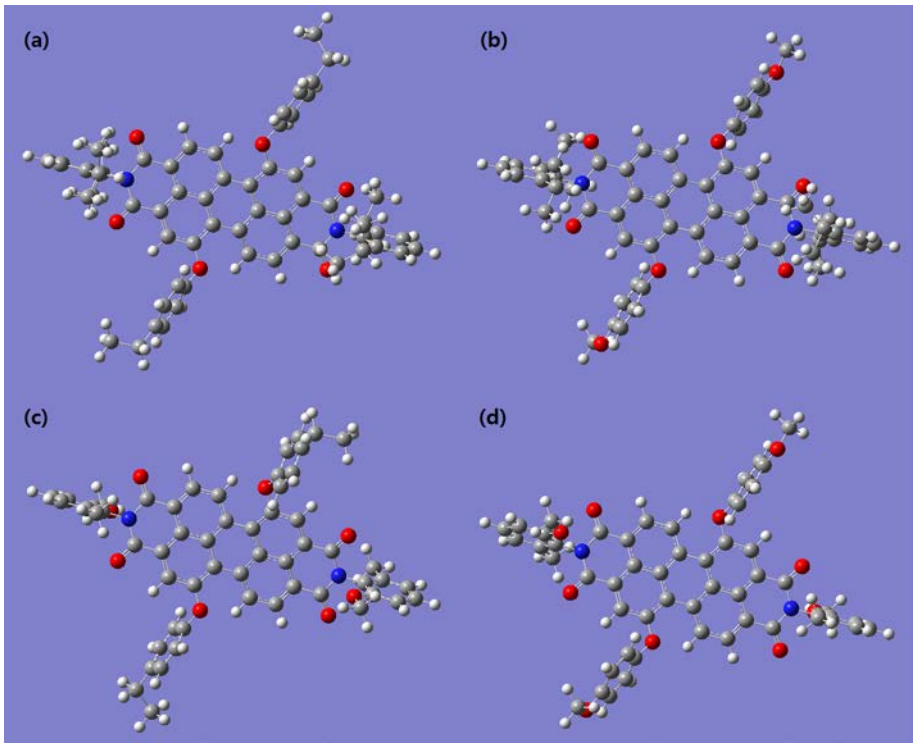

Fig. 4.2 Geometry-optimized structures of the synthesized dyes. (a) **PI-4EP**, (b) **PI-4ME**, (c) **PM-4EP**, and (d) **PM-4ME**

Table 4.2 Dihedral angels of the perylene main body and calculated lengths of the substituents [a]

Dye		PI-4EP	PI-4ME	PM-4EP	PM-4ME
Dihedral angle of the perylene main body (°)		13.13923	13.55246	13.18118	13.51070
Calculated lengths of substituents (Å)	**Bay-substituent**	7.50721	7.39420	7.50609	7.39358
	Terminal-substituent	8.91795	8.85661	7.76817	7.76834

[a] dihedral angle and calculated lengths are not symmetric, average values are listed.

similar, thus, the geometrical structures of the synthesized dyes would be naturally analogous to each other. Geometry-optimized structures of the synthesized dyes are shown in **Fig. 4.2** and dihedral angle of the perylene main body and calculated lengths of the substituents are listed in **Table 4.2**. As shown in **Table 4.2**, the differences in the geometrical structures of the synthesized dyes were very small to relate the influences on the intermolecular interactions. Especially, all synthesized dyes show almost identical the dihedral angles that mostly affect the planarities of them [8, 41, 42]. Therefore, the differences in optical properties of the color filters resulting from dye aggregation and intermolecular interactions would also be minimized.

Introduction of bulky substituents is the most popular method to enhance the fluorescence of dyes by inhibiting both aggregation quenching and energy transfer such as Förster resonance energy transfer (FRET) [21, 26, 43]. Therefore, in addition to enhancing the solubilities with structure distortion and steric hindrance, the fluorescence of the dyes would be naturally increased when bulky substituents were introduced to the perylene main body [14]. However, as mentioned in our previous study [9], dyes for LCD color filters have to be highly

soluble in organic solvents and show minimized fluorescence. Accordingly, we designed dyes containing methoxy groups in the terminal-, bay-, or both positions for developing fluorescence quenched dyes. Generally, methoxy groups are used to cause bathochromic shifts by electron donating effects or to sterically broaden the intermolecular distance [44-47]. And, in some preceding reports [45, 46], it has been reported that the introduction of a methoxy group leads to decreased fluorescence in certain dyes. A methoxy group in the para-position of the bay-substituents is highly efficient at decreasing dye fluorescence [48]. Therefore, we designed dyes having a methoxy group at this position. As a result, we successfully designed dyes that highly soluble in organic solvents, exhibit very weak fluorescence, and can be easily synthesized due to their simple molecular structures. Dyes showing strong fluorescence were designed to contain alkyl groups that have a similar geometrical size as methoxy groups in order to minimize the differences in molecular behavior among them.

4.3.2 Spectral and fluorescence properties of synthesized dyes

The absorption spectra of the synthesized dyes in chloroform are shown in **Fig. 4.3**. As mentioned before, the conjugation systems of all synthesized dyes are similar to each other. Therefore, the synthesized dyes exhibit similar spectral properties as shown in **Fig. 4.3** and **Table 4.3** [37, 39, 49]. Namely, the effect of the spectral properties of synthesized dyes on the optical properties of the fabricated color filters would be minimized. Although, the dyes with methoxy groups in bay-positions show a small bathochromic shift of about 4 nm due to the electron donating effect of the methoxy groups [45, 46, 50]. But, this shift would not seriously influence the optical properties of the manufactured color filters because the color filters were fabricated with low color content concentration.

The fluorescence properties of the synthesized dyes are listed in **Fig. 4.4** and **Table 4.3**. All of the measured fluorescence properties except quantum yield were measured at an excitation wavelength corresponding to the wavelength of maximum absorption. The quantum yield was measured with an excitation wavelength of 480 nm [51, 52]. Chloroform was used as a solvent for all measurements in **Table 4.3**.

In our previous study [9], dyes with various geometrical structures

would severely affect their molecular behavior and aggregation resulting in a variation of fluorescence properties. It is well-known that the two main factors affecting fluorescence quenching of organic dyes are static quenching derived from H-aggregation and energy transfer which occurs via intermolecular interactions [20, 22, 53-55]. However, as shown in **Table 4.2**, the synthesized dyes in this study have similar geometrical molecular structures. Therefore, the intermolecular interactions of the dyes would not be different from each other. In other words, the main factor affecting the fluorescence properties of the synthesized dyes is not H-aggregation or energy transfer. This result also could be verified from the presented data. For example, the solubilities in **Table 4.1** and the fluorescence intensities of the synthesized dyes in **Table 4.3** do not show a correlation. If the fluorescence of the synthesized dyes resulted mainly from intermolecular behavior, the solubility and the fluorescence intensity would show a certain trend. Eventually, it could be concluded that the dyes synthesized in this study exhibit different fluorescence properties which are mainly attributed to the introduced methoxy groups.

The methoxy groups introduced in the terminal-positions have no effect on the fluorescence quenching. On the contrary, methoxy groups

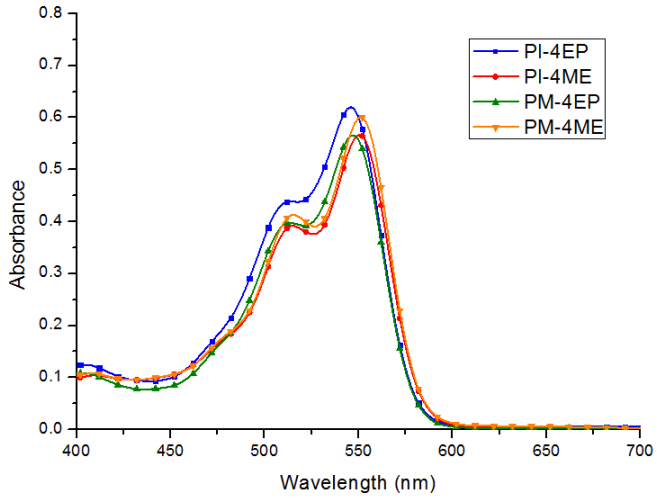

Fig. 4.3 Absorption spectra of the synthesized dyes in chloroform (10^{-5} mol/L)

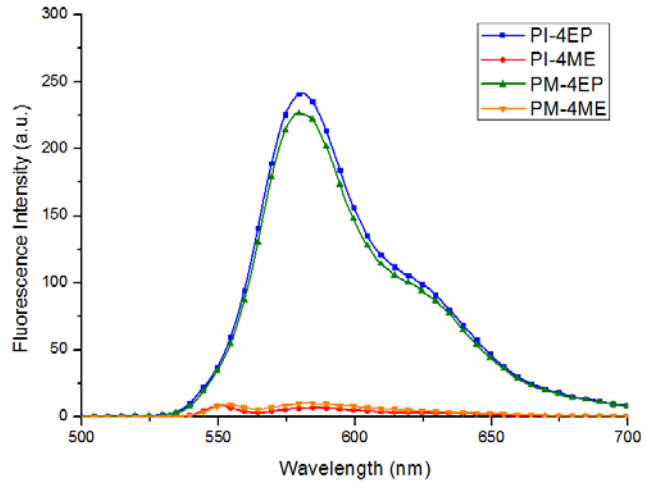

Fig. 4.4 Fluorescence of the synthesized dyes in chloroform (10^{-8} mol/L)

Table 4.3 Spectral and fluorescence properties of the synthesized dyes

Dye	PI-4EP	PI-4ME	PM-4EP	PM-4ME
λ_{abs} [a]	546	550	548	552
ε_{abs} [b]	62,050	56,650	56,510	60,000
λ_{em} [c]	581	586	580	582
Max. Emission Intensity	241.82	7.07	226.75	10.20
Σ(emission) [d]	29,305.99	856.53	27,623.99	1257.39
Δss [e]	35	36	32	30
Q_y [f]	0.966	0.054	0.948	0.079

[a] λ_{abs} : maximum absorption wavelength (nm).

[b] ε_{abs} : molar extinction coefficient (L/mol·cm).

[c] λ_{em} : maximum emission wavelength (nm).

[d] Σ(emission) : integral of 'Fluorescence Intensity' in visible-ray region, total emission intensity.

[e] Δss : stokes shift.

[f] Q_y : quantum yield (10^{-5} mol/L in chloroform, excited at 480 nm).

in the bay-positions severely diminish the fluorescence. It is widely known that substituents at the bay-positions have a strong conjugation link with the perylene main body [29, 33, 34]. Contrastively, the terminal-substituents have no or very slight conjugation linkage [5, 8]. Therefore, bay-substituents have a strong influence on the π-conjugation system and the electrochemical properties of the dyes. This phenomenon could be verified from the bathochromic shift of the spectral properties of the synthesized dyes with methoxy groups in the bay-positions.

Dyes with bay-substituents containing ethyl groups exhibited more powerful fluorescence in the visible region than dyes with bay-substituents containing methoxy groups. The difference in the total emission intensity is 22–34-fold and the difference in the quantum yield is 12–18-fold between dyes with bay-substituents containing methoxy groups and dyes with ethyl groups. Namely, introduction of methoxy groups in the para-position of the bay-substituents is a powerful method to quench dye fluorescence that would rarely affect molecular behavior and aggregation. To sum up, with just a simple modification, we successfully designed and synthesized fluorescence reduced dyes exhibiting sufficient solubilities in organic solvents. These novel

perylene-based dyes have more desirable properties than those previously used as colorants in LCD color filters.

4.3.3 Time-resolved fluorescence properties of synthesized dyes

The results of the time-resolved fluorescence decay of the synthesized dyes measured by a time-correlated single photon counting (TCSPC) system are illustrated in **Fig. 4.5** and **Table 4.4** [56, 57]. The represented fluorescence decay data were measured with an excitation wavelength of 520 nm and fitted using a bi-exponential function [58, 59].

The dyes with methoxy groups in the bay-positions exhibited shorter fluorescence lifetimes than those with ethyl groups. In other words, the methoxy group in the bay-position affects both fluorescence intensity and lifetime. Therefore, the total emission quantity from the dyes with methoxy groups in the bay-substituents would be much smaller than that of the dyes with ethyl groups. This is the same result as the tendencies of the total emission intensity in the visible region and the quantum yield data that were presented ahead.

Energy injected from the excitation light is released in radiative or

non-radiative form [60-62]. The radiative decay rate constant and the non-radiative decay rate constant can be simply calculated from the fitted lifetime (τ) and the quantum yield (Q_y) with the following equations [59, 63-66]. The results are listed in **Table 4.5**.

$$K_r = \frac{1}{\tau_r} = \frac{Q_y}{\tau} \quad \text{--- (1)}$$

$$K_{nr} = \frac{1}{\tau_{nr}} = \frac{1}{\tau} - \frac{1}{\tau_r} = \frac{1}{\tau}\left(1 - Q_y\right) \quad \text{--- (2)}$$

All synthesized dyes show similar radiative decay constants (K_r), however, their non-radiative decay constant (K_{nr}) are tremendously different depending on the substituents at the bay-position. The dyes with methoxy groups in the bay-positions show extremely higher value of non-radiative decay constant than that of the dyes with ethyl groups. It could be regarded that the dyes with bay-substituents containing methoxy groups exhibit intensely stronger non-radiative energy release than the radiative form [60, 61, 67], contrary to the dyes containing ethyl groups in the bay-positions. Due to this reason, dyes with methoxy groups in bay-positions seem to exhibit quenched fluorescence. The trend is reversed in the case of the dyes with ethyl groups in bay-positions, although all of the synthesized dyes have similar geometrical molecular structures and conjugation systems.

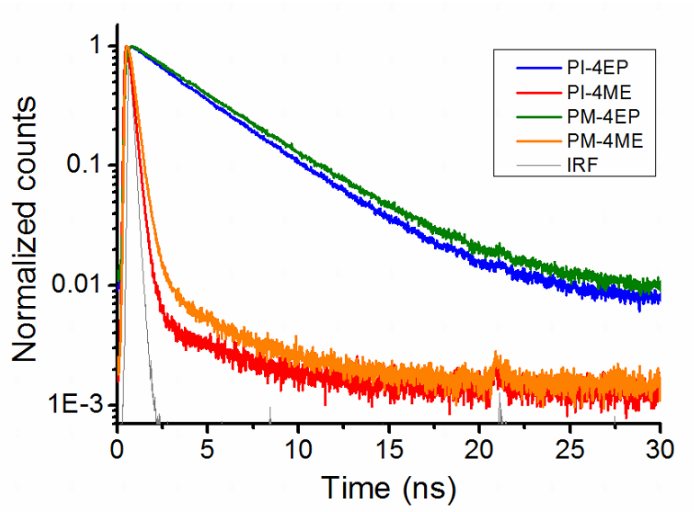

Fig. 4.5 Time-correlated single-photon-counting (TCSPC) results of the synthesized dyes and instrumental response function of the TCSPC setup (10^{-5} mol/L in chloroform)

Table 4.4 Fluorescence decay time (τ) of the synthesized dyes (ns)

Dye	PI-4EP	PI-4ME	PM-4EP	PM-4ME
Decay	3.95	0.23	4.25	0.35

Table 4.5 Calculated radiative decay rate constant (K_r) and non-radiative decay rate constant (K_{nr}) (ns^{-1})

Dye	PI-4EP	PI-4ME	PM-4EP	PM-4ME
K_r	0.244557	0.234783	0.223059	0.225714
K_{nr}	0.008608	4.113043	0.012235	2.631429

4.3.4 Optical properties of fabricated dye-based color filters

Color filters are located between two polarizing films in the LCD devices. Light radiated from a backlight unit is polarized by the first polarizer when entering into the color filters. Most light that passes through the color filters maintains its polarized state, however, non-polarized light can be generated by scattering or emission. This non-polarized light can passes through the second polarizer even in full-black state, and increases the minimum brightness. As scattering from the traditional pigment-based color filters gives rise to the unexpected increment of minimum brightness, fluorescence emitted from the dye-based color filters also causes the same effect in spite of the smaller particle size compared to pigment-based ones. We reported this phenomenon in our previous study through experimental investigations [9].

Dye-based color filters were fabricated using the synthesized dyes that were added in the proportion of 1, 2 or 3 wt% to the acrylate binder. The measured fluorescence spectrometer results are shown in **Fig. 4.6** (a). The measurements were obtained with an excitation wavelength

corresponding to the wavelength of maximum absorption. Both the incident light that passed through the color filters and the emission from the color filters can be observed in all of the fluorescence spectra. The fluorescence spectrum of the color filter fabricated with **PI-4EP** with 3 wt% dye content is separately illustrated in **Fig. 4.6** (b). In the results of the color filters fabricated with **PM-4EP**, the intensity of the incident light exceeded the detectable range of our instrument. Therefore, the intensity of the incident light is saturated in the maximum detectable value of the instrument in every dye content concentration. The absolute values of the spectra are not precise because the measurements of the fluorescence spectrometer of the fabricated dye-based color filters were operated without consideration of the emission toward every spherical direction. However, it can be argued that the observed trend of incident light and emission varying according to dye content concentration is definitely a meaningful result.

As shown in the spectra, the intensity of the incident light is decreasing with increasing dye concentration. Contrastively, the intensity of the emission from the color filters is increasing according to the dye concentration. The maximum emission intensities from the

prepared color filters are plotted in **Fig. 4.6** (c). As shown in the figures, the emission intensity increase of the color filters depends on the added dye concentration with a certain linear trend. These phenomena result from the fact that the color filters were fabricated with a low color content concentration [9]. In accordance with the dye concentration increase, the increase of the aggregation fluorescence quenching would be smaller than the increase of the emission from the added dyes in the concentration range of our investigation [68, 69].

The color filters fabricated with dyes containing ethyl groups in bay-positions exhibited strong fluorescence within the visible region in the film state. As mentioned in our previous study [9], the fluorescence properties of the prepared color filters show a similar tendency to the properties of the dyes in the solution state. Therefore, the fluorescence of the added dyes would significantly affect the optical properties of the color filters.

The optical properties of the fabricated color filters are listed in **Table 4.6**. All represented data were measured 3 times and the average value is provided. The brightness of the color filters decreased with the increase in dye content concentration. This results from the fact that the

transmittance of the color filters would decrease with the amount of additionally added dyes. Namely, the effect of the fluorescence from the added dyes on the brightness increase is much weaker than the effect of the transmittance reducing that derives the brightness decrease. Therefore, it would be hard to expect a remarkable brightness increase from the fluorescence of the dyes added in dye-based color filters.

Contrast ratio is the proportion of maximum brightness to minimum brightness [5, 8, 70-72]. The maximum and minimum brightness values are represented after normalization to a blank brightness of 30,000. The minimum brightness of the color filters was increased according to the fluorescence of the added dyes. Both the maximum and minimum brightness of the color filters with highly fluorescent dyes generally show higher values than those with less fluorescent dyes. However, the influence of the fluorescence seems more effective on the minimum brightness. Therefore, the color filters with highly fluorescent dyes exhibited a lower contrast ratio than those with fluorescence quenched dyes.

It can be concluded that the fluorescence properties of the fabricated color filters show the same tendency to those of the dyes in the solution

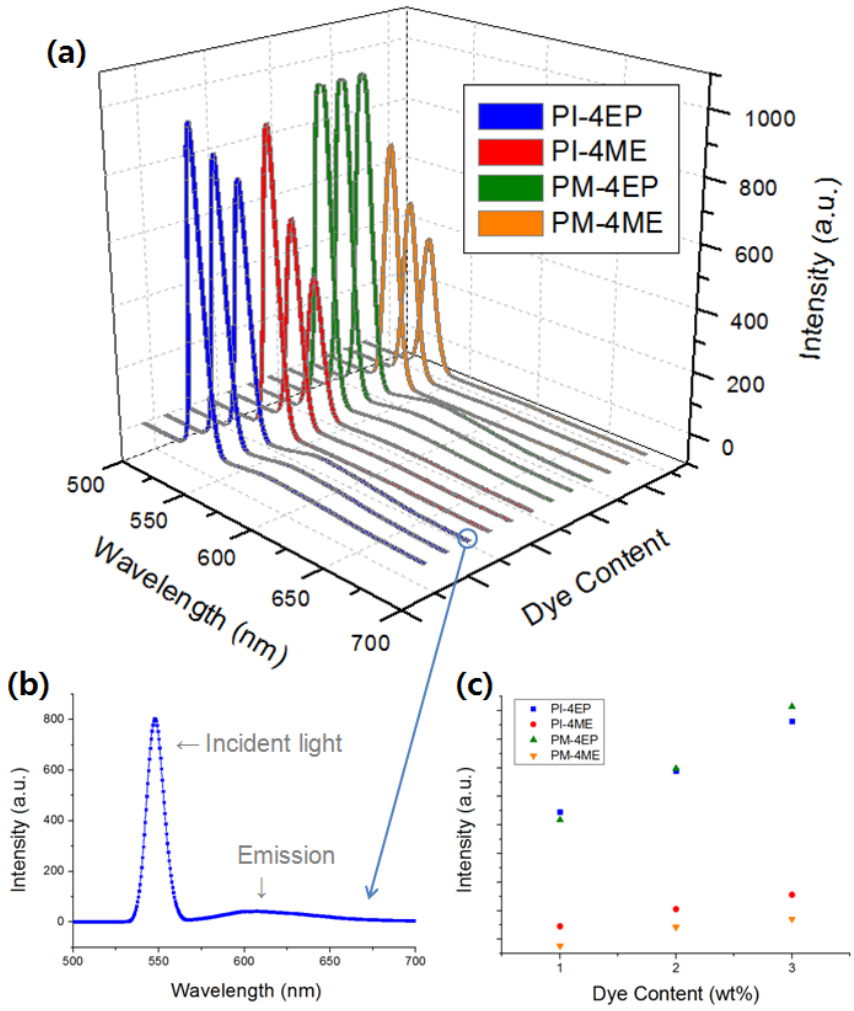

Fig. 4.6 (a) Fluorescence spectrometer results of the fabricated dye-based color filters (each dye contents were 1, 2 and 3 wt% increasing toward right-side). (b) Detailed fluorescence spectrometer results of the color filter fabricated with **PI-4EP** in 3 wt% dye content. (c) Plot of maximum emission intensity of the fabricated color filters.

Table 4.6 Optical properties of the fabricated dye-based color filters

Dye	Dye Content	Brightness			Contrast Ratio - Blank 30,000		
		Rx	Ry	Value	Max. Brightness	Min. Brightness	Value
PI-4EP	1	0.3237	0.2977	62.1513	1,765.1667	20.8607	84.62
	2	0.3244	0.2953	59.9033	1,729.9333	22.2023	77.92
	3	0.3251	0.2886	52.3643	1,617.0000	27.6647	58.45
PI-4ME	1	0.3228	0.3023	70.8803	1,839.9000	3.5033	525.19
	2	0.3334	0.2804	56.4173	1,509.5667	4.2287	356.98
	3	0.3310	0.2765	51.4653	1,428.0000	6.6037	216.24
PM-4EP	1	0.3157	0.3213	82.4580	2,184.0667	7.3437	297.41
	2	0.3168	0.3187	80.0553	2,136.9667	10.1030	211.52
	3	0.3185	0.3157	73.0377	2,032.0000	17.5680	115.66
PM-4ME	1	0.3310	0.2918	63.1287	1,642.8000	3.5767	459.31
	2	0.3382	0.2805	55.9787	1,456.0000	3.3073	440.23
	3	0.3483	0.2674	46.2667	1,228.4333	6.4457	190.58

state. Additionally, the fluorescence of the added dyes has a limitative effect on the maximum brightness increase of the fabricated color filters. However, the fluorescence mainly influences the minimum brightness increase and causes the contrast ratio decrease. In conclusion, color filters prepared with synthesized dyes containing methoxy groups in the bay-substituents have remarkable effects in minimizing the increment of minimum brightness and prohibiting the contrast ratio decrease.

4.4 Conclusions

The most popular method to enhance the solubilities of dyes is the introduction of bulky substituents. However, bulky substituents usually enhance the fluorescence of dyes by preventing both static fluorescence quenching with H-aggregation and energy transfer via intermolecular interaction. Therefore, it is difficult to devise dyes exhibiting both sufficient solubilities in organic industrial solvents and significantly quenched fluorescence.

Dyes have to be sufficiently soluble in organic solvents and show minimized fluorescence to be used as a colorant in LCD color filters. In

this study, we successfully designed and synthesized dyes meeting this purpose by introducing substituents containing methoxy groups. Moreover, we also synthesized highly fluorescent dyes which have similar molecular structures to the fluorescence quenched dyes. Finally, we fabricated dye-based color filters using the synthesized dyes and analyzed the optical performances of the color filters.

In conclusion, the methoxy group in the para-position of the bay-substituents has an enormous effect on the fluorescence quenching without the conspicuous influences on molecular behavior or dye aggregation. On the contrary, there is no fluorescence quenching effect by the methoxy group in the terminal-substituents. This difference seems to be caused by the π-conjugation system of the substituents. The color filters fabricated with the synthesized dyes containing methoxy groups in the bay-positions exhibited lower minimum brightness than those with ethyl groups. Therefore, they show superior performance in preventing contrast ratio decrease caused by fluorescence of added dyes.

4.5 References

[1] Kim YD, Kim JP, Kwon OS, Cho IH, Dyes Pigm., 2009, **81**, 45-52

[2] Kim YD, Cho JH, Park CR, Choi JH, Yoon C, Kim JP, Dyes Pigm., 2011, **89**, 1-8

[3] Choi J, Lee W, Sakong C, Yuk SB, Park JS, Kim JP, Dyes Pigm., 2012, **94**, 34-39

[4] Kim SH, Namgoong JW, Yuk SB, Kim JY, Lee W, Yoon C, Kim JP, J. Incl. Phenom. Macrocycl. Chem., 2015, **82**, 195-202

[5] Choi J, Sakong C, Choi JH, Yoon C, Kim JP, Dyes Pigm., 2011, **90**, 82-88

[6] Sakong C, Kim YD, Choi JH, Yoon C, Kim JP, Dyes Pigm., 2011, **88**, 166-173

[7] Choi J, Lee W, Namgoong JW, Kim TM, Kim JP, Dyes Pigm., 2013, **99**, 357-365

[8] Kim JY, Choi J, Namgoong JW, Kim SH, Sakong C, Yuk SB, Choi S, Lee W, Kim JP, J. Incl. Phenom. Macrocycl. Chem., 2015, **82**, 203-212

[9] Kim JY, Sakong C, Choi S, Jang H, Kim SH, Chang KS, Han MS, Lee JS, Kim JP, Dyes Pigm., 2016, **131**, 293-300

[10] Nagao Y, Prog. Org. Coat., 1997, **31**, 43-49

[11] Huang C, Barlow S, Marder SR, J. Org. Chem., 2011, **76**, 2386-2407

[12] Zhang X, Pang S, Zhang Z, Ding X, Zhang S, He S, Tetrahedron Lett., 2012, **53**, 1094-1097

[13] Wei ZJ, Xu YW, Zhang L, Luo MM, Chin. Chem. Lett., 2014, **25**, 1367-1370

[14] Kraub S, Lysetska M, Wurthner F, Lett. Org. Chem., 2005, **2**, 349-353

[15] Tsai HY, Chen KY, J. Lumin., 2014, **149**, 103-111

[16] Mayorova JY, Troshin PA, Peregudov AS, Peregudova SM, Kaplunova MG, Lyubovskaya RN, Mendeleev Commun., 2007, **17**, 156-158

[17] Turkmen G, Erten-Ela S, Icli S, Dyes Pigm., 2009, **83**, 297-303

[18] Choi J, Kim SH, Lee W, Chang JB, Namgoong JW, Kim YH, Han SH, Kim JP, Dyes Pigm., 2014, **101**, 186-195

[19] Karolin J, Johansson LBA, Ring U, Langhals H, 1996, **52**, 747-753

[20] Wurthner F, Thalacker C, Diele S, Tschierske C, Chem. Eur. J., 2001, **7**, 2245-2253

[21] Chakraborty S, Debnath P, Dey D, Bhattacharjee D, Hussain SA, J.

Photochem. Photobiol., A, 2014, **293**, 57-64

[22] Moon H, Xuan QP, Kim D, Kim Y, Park JW, Lee CH, Cryst. Growth Des., 2014, **14**, 6613-6619

[23] Holmes AS, Birch DJS, Salthammer T, J. Fluoresc., 1993, **3**, 77-84

[24] Langhals H, Ismael R, Yuruk O, 2000, **56**, 5435-5441

[25] Langhals H, Krotz O, Polborn K, Mayer P, Angew. Chem. Int. Ed., 2005, **44**, 2427-2428

[26] Gao B, Li H, Liu H, Zhang L, Bai Q, Ba X, Chem. Commun., 2011, **47**, 3894-3896

[27] Reghu RR, Bisoyi HK, Grazulevicius JV, Anjukandi P, Gaidelis V, Jankauskas V, J. Mater. Chem., 2011, **21**, 7811

[28] Shin EJ, Kim D, J. Photochem. Photobiol., A, 2002, **152**, 25-31

[29] Dincalp H, Askar Z, Zafer C, Icli S, Dyes Pigm., 2011, **91**, 182-191

[30] Yuk SB, Lee W, Namgoong JW, Choi J, Chang JB, Kim SH, Kim JY, Kim JP, J. Incl. Phenom. Macrocycl. Chem., 2015, **82**, 187-194

[31] Zhang X, Wu Y, Li J, Li F, Li M, Dyes Pigm., 2008, **76**, 810-816

[32] Biedermann F, Elmalem E, Ghosh I, Nau WM, Scherman OA, Angew. Chem. Int. Ed., 2012, **51**, 7739-7743

[33] Osswald P, Würthner F, Chem. Eur. J., 2007, **13**, 7395-7409

[34] Dincalp H, Kizilok S, Icli S, Dyes Pigm., 2010, **86**, 32-41

[35] Farooqi MJ, Penick MA, Burch J, Negrete GR, Brancaleon L, Spectrochim. Acta, Part A, 2016, **153**, 124-131

[36] Hutchings MG, Dyes Pigm., 1991, **17**, 227-240

[37] Durbeej B, Eriksson LA, Chem. Phys. Lett., 2003, **375**, 30-38

[38] Chen J, Shi MM, Hu XL, Wang M, Chen HZ, Polymer, 2010, **51**, 2897-2902

[39] Lakshmi Praveen P, Ojha DP, J. Mol. Liq., 2014, **197**, 106-113

[40] Lee IL, Li SR, Chen KF, Ku PJ, Singh AS, Kuo HT, Eur. J. Org. Chem., 2012, **15**, 2906-2915

[41] Lee SK, Zu Y, Herrmann A, Geerts Y, Mullen K, Bard AJ, J. Am. Chem. Soc., 1999, **121**, 3513-3520

[42] Yang L, Liu Y, Ma C, Liu W, Li Y, Li L, Dyes Pigm., 2015, **122**, 1-5

[43] Wrona-Piotrowicz A, Plazuk D, Zakrzewski J, Metivier R, Nakatani K, Makal A, Dyes Pigm., 2015, **121**, 290-298

[44] Sun B, Zhao Y, Qiu X, Han C, Yu Y, Shi Z, Supramol. Chem., 2008, **20**, 537-544

[45] Pu S, Fan C, Miao W, Liu G, Dyes Pigm., 2010, **84**, 25-35

[46] Kim SH, Choi J, Sakong C, Namgoong JW, Lee W, Kim DH, Dyes Pigm., 2015, **113**, 390-401

[47] Suzuki R, Tada R, Miura Y, Yoshioka N, J. Mol. Struct., 2016, **1106**, 399-406

[48] Saeed A, Shabir G, Spectrochim. Acta, Part A, 2014, **133**, 7-12

[49] Johansson LBA, Langhals H, Spectrochim. Acta, Part A, 1991, **47**, 857-861

[50] Al Ani KE, Suleiman AM, J. Photochem. Photobiol., A, 2007, **188**, 177-184

[51] Stolarski R, Fiksinski KJ, Dyes Pigm., 1994, **24**, 295-303

[52] Erdoğmuş A, Nyokong T, Dyes Pigm., 2010, **86**, 174-181

[53] Masuko M, Ohuchi S, Sode K, Ohtani H, Shimadzu A, Nucleic Acids Res., 2000, **28**, e34-e

[54] Georgiev NI, Sakr AR, Bojinov VB, Dyes Pigm., 2011, **91**, 332-339

[55] Georgieva I, Aquino AJA, Plasser F, Trendafilova N, Kohn A, Lischka H, J. Phy. Chem. A, 2015, **119**, 6232-6243

[56] Aaron JJ, Fall M, Spectrochim. Acta, Part A, 2000, **56**, 1391-1397

[57] Yang I, Kim E, Kang J, Han H, Sul S, Park SB, Chem. Commun., 2012, **48**, 3839-3841

[58] Kwon J, Hwang J, Park J, Han GR, Han KY, Kim SK, Sci. Rep., 2015, **5**, 17804

[59] Bae S, Lim E, Hwang D, Huh H, Kim SK, Chem. Phys. Lett., 2015, **633**, 109-113

[60] Andreussi O, Corni S, Mennucci B, Tomasi J, J. Chem. Phys., 2004, **121**, 10190-101202

[61] Kim M, Park WB, Bang B, Kim CH, Sohn KS, J. Mater. Chem. C., 2015, **3**, 5484-5489

[62] Carminati R, Greffet JJ, Henkel C, Vigoureux JM, Opt. Commun., 2006, **261**, 368-375

[63] Barqawi KR, Murtaza Z, Meyer TJ, J. Phy. Chem., 1991, **95**, 47-50

[64] Mazurak Z, Wanic A, Karolczak J, Czaja M, J. Lumin., 2015, **158**, 103-109

[65] Liu Y, Zhao J, Chem. Commun., 2012, **48**, 3751-3753

[66] Kang J, Jung J, Kim SK, Biophys. Chem., 2014, **195**, 49-52

[67] Lee Y, Yang I, Lee JE, Hwang S, Lee JW, Um SS, J. Phy. Chem. C, 2013, **117**, 3298-3307

[68] Campos PJ, Caro M, Rodríguez MA, Tetrahedron, 2013, **69**, 7950-7955

[69] Kufazvinei C, Ruether M, Wang J, Blau W, Org. Electron., 2009, **10**, 674-680

[70] Hwang YJ, Shin DM, Mol. Cryst. Liq. Cryst., 2007, **472**, 25-32

[71] Yoon C, Choi Jh, Dyes Pigm., 2014, **101**, 344-350

[72] Mat Raffei AF, Asmuni H, Hassan R, Othman RM, Knowledge Based Syst., 2015, **74**, 40-48

Chapter 5

A Study on the Fluorescence Property of the Perylene Derivatives with Methoxy Groups

5.1 Introduction

Perylene-based dyes generally show superior thermal stability and optical properties owing to the planarity of their molecular structures [1-5]. Because of these advantages, perylene-based dyes are widely used as optical coloring materials for displays among many other useful applications [5-11]. Moreover, perylene dyes are easily functionalized through the introduction of substituents at their terminal- and bay-positions, which enables the modification of characteristics such as their spectral properties and solubilities [12-14]. Perylene diimide derivatives having two bulky substituents at their terminal-positions are commonly used, and these molecules are often modified for various purposes by the introduction of 1 – 4 substituents at their bay-positions.

Previously, we have reported many novel perylene-based dyes for use as the red colorants in LCD color filters [7, 8, 12-22]. Since the fluorescence of these dyes can negatively affect the optical performance of the color filters fabricated with them [21], we have also suggested solutions for this problem, in which the decrease of contrast ratios of color filters was inhibited by using perylene-based dyes with high solubility and low fluorescence [22]. Based on our previous reports, the effect of methoxy groups on the fluorescence properties of perylene-based dyes and the relationships between the fluorescence of the dyes and the position of the introduced methoxy groups are studied in this paper, both experimentally and theoretically.

In this study, perylene-based dyes which contained methoxy groups in the terminal-, bay-, or both positions were synthesized. The methoxy groups were sequentially placed at the *ortho*-, *meta*-, or *para*-position of each substituent. Additionally, the dyes with ethyl substituents instead of methoxy groups were designed and synthesized, these dyes have similar geometrical molecular structures and conjugation systems with the dyes containing methoxy groups [22]. The absorption and fluorescence properties of the synthesized dyes were measured and compared. The

geometrical structures of the dyes were analyzed by density functional theory (DFT) calculations, and excitations from the highest occupied molecular orbitals (HOMOs) to the lowest occupied molecular orbitals (LUMOs) of the dyes were simulated with time-dependent density functional theory (TD-DFT) [23, 24]. Using these methods, the influence of the position of the methoxy groups on the electrochemical and the fluorescence properties of the dyes were studied.

5.2 Experimental

5.2.1 Materials and instrumentation

Perylene-3,4,9,10-tetracarboxylic dianhydride, iodine, sulfuric acid, bromine, and acetic acid were purchased from Sigma-Aldrich, 2,6-diisopropylaniline, 2-methoxy-6-methylaniline, 4-methoxy-2-methylaniline, 4-methoxyphenol, 4-ethylphenol, 3-methoxyphenol, 3-ethylphenol, 2-methoxyphenol, and 2-ethylphenol were purchased from TCI. Potassium carbonate anhydrous, methylene chloride, and other chemical solvents were purchased from Samchun Pure Chemical. All

chemicals were used without any additional purification.

Absorption spectra were measured using a Perkin Elmer Lambda 25 UV/Vis spectrophotometer. Fluorescence spectra and quantum yield data were measured on a Perkin Elmer LS 55 and a PTI Quanta Master 40 fluorescence spectrometer, respectively. Elemental Analysis (EA) was completed on a CE Instruments EA1112 analyzer. ^{1}H and ^{13}C Nuclear Magnetic Resonance (NMR) spectra were recorded on a Bruker Avance 500 spectrometer running at 500 MHz using chloroform-d as a solvent with TMS as an internal standard. Matrix Assisted Laser Desorption/Ionization Time of Flight (MALDI-TOF) mass spectra were recorded on an Applied Biosystems Voyager-DE STR Biospectrometry Workstation using α-cyano-4-hydroxycinnamic acid (CHCA) as a matrix.

5.2.2 Syntheses of the dyes

All synthetic procedures were carried out by following our previous reports [20-22]. The dyes **PI-4EP**, **PI-4ME**, **P2M-4EP**, and **P2M-4ME** were already reported in chapter 4. The specified name of the dyes **P2M-4EP** and **P2M-4ME** were **PM-4EP** and **PM-4ME** in chapter 4,

respectively. The syntheses of these dyes are repeated in this chapter.

5.2.2.1 1,7-Dibromoperylene-3,4,9,10-tetracarboxydiimide :

Bromination

Perylene-3,4,9,10-tetracarboxylic dianhydride (32.00 g, 81.40 mmol), iodine (0.78 g, 3.04 mmol) and sulfuric acid (98 %, 450 mL) were mixed and stirred for 2 h at room temperature. The temperature of the mixture was raised to 80 ℃ and bromine (8.33 mL, 162.80 mmol) was added dropwise over 1 h. The resulting mixture allowed to react for 16 h as sealed, upon which time, it was cooled to room temperature and the remaining bromine gas was displaced by nitrogen gas. The mixture was slowly poured into 3 L of ice water and the crude precipitate formed was collected by suction filtration followed by washing several times with distilled water. The crude product was dried at 80 ℃ under reduced pressure and used in the next step without further purification. The crude product containing both mono- and di-bromoperylene derivatives was separated by column chromatography in next step, after introducing bulky substituents in the terminal-position to increase their solubilities.

5.2.2.2 N,N'-bis(R_1)-1,7-dibromoperylene-3,4,9,10-tetracarboxydiimide : *Terminal-position substitution*

Crude 1,7-dibromoperylene-3,4,9,10-tetracarboxydiimide (8.00 g, 14.55 mmol), R_1-NH_2 (45.00 mmol), acetic acid (4.60 mL) and N-methyl-2-pyrrolidone (NMP, 100 mL) were mixed and heated to 120 ℃ under nitrogen atmosphere for 96 h. Water was added to the mixture and the resulting precipitate was collected by suction filtration. The crude product was washed with water and dried under reduced pressure. The crude product was purified by column chromatography in silica gel using CH_2Cl_2 as an eluent. Three bands were collected. The first band contained a small amount of tribrominated diimide, the second band contained the dibrominated diimide, and the third contained the monobrominated diimide. Detailed structural analysis was conducted after the next step. To obtain the **PI-series**, 2,6-diisopropylaniline was used as R_1-NH_2, to obtain **PM-series**, 2-methoxy-6-methylaniline was used and to obtain **P2M-series**, and 4-methoxy-2-methylaniline was used for **P4M-series**.

5.2.2.3 N,N'-Bis(R_1)-1,7-bis(R_2)-perylene-3,4,9,10-tetracarboxydiimide : *Bay-position substitution*

N,N'-bis(R_1)-1,7-dibromoperylene-3,4,9,10-tetracarboxydiimide (0.58 mmol) was mixed with anhydrous potassium carbonate (0.35 g, 2.54 mmol), R_2-OH (1.60 mmol) and NMP (60 mL). The mixture was heated at 40 ℃ under nitrogen and was stirred for 1.5 h. Thin layer chromatography (TLC) of the crude was repetitively performed during the reaction to check the progress. After the reaction, the mixture was cooled to room temperature, and then poured into HCl aqueous solution (400 mL, 5 %). The precipitate was collected by suction filtration, washed with water and dried under vacuum at 80 ℃. The crude product was purified by column chromatography in silica gel using CH_2Cl_2 as an eluent to obtain the products as red solids.

5.2.2.4 Structural analysis

PI-3EP, Yield 74.4 %; ^{1}H NMR ($CDCl_3$, ppm): 9.65 (d,2H), 8.70 (d,2H), 7.46 (m,4H), 7.34 (m,4H), 6.97 (m,4H), 2.72 (m,4H), 1.59 (s,2H),

1.23 (d,24H), 1.13 (s,12H); ^{13}C NMR (126 MHz, $CDCl_3$): δ= 15.55, 22.64, 24.17, 24.19, 28.98, 29.37, 31.14, 76.97, 77.22, 77.47, 116.46, 116.59, 118.95, 119.05, 122.54, 123.88, 124.24, 124.86, 124.97, 125.21, 126.10, 128.16, 129.21, 129.82, 129.89, 130.51, 130.63, 131.01, 132.02, 133.96, 145.78, 147.51, 155.41, 155.44, 163.13, 163.65; MALDI-TOF MS: m/z 952.3 (100 %, [M+2K]+)

PI-2EP, Yield 67.6 %; ^{1}H NMR ($CDCl_3$, ppm): 9.72 (d,2H), 8.70 (d,2H), 7.46 (m,4H), 7.25 (m,4H), 6.98 (m,4H), 2.70 (m,4H), 1.57 (s,2H), 1.32 (d,24H), 1.14 (s,12H); ^{13}C NMR (126 MHz, $CDCl_3$): δ= 15.03, 22.65, 23.53, 24.17, 24.21, 29.36, 31.15, 76.96, 77.22, 77.47, 119.46, 119.66, 122.14, 122.46, 122.97, 123.63, 123.73, 124.10, 124.22, 124.25, 125.85, 125.78, 125.99, 127.91, 128.09, 129.04, 129.80, 129.97, 130.64, 130.78, 130.86, 131.97, 134.06, 135.91, 145.78, 152.70, 155.90, 157.02, 162.92, 163.10, 163.68, 163.91; MALDI-TOF MS: m/z 952.3 (100 %, [M+2K]+)

PI-3ME, Yield 73.5 %; ^{1}H NMR ($CDCl_3$, ppm): 9.61 (d,2H), 8.69 (d,2H), 8.45 (d,4H), 7.47 (m,4H), 6.77 (m,4H), 2.73 (m,4H), 2.69 (s,2H), 1.16 (d,20H), 1.15 (m,12H); ^{13}C NMR (126 MHz, $CDCl_3$): δ= 24.20, 29.37, 31.14, 55.76, 76.96, 77.47, 105.63, 110.29, 111.23, 111.34,

122.64, 124.25, 124.35, 124.60, 125.19, 125.79, 126.33, 128.22, 129.22, 129.84, 130.59, 131.16, 131.19, 133.82, 145.79, 154.86, 156.52, 161.64, 163.04, 163.61; MALDI-TOF MS: m/z 956.3 (100 %, [M+2K]+)

PI-2ME, Yield 67.0 %; ^{1}H NMR ($CDCl_3$, ppm): 9.76 (d,2H), 8.69 (d,2H), 7.45 (d,4H), 7.31 (m,4H), 7.18 (m,4H), 2.73 (septet,4H), 1.56 (s,2H), 1.17 (d,20H), 1.12 (s,12H); ^{13}C NMR (126 MHz, $CDCl_3$): δ= 24.14, 24.20, 29.34, 31.14, 56.13, 76.96, 77.22, 77.47, 113.52, 120.62, 121.83, 121.88, 122.03, 122.15, 122.18, 123.13, 123.85, 124.18, 124.22, 125.66, 126.88, 127.00, 128.34, 129.47, 129.73, 130.00, 130.61, 130.78, 131.91, 134.21, 134.41, 142.87, 145.79, 145.86, 151.60, 156.15, 157.25, 163.18, 163.34, 163.79, 164.02; MALDI-TOF MS: m/z 956.3 (100 %, [M+2K]+)

P4M-4EP, Yield 65.9 %; ^{1}H NMR ($CDCl_3$, ppm): 9.67 (d,2H), 8.67 (d,2H), 7.27 (d,4H), 7.10 (m,4H), 6.91 (m,4H), 2.69 (septet,4H), 1.56 (s,2H), 1.25 (d,14H), 0.88 (m,6H); ^{13}C NMR (126 MHz, $CDCl_3$): δ= 15.86, 18.16, 28.45, 29.91, 31.14, 55.61, 77.22, 77.47, 112.59, 116.53, 119.74, 119.85, 122.53, 123.04, 124.11, 124.28, 124.37, 125.71, 127.03, 129.20, 130.11, 130.79, 131.88, 134.02, 134.09, 137.25, 141.57, 152.98, 155.90, 160.00, 163.21, 163.59; MALDI-TOF MS: m/z 872.2 (100 %,

[M+2K]+)

P4M-4ME, Yield 62.1 %; ^{1}H NMR ($CDCl_3$, ppm): 9.63 (d,2H), 8.76 (d,2H), 8.34 (s,4H), 7.13 (m,4H), 6.88 (m,4H), 3.83 (s,2H), 2.17 (d,14H), 1.56 (s,6H); ^{13}C NMR (126 MHz, $CDCl_3$): δ= 19.16, 29.91, 31.15, 55.62, 55.92, 77.22, 77.47, 112.58, 115.87, 116.51, 121.29, 121.40, 122.20, 122.48, 123.58, 124.04, 125.53, 127.04, 128.08, 129.23, 129.49, 129.80, 130.70, 131.87, 134.05, 137.25, 148.38, 156.47, 157.35, 160.00, 163.01, 163.24, 163.60; MALDI-TOF MS: m/z 876.2 (100 %, [M+2K]+)

5.2.3 Geometry optimization of the dyes

Density functional theory (DFT) and Time-dependent density functional theory (TD-DFT) calculations were carried out with the Gaussian 09 program package. We used the 6-311++G(d,p) Pople basis set for all elements and the conventional B3LYP exchange-correlation function. The intermolecular interactions were analyzed by examining the core twist angles and the size of substituents. Dihedral angles of perylene main body were calculated by measuring the distortion angle of benzene ring in the center of perylene main body. Calculated lengths of

substituents were indicated by measuring the longest lineal distance of the atoms in the substituents. The spaces of the substituents away from the plane of perylene back bone were assessed by measuring the inserted angle between the substituents and the plane.

5.3 Results and discussion

5.3.1 Design concept of the synthesized dyes

The synthetic route and molecular structures of the synthesized dyes are shown in **Scheme 5.1** and **Fig. 5.1**, respectively. Seven dyes containing methoxy groups and three without methoxy groups were synthesized. The methoxy group, a readily available organic substituent and powerful electron donor, usually inhibits fluorescence when introduced into organic coloring materials [22, 25-28]. To observe the effects of methoxy groups incorporated into bay-substituents, dyes containing methoxy groups in the *ortho*-, *meta*-, or *para*-position of bay-position benzene rings were designed. For comparison, analogs with ethyl groups introduced in place of the methoxy groups were also

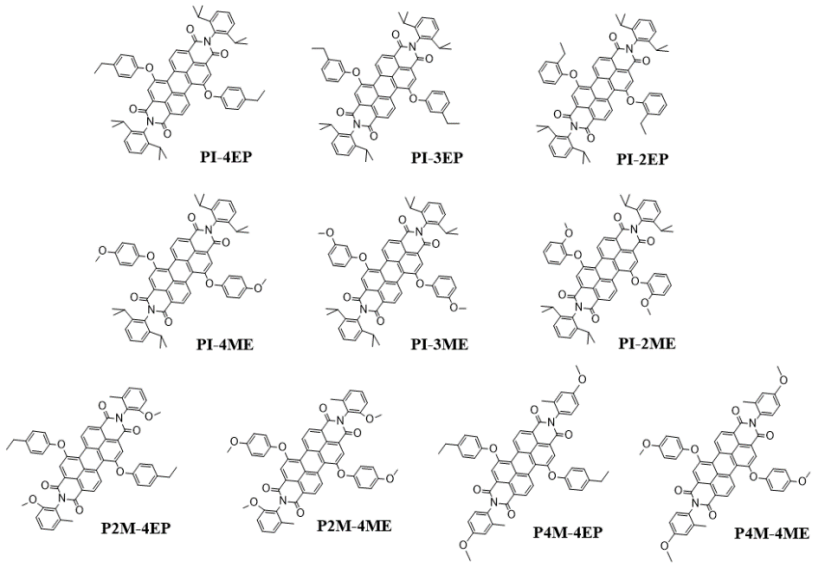

Fig. 5.1 Structure of the synthesized dyes

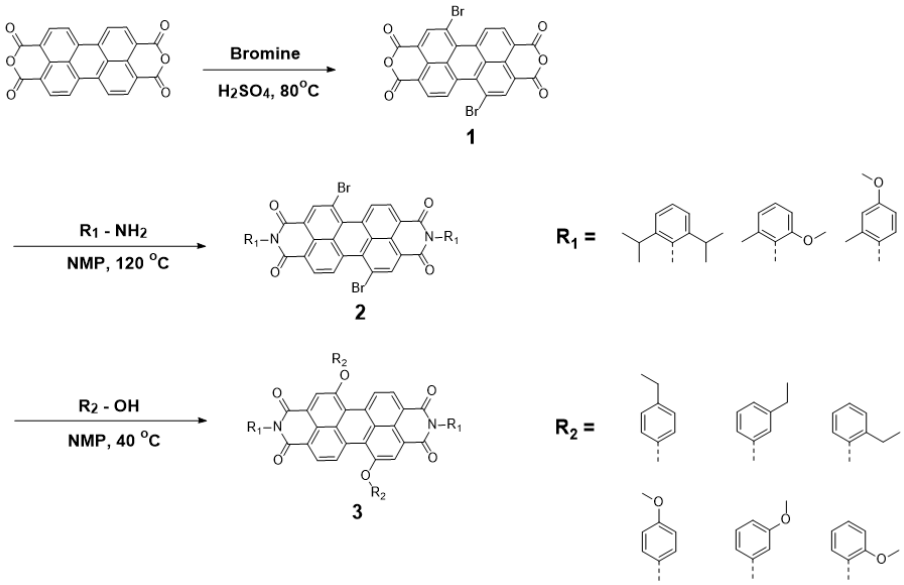

Scheme 5.1 Synthetic routes of the designed dyes

designed. To observe the effects of methoxy groups on the terminal-substituents, *ortho*- or *para*-methoxylated aryl substituents were introduced at the terminal-substituents of the dyes. Finally, the dyes with the methoxylated terminal-substituents carried only *para*-methoxy- or *para*-ethyl-aryl groups as their bay-substituents.

All the dyes were designed to have similar conjugation lengths and steric bulkiness, to minimize differences in the spectral properties and intermolecular interactions. As is widely known, the most impactful principal factor influencing the fluorescence of organic coloring materials is quenching through intermolecular interactions [29-33]. If H-aggregation intensively occurs, the excited energy is significantly consumed via non-radiative decay accompanied by intermolecular energy transfer, and as a result, radiative decay processes such as emission are inhibited [30, 34-36]. Therefore, the dyes used in this study were designed to have similar geometrical structures and intermolecular interactions so that their fluorescence properties would be primarily dependent on their electrochemical properties rather than their physical molecular behaviors [22].

5.3.2 Geometry optimization of the synthesized dyes

The optimized geometries of the synthesized dyes obtained via DFT calculations are shown in **Fig. 5.2**. The images as observed from the normal to the perylene main body plane are presented in **Fig. 5.2**. All the designed dyes have similar molecular morphologies, despite the introduction of the various substituents. The size of a dye molecule and its substituents majorly influence the distance between molecules [20], which, in turn, affects intermolecular interactions and fluorescence properties.

The dihedral angle of the perylene main body and the calculated lengths of the introduced substituents are listed in **Table 5.1**. The dihedral angle of the perylene main body was measured on the benzene ring at the center of perylene backbone [20]. All the introduced substituents are symmetrically oriented at each substitution position, but the dye molecules are not three-dimensionally symmetric according to the DFT simulations [20]. Therefore, all values were measured for both sides of the molecules and the average values are provided in **Table 5.1**. The synthesized dyes exhibited similar values for the dihedral angle of

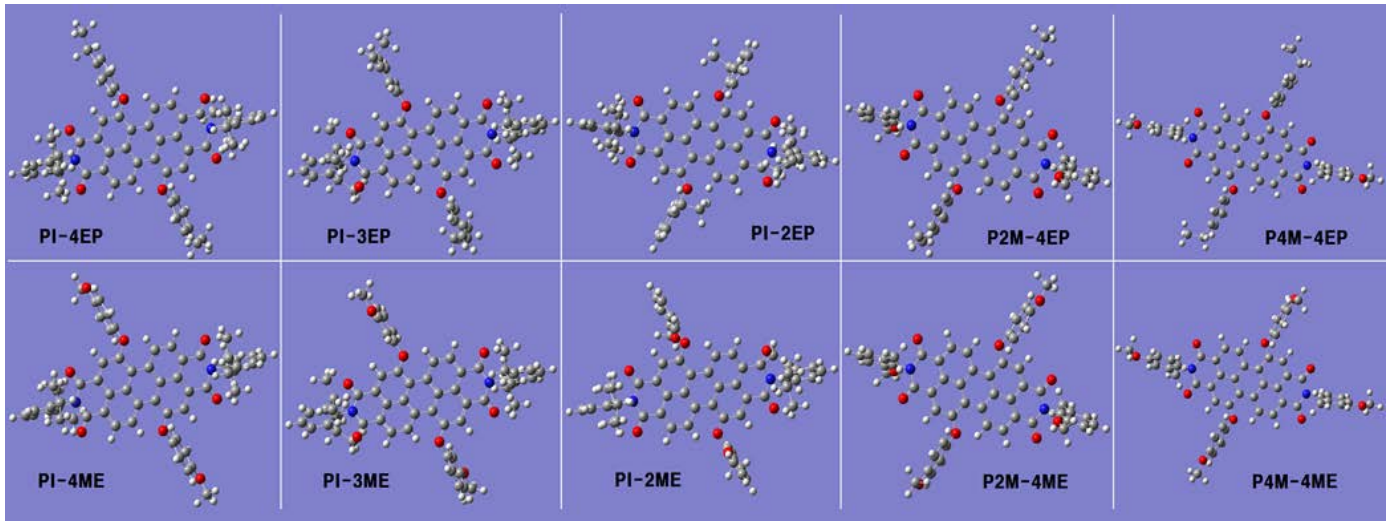

Fig. 5.2 Geometry-optimized structure of the synthesized dyes

Table 5.1 Dihedral angles of the perylene main body and calculated lengths of the substituents [a]

Dye	Dihedral angle of the perylene main body (°)	Calculated lengths of substituents (Å)	
		Bay-substituent	Terminal-substituent
PI-4EP	13.66954	7.61265	8.91653
PI-4ME	13.65821	7.39409	8.91467
PI-3EP	12.70249	7.22121	8.83280
PI-3ME	12.90190	7.10929	8.90940
PI-2EP	12.82097	7.23594	8.82305
PI-2ME	13.89031	7.11218	8.90961
P2M-4EP	13.58233	7.61336	7.76763
P2M-4ME	13.65405	7.39385	7.76759
P4M-4EP	13.18395	7.50709	7.56291
P4M-4ME	13.57888	7.39411	7.56386

[a] dihedral angle and calculated lengths are not symmetric for each side of perylene main body, therefore, the average values are listed.

the perylene main body, which principally determines its planarity. The difference in the dihedral angles among the dyes is within about 1°, except for **PI-2ME**, therefore, it can be assumed that the planarity of the dyes is generally analogous to each other. As can be observed in **Table 5.1**, the dihedral angle data of **PI-2ME** is slightly out of the tendency. Our guess is that an unexpected error occurred in the case of **PI-2ME**, because the molecular structure of **PI-2ME** dye is less stable than the other dyes owing to the close proximity of the branches of the bay-substituents and the perylene backbone. This would increase the interference factor, and as a result, an error would be observed in the DFT calculations.

The sizes of introduced substituents are similar. Commonly, the bay-substituents with methoxy groups are smaller than those bearing ethyl groups by ~0.2 Å, and the terminal-substituents with methoxy groups are smaller than those without methoxy groups by ~1.2 Å. Generally, bulky substituents that contain several alkyl groups or benzene rings are used to prevent the intermolecular interactions of perylene-based dyes [3, 21, 22, 37-43]. From this point of view, the difference of the physical morphologies of the dyes used in this study would not have a significant

influence on the molecular interactions or the fluorescence behaviors of them.

5.3.3 Absorption properties of the synthesized dyes

The absorption properties of the synthesized dyes are shown in **Fig. 5.3** and **Table 5.2**. The absorption properties of the dyes have been reported in our previous study were remeasured and the measured results under this research are provided [22]. As intended, the overall shapes of the absorption spectra are similar, owing to the similar conjugation lengths designed for the synthesized dyes.

The dyes with *ortho*- or *para*-methoxylated bay-substituents exhibit bathochromic shifts of ~4 nm due to the electron donating effects of the methoxy groups. In contrast, the dye with *meta*-methoxylated bay-substituents shows a hypsochromic shift compared to the analogous dye with ethylated bay-substituents. These phenomena result from the well-known electron donating ability of the introduced organic substituents [25-27, 44-46]. The same tendency is observed when methoxy groups are introduced in the terminal-substituents. However, the effects of

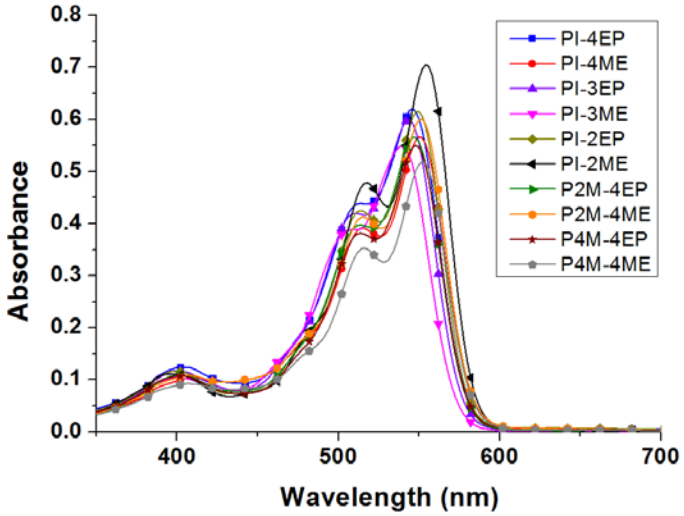

Fig. 5.3 Absorption spectra of the synthesized dyes in chloroform (10^{-5} mol/L)

Table 5.2 Spectral properties of the synthesized dyes

Dye	λ_{abs} [a]	ε_{abs} [b]
PI-4EP	546	62,050
PI-4ME	550	56,650
PI-3EP	544	59,880
PI-3ME	540	54,940
PI-2EP	550	61,520
PI-2ME	554	70,520
P2M-4EP	548	56,510
P2M-4ME	552	60,000
P4M-4EP	548	55,040
P4M-4ME	552	51,940

[a] λ_{abs} : maximum absorption wavelength (nm)

[b] ε_{abs} : molar extinction coefficient (L/mol·cm)

electron donation by the methoxy groups appear to be more powerful when these groups are incorporated in the bay-substituents than in the terminal-substituents. The dyes with methoxylated terminal-substituents exhibited bathochromic shifts of only ~2 nm compared to the dyes without methoxy groups in the terminal-substituents.

5.3.4 Fluorescence properties of the synthesized dyes

The fluorescence properties of the synthesized dyes are presented in **Fig. 5.4** and **Table 5.3**. All fluorescence properties except quantum yield were measured at an excitation wavelength corresponding to the wavelength of maximum absorption. The quantum yield was measured at an excitation wavelength of 480 nm. Similarly to the absorption properties, the fluorescence properties of the dyes that were reported in our previous study were remeasured for comparison with the new dyes in this study [22]. The optical image of the synthesized dyes in chloroform solutions are shown in **Fig. 5.5**. The images were photographed under 365 or 254 nm of UV light.

Among the ten synthesized compounds, dyes **PI-4ME**, **P2M-4ME**,

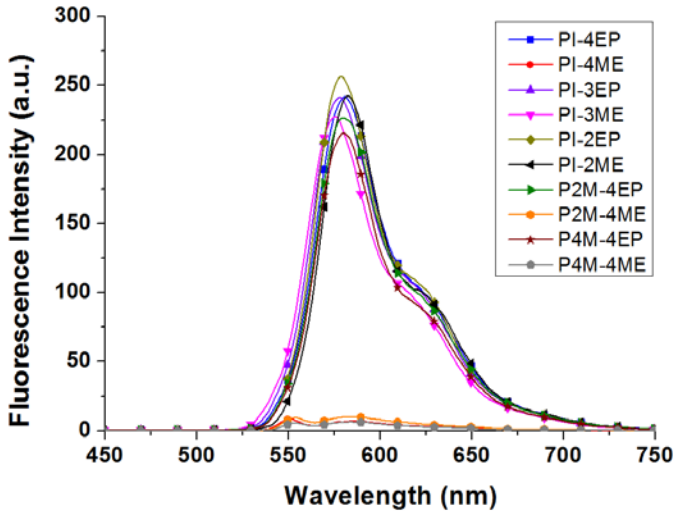

Fig. 5.4 Fluorescence spectra of the synthesized dyes in chloroform (10^{-8} mol/L)

Table 5.3 Fluorescence properties of the synthesized dyes

Dye	λ_{em} [a]	Maximum emission intensity (a.u.)	Q_y [b]
PI-4EP	581	241.82	0.976
PI-4ME	586	7.08	0.054
PI-3EP	578	241.62	0.938
PI-3ME	576	227.61	0.926
PI-2EP	579	256.49	0.947
PI-2ME	582	242.51	0.961
P2M-4EP	580	226.75	0.985
P2M-4ME	582	10.20	0.080
P4M-4EP	580	215.44	0.880
P4M-4ME	584	6.38	0.040

[a] λ_{em} : maximum emission wavelength (nm) ;

[b] Q_y : quantum yield (10^{-5} mol/L in chloroform, excited at 480 nm)

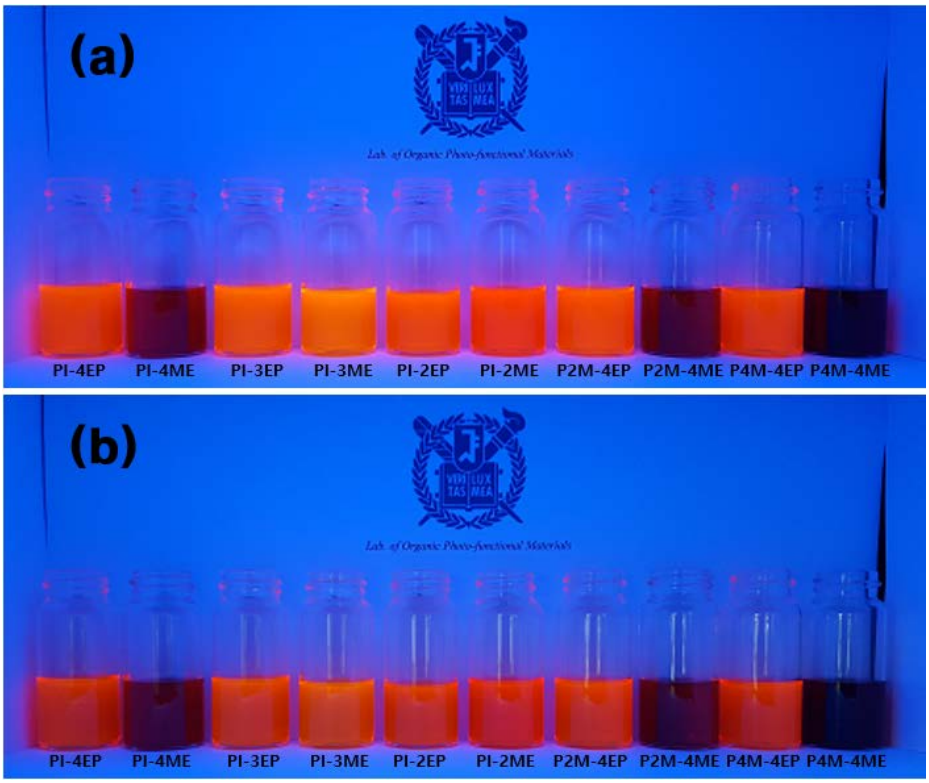

Fig. 5.5 Optical image of the synthesized dyes in chloroform solutions (10^{-4} mol/L) under UV light of (a) 365 nm and (b) 254 nm

and **P4M-4ME** show quenched fluorescence, with differences in quantum yield of ~20-fold from the highly fluorescent dyes. The dyes with low fluorescence all bear methoxy groups at the *para*-positions of the bay-substituents. Compounds with methoxy groups at the *ortho*- or *meta*-positions of the bay-substituents show no fluorescence quenching. The differences in the fluorescence of the highly fluorescent dyes appear less significant compared to the obvious influences of *para*-methoxy groups in the bay-substituents. As observed above, methoxy groups electronically affect the absorption properties of perylene-based dyes irrespective of their positions. However, only the methoxy groups at the *para*-position of the bay-substituents inhibit fluorescence. Thus, the electrochemical influence of the introduced substituents on the fluorescence properties is dependent on their positions.

Methoxy groups introduced into terminal-substituents exerted a weaker influence on the fluorescence of dyes. *Ortho*-methoxylated terminal-substituents showed no fluorescence quenching effects, and those were *para*-methoxylated exhibited limited effects on fluorescence quenching compared to the cases with methoxy-bearing bay-substituents. It is widely known that the terminal-substituents have no or little

influence on the conjugation systems of perylene-based dyes [41-43, 47]. Comprehensively judged with the results of this study, it would seem that the terminal-substituents exert a very weak influence on the electrochemical properties of the perylene-based dyes, especially on their spectral properties, and these effects are very minor compared to the influences of bay-substituents. However, it is not reasonable to assume that the terminal-substituents have no relationship with the conjugation systems of the perylene-based dyes.

5.3.5 Molecular orbital modeling of the synthesized dyes

The TD-DFT simulation results for excitation from the HOMOs to the LUMOs of the synthesized dyes are presented in **Table 5.4**. For each dye, the excitation system with the highest oscillator strength among the theoretically possible excitation systems is presented [23, 24]. The maximum theoretical absorption wavelength changes along with the electron donating effect of the introduced substituents, although the results are not perfectly correlated with the measured data. Similar to the results of the DFT calculations, the simulations of dyes with groups at

the *ortho*-positions of the bay-substituents show slight errors due to structural instability and the increase of interference factors.

The HOMO and LUMO molecular orbital models of the **PI-4EP**, **PI-4ME**, **PI-3ME**, **PI-2ME**, **P2M-4ME**, and **P4M-4ME** dyes are illustrated in **Fig. 5.6 – 5.11**, respectively. The HOMO and LUMO states are based on the results presented in **Table 5.4**, with the highest oscillator strength for each dye. For each figure, images of the HOMO state are presented in the upper three panels, and those of the LUMO state are presented below. The images as observed from the direction of x (terminal-substituents), y (bay-substituents), or z (normal of perylene main body plane) axis are sequentially presented for each state.

The **PI-4ME**, **P2M-4ME**, and **P4M-4ME** dyes show inhibited fluorescence and have methoxy groups in the *para*-positions of the bay-substituents. Dyes **PI-3ME** and **PI-2ME** exhibit strong fluorescence and have methoxy groups in the *meta*- and *ortho*-positions, respectively. In the HOMO states of the fluorescence quenched dyes, electron density is clearly visible on the methoxy groups at the *para*-positions of the bay-substituents. In contrast, electron density is not observed on the methoxy groups in either the HOMO or LUMO states of the highly fluorescent

Table 5.4 Calculated result of TD-DFT for the excitation from HOMO to LUMO of the synthesized dyes

Dye	Definition	Transition	Excitation energy (eV)	Theoritical λ_{abs} (nm)	Oscillator strength
PI-4EP	252 → 253	$S_0 \rightarrow S_1$	2.2911	541.15	0.7918
PI-4ME	252 → 253	$S_0 \rightarrow S_1$	2.2661	547.13	0.7547
PI-3EP	252 → 253	$S_0 \rightarrow S_1$	2.2710	545.95	0.7629
PI-3ME	252 → 253	$S_0 \rightarrow S_1$	2.2861	542.34	0.7632
PI-2EP	252 → 253	$S_0 \rightarrow S_1$	1.8731	661.91	0.7067
PI-2ME	252 → 253	$S_0 \rightarrow S_1$	2.2541	550.04	0.7775
P2M-4EP	228 → 229	$S_0 \rightarrow S_1$	2.3215	534.06	0.7583
P2M-4ME	228 → 229	$S_0 \rightarrow S_1$	2.2951	540.20	0.7268
P4M-4EP	228 → 229	$S_0 \rightarrow S_1$	2.2817	543.38	0.7525
P4M-4ME	228 → 229	$S_0 \rightarrow S_1$	2.2846	542.69	0.7405

Table 5.5 Structural angle between the methoxy group at bay-substituents and the plane of perylene main body

Dye	PI-4ME	PI-3ME	PI-2ME	P2M-4ME	P4M-4ME
Angle (°)	26.287	58.863	74.911	28.109	27.657

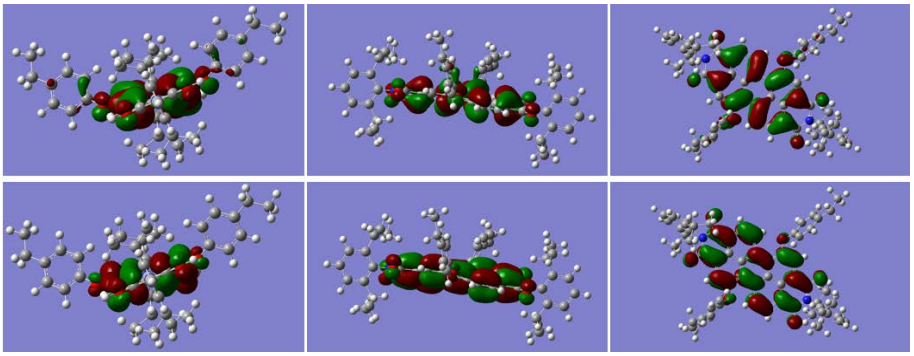

Fig. 5.6 Molecular orbital model of **PI-4EP** at HOMO and LUMO

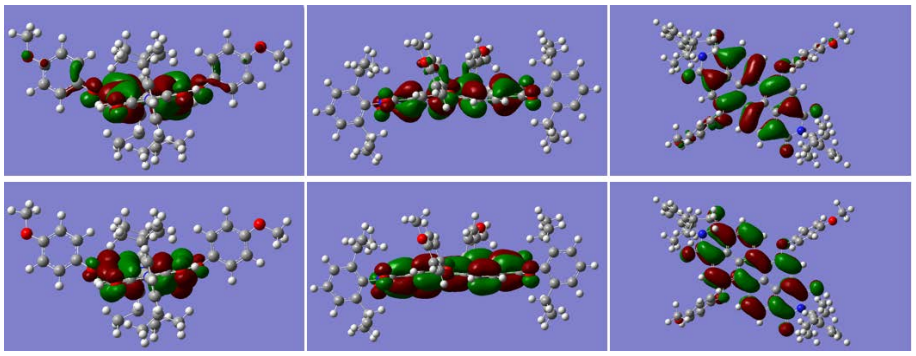

Fig. 5.7 Molecular orbital model of **PI-4ME** at HOMO and LUMO

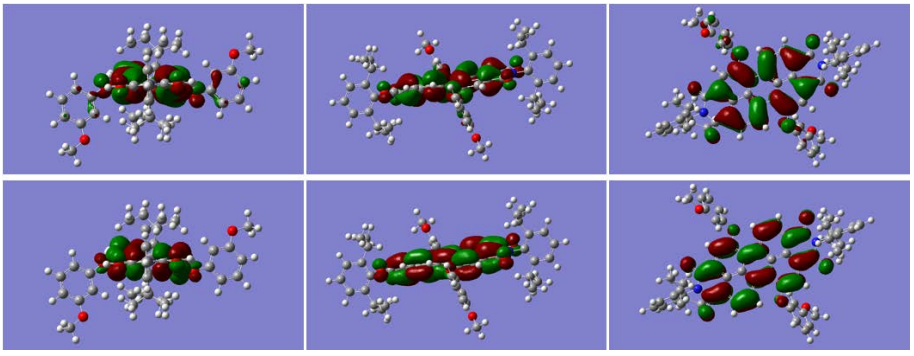

Fig. 5.8 Molecular orbital model of **PI-3ME** at HOMO and LUMO

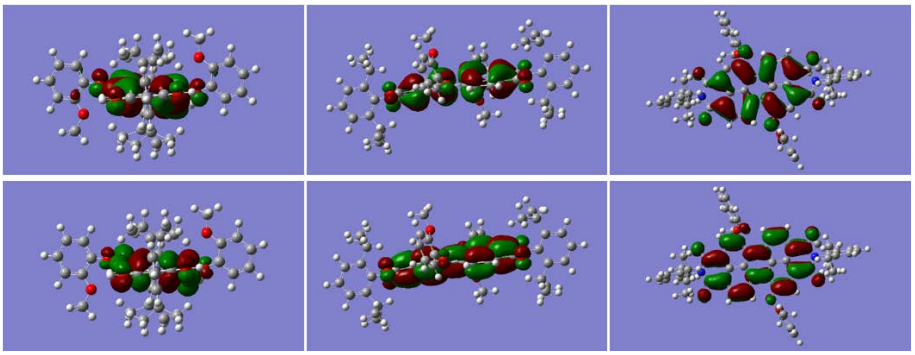

Fig. 5.9 Molecular orbital model of **PI-2ME** at HOMO and LUMO

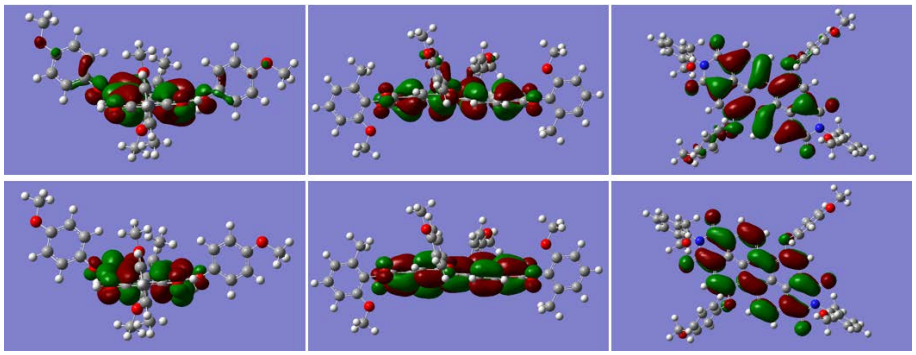

Fig. 5.10 Molecular orbital model of **P2M-4ME** at HOMO and LUMO

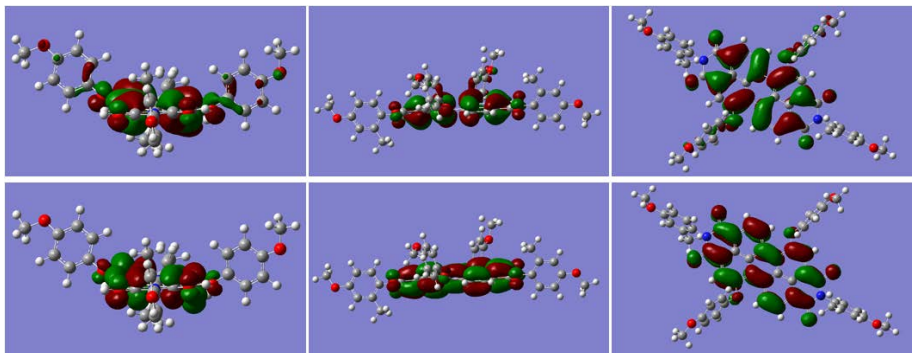

Fig. 5.11 Molecular orbital model of **P4M-4ME** at HOMO and LUMO

dyes. Thus, the methoxy groups exert an electrochemical influence through electron donation when they can overlap with the conjugation system of the perylene main body, effectively resulting in a fluorescence quenching effect.

The structural angles between the methoxy groups introduced in the bay-substituents and the perylene main body are listed in **Table 5.5**. *Para*-methoxy groups in the bay-substituents are oriented at an angle of 27° with respect to the perylene backbone, whereas the angle of methoxy groups in the *meta*-position is ~59° and that of the *ortho*-position is ~75°. Since the average observed dihedral angle of the perylene main body is ~13°, it can be assumed that the structural estranged degrees of the methoxy groups in the *para*-position of the bay-substituents are only about 15° when the plane of the perylene main body is assumed as a curved face. Therefore, the possibility that the methoxy groups at the *para*-positions of the bay-substituents overlap with the conjugation system of the perylene main body would be much higher than those of methoxy groups at other positions [48, 49]. As a result, it could be concluded that the methoxy groups differently influence fluorescence quenching, dependent on their introduced position.

5.4 Conclusion

In this study, the effects of methoxy groups on the fluorescence of perylene-based dyes were studied with dyes that contained methoxy groups in various positions. To observe the effects of the methoxy group at the bay-substituents, dyes bearing *ortho*-, *meta*-, or *para*-methoxybenzene groups as bay-substituents were designed. To observe the effects of the methoxy groups in the terminal-substituents, dyes with *ortho*- or *para*-methoxyaryl groups as terminal-substituents were designed. Additionally, dyes with ethyl groups introduced instead of methoxy groups were also designed for comparison.

The geometries of the dyes were analyzed by the DFT method to assure the similarity of their structural morphologies. The introduced methoxy groups show a significant relationship with the spectral properties of the dyes. In particular, methoxy groups incorporated in the bay-substituents exhibited a stronger influence than those in the terminal-substituents. Dyes with *para*-methoxylated bay-substituents showed significantly quenched fluorescence. These *para*-methoxy groups in the bay-substituents exhibit the smallest structural dihedral

angle with respect to the perylene main body, and therefore, would easily contribute to the conjugation system and affect the electrochemical properties. According to the TD-DFT calculations, electron density is only exhibited on the methoxy groups at the *para*-positions of the bay-substituents in the HOMO states of fluorescence quenched dyes. In conclusion, the methoxy groups that can overlap with the conjugation plane of the perylene main body influence the electrochemical and fluorescence properties of the dyes.

5.5 Reference

[1] Chao CC, Leung Mk, J. Org. Chem., 2005, **70**, 4323-4331

[2] Zhao C, Zhang Y, Renjie Li XL, Jiang J, J. Org. Chem., 2006, **72**, 2402-2410

[3] Dincalp H, Askar Z, Zafer C, Icli S, Dyes Pigm., 2011, **91**, 182-191

[4] Huang C, Barlow S, Marder SR, J. Org. Chem., 2011, **76**, 2386-2407

[5] Reghu RR, Bisoyi HK, Grazulevicius JV, Anjukandi P, Gaidelis V, Jankauskas V, J. Mater. Chem., 2011, **21**, 7811

[6] Lee SK, Zu Y, Herrmann A, Geerts Y, Mullen K, Bard AJ, J. Am.

Chem. Soc., 1999, **121**, 3513-3520

[7] Kim YD, Kim JP, Kwon OS, Cho IH, Dyes Pigm., 2009, **81**, 45-52

[8] Choi J, Kim SH, Lee W, Chang JB, Namgoong JW, Kim YH, Dyes Pigm., 2014, **101**, 186-195

[9] Biedermann F, Elmalem E, Ghosh I, Nau WM, Scherman OA, Angew. Chem. Int. Ed., 2012, **51**, 7739-7743

[10] Stolarski R, Fiksinski KJ, Dyes Pigm., 1994, **24**, 295-303

[11] Qiao Y, Chen J, Yi X, Duan W, Gao B, Wu Y, Tetrahedron Lett., 2015, **56**, 2749-2753

[12] Choi J, Sakong C, Choi JH, Yoon C, Kim JP, Dyes Pigm., 2011, **90**, 82-88

[13] Kim YD, Cho JH, Park CR, Choi JH, Yoon C, Kim JP, Dyes Pigm., 2011, **89**, 1-8

[14] Sakong C, Kim YD, Choi JH, Yoon C, Kim JP, Dyes Pigm., 2011, **88**, 166-173

[15] Choi J, Lee W, Sakong C, Yuk SB, Park JS, Kim JP, Dyes Pigm., 2012, **94**, 34-39

[16] Choi J, Lee W, Namgoong JW, Kim TM, Kim JP, Dyes Pigm., 2013, **99**, 357-365

[17] Kim SH, Choi J, Sakong C, Namgoong JW, Lee W, Kim DH, Dyes Pigm., 2015, **113**, 390-401

[18] Kim SH, Namgoong JW, Yuk SB, Kim JY, Lee W, Yoon C, J. Inclusion Phenom. Macrocyclic. Chem., 2015, **82**, 195-202

[19] Yuk SB, Lee W, Namgoong JW, Choi J, Chang JB, Kim SH, J. Inclusion Phenom. Macrocyclic. Chem., 2015, **82**, 187-194

[20] Kim JY, Choi J, Namgoong JW, Kim SH, Sakong C, Yuk SB, J. Inclusion Phenom. Macrocyclic. Chem., 2015, **82**, 203-212

[21] Kim JY, Sakong C, Choi S, Jang H, Kim SH, Chang KS, Dyes Pigm., 2016, **131**, 293-300

[22] Kim JY, Hwang TG, Kim SH, Namgoong JW, Kim JE, Sakong C, Dyes Pigm., 2017, **136**, 836-845

[23] Tretiak S, Nano Lett., 2007, **7**, 2201-2206

[24] Li GY, Chu T, Phys. Chem. Chem. Phys., 2011, **13**, 20766-22071

[25] Pu S, Fan C, Miao W, Liu G, Dyes Pigm., 2010, **84**, 25-35

[26] Saeed A, Shabir G, Spectrochim. Acta A., 2014, **133**, 7-12

[27] Suzuki R, Tada R, Miura Y, Yoshioka N, J. Mol. Struct., 2016, **1106**, 399-406

[28] Korzdorfer T, Tretiak S, Kummel S, J. Chem. Phys., 2009, **131**,

034310

[29] Andreussi O, Corni S, Mennucci B, Tomasi J, J. Chem. Phys., 2004, **121**, 10190-10202

[30] Kang J, Jung J, Kim SK, Biophys. Chem., 2014, **195**, 49-52

[31] Kim M, Park WB, Bang B, Kim CH, Sohn KS, J. Mater. Chem. C, 2015, **3**, 5484-5489

[32] Kwon J, Hwang J, Park J, Han GR, Han KY, Kim SK, Sci. Rep., 2015, **5**, 17804

[33] Mazurak Z, Wanic A, Karolczak J, Czaja M, J. Lumin., 2015, **158**, 103-109

[34] Bae S, Lim E, Hwang D, Huh H, Kim SK, Chem. Phys. Lett., 2015, **633**, 109-113

[35] Karolin J, Johansson LBA, Ring U, Langhals H, Spectrochim. Acta A. 1996, **52**, 747-753

[36] Wurthner F, Thalacker C, Diele S, Tschierske C, Chem. Eur. J., 2001, **7**, 2245-2253

[37] Turkmen G, Erten-Ela S, Icli S, Dyes Pigm., 2009, **83**, 297-303

[38] Gao B, Li H, Liu H, Zhang L, Bai Q, Ba X, Chem. Commun., 2011, **47**, 3894-3896

[39] Osswald P, Wurthner F, Chem. Eur. J., 2007, **13**, 7395-7409

[40] Zhang X, Wu Y, Li J, Li F, Li M, Dyes Pigm., 2008, **76**, 810-816

[41] Georgiev NI, Sakr AR, Bojinov VB, Dyes Pigm., 2011, **91**, 332-339

[42] Lee IL, Li SR, Chen KF, Ku PJ, Singh AS, Kuo HT, Eur. J. Org. Chem., 2012, **15**, 2906-2915

[43] Tsai HY, Chen KY, J. Lumin., 2014, **149**, 103-111

[44] Hutchings MG, Dyes Pigm., 1991, **17**, 227-240

[45] Durbeej B, Eriksson LA, Chem. Phys. Lett., 2003, **375**, 30-38

[46] Lakshmi Praveen P, Ojha DP, J. Mol. Liq., 2014, **197**, 106-113

[47] Erdogmuş A, Nyokong T, Dyes Pigm., 2010, **86**, 174-181

[48] Chen J, Shi MM, Hu XL, Wang M, Chen HZ, Polymer, 2010, **51**, 2897-2902

[49] Dincalp H, Kizilok S, Icli S, Dyes Pigm., 2010, **86**, 32-41

Summary

Novel perylene derivatives were designed and synthesized for application in red dye-based and pigment-dye hybrid LCD color filters. Two substituents were introduced at the terminal-position of the perylene molecule; additional one or two substituents were further introduced at the bay-position. The synthesized dyes were soluble in organic solvents, possessed acceptable spectral properties for use in red color filters, and were thermally stable such that the dyes could be used in color filters. The solubility in organic solvents and other physical properties were related to the intermolecular interactions of the dyes, which were influenced by the planarity of the molecular structures and the size of the introduced substituent groups.

On the contrary to most of the previously reported studies, this study focused on the negative implications arising from the strong fluorescence of perylene derivatives on the performance, specifically the contrast ratio, of LCD color filters. The strong fluorescence of perylene-based dyes has been consistently revealed when used in dye-based and pigment-dye hybrid color filters. In addition, non-polarized light, generated from the

emission of perylene-based dyes, can then pass through the second polarizer even in full-black state and increases the minimum brightness. To overcome this drawbacks, additional perylene-based dyes with high solubility and low fluorescence were developed and used in color filters. The color filters made with the low-fluorescent dyes were optically superior, especially in terms of the contrast ratio, to the color filters made with high-fluorescent dyes.

The perylene derivatives with low fluorescence were designed by introducing electron-donating substituents such as the methoxy group, which had a strong effect on fluorescence quenching. The quantum yield were higher than 0.88 for the high-fluorescent dyes and less than 0.08 for the low-fluorescent dyes. Methoxy groups introduced at the *para*-position of bay-substituents had the strongest effect on fluorescence quenching compared to the methoxy groups introduced at the *ortho*- and *meta*-positions, which had no effect on fluorescence quenching. Therefore, the effectiveness of the methoxy groups on the fluorescence quenching is dependent on the position and orientation. The methoxy groups should be located close to the plane and conjugation system of the perylene molecule for the electron-donating property of the methoxy

groups to affect the electrochemical properties of the dyes and enhance the fluorescence quenching.

초 록

최근 다양한 형태의 평판 디스플레이가 개발되고 있지만 LCD는 여전히 높은 시장 점유율을 차지하고 있다. LCD 모듈은 백색광을 발광하는 back light unit과 화상을 구현하는 액정 패널로 구성되어 있는데, 컬러필터는 액정 패널의 한 구성요소이다. LCD는 컬러필터가 백색광을 각각 적색, 녹색, 청색 3개의 빛으로 변환하고, 이를 편광 필름과 액정을 사용해 적절히 혼합함으로써 컬러를 구현하는 방식으로 작동한다. 컬러필터는 LCD의 성능을 결정하는 가장 중요한 요소로, 컬러필터의 광학적 특성을 향상시켜 LCD의 성능을 높이려는 연구가 다양하게 진행되어 왔다. 기존의 전통적인 LCD 컬러필터는 안료를 그 색재로 사용하고 있는데, 안료는 내구성이 매우 우수하지만 입자 크기가 커, 안료형 컬러필터를 도입한 LCD의 광학적 성능에는 한계가 있다. 이런 안료형 LCD 컬러필터의 한계는 염료를 색재로 사용함으로써 해결이

가능하다. 염료는 안료에 비해 안정성이 다소 부족하지만, 색순도나 투과도 등의 광학적 특성이 우수하고, 컬러필터 제조 시 비교적 작은 입자 크기를 가질 수 있다. 염료를 LCD 컬러필터에 적용하기 위해, 액정 배향막 공정 온도에서 충분한 열적 안정성을 가지며, 산업적 공정 용매에 충분한 용해도를 가지고, 색순도와 투과도 등의 광학적 특성이 우수한 염료를 개발할 필요가 있다.

본 연구에서는, LCD 컬러필터에 적용 가능한 perylene 계 염료를 합성하기 위해, perylene 모체의 terminal과 bay 위치에 다양한 치환체를 도입하여 다수의 신규 염료들을 합성하였다. 특히, 기존에 한정적인 치환체만 도입되던 terminal 위치에 새로운 구조의 치환체를 도입하였다. 합성된 염료들이 적색 컬러필터용 색재로 사용 가능한지를 판단하기 위해, 염료의 색특성, 내열성, 용해도 등을 평가하였다. 또한, 염료의 구조를 Density functional theory로 모델링하여 염료의 구조적 특징이 광학적 특성과 내열성 등에 미치는 영향을 분석하였다.

Perylene 계 염료는 일반적으로 강한 형광을 가진다. 염료의 형광은 컬러필터를 제조하였을 때 휘도를 향상시키는 긍정적인 효과가 있기는 하지만, 컬러필터의 명암비를 떨어뜨리는 주요 원인이 된다. 신규 합성된 perylene 계 염료들로 염료형, 염안료형 컬러필터를 제조하여 광학적 특성을 비교해 본 결과, 염료가 발현하는 형광의 세기는 컬러필터를 제조하였을 때에도 일관성 있게 발현하였다. 이를 해결하기 위해, 공정 용매에 충분한 용해도를 가지면서 형광이 약한 염료를 신규 개발하였다. 염료 분자에 methoxy 그룹을 포함하는 치환체를 도입하였고, methoxy 그룹의 electron donating effect로 인해 염료의 형광이 감소하는 것을 확인하였다. 신규 개발된 고용해성, 저형광성 염료를 염료형, 염안료형 컬러필터에 적용한 결과, 형광이 강한 염료를 사용하였을 때 보다 컬러필터가 최소 밝기 값이 감소하고, 명암비가 향상되는 것을 확인하였다.

염료의 치환체에 포함된 methoxy 그룹이 염료의 형광에 미치는 영향을 분석하기 위해, methoxy 그룹이 도입된 위치와

방향을 다양화한 염료들을 합성하였다. 그리고 methoxy 그룹 대신 ethyl 그룹이 도입된 염료들 또한 대조군으로 합성하여, 염료들의 광학적 특성을 비교 분석하였다. Terminal 위치에 도입된 methoxy 그룹은 bay 위치에 도입된 methoxy 그룹에 비해 형광 억제 효과가 훨씬 적었으며, bay 위치의 치환체의 para-방향에 도입된 methoxy 그룹들만 형광 억제 효과를 보였다. 이는 perylene 본체가 주요하게 형성하고 있는 conjugation 구조에 methoxy 그룹이 포함될 수 있을 때에만 형광 억제 효과가 있기 때문으로 보인다. 염료의 구조에 따른 치환체의 molecular orbital modeling을 통해, 다양한 위치와 방향에 도입된 methoxy 그룹이 염료의 conjugation에 관여하는 정도를 분석하였다.

주요어: 액정디스플레이, 컬러필터, 퍼릴렌, 용해도, 형광, 분자간 회합, 명암비

학번: 2010-23182

List of Publications

Original Papers

1. Chun Sakong, Se Hun Kim, Sim Bum Yuk, **Jeong Yun Kim**, Se Woong Park, Min Jae Ko, Jae Pil Kim, ‘Synthesis of novel quinacridone dyes and their photovoltaic performances in organic dye-sensitized solar cells’, Bull. Korean Chem. Soc., **2011**, 32, 2553-2559.
2. **Jeong Yun Kim**, Jun Choi, Jin Woong Namgoong, Se Hun Kim, Chun Sakong, Sim Bum Yuk, Sang-a Choi, Woosung Lee, Jae Pil Kim, ‘Synthesis and characterization of novel perylene dyes with new substituents at terminal-position as colorants for LCD color filter’, J. Incl. Phenom. Macrocycl. Chem., **2015**, 82, 203-212.
3. Sim Bum Yuk, Woosung Lee, Jun Woong Namgoong, Jun Choi, Jae Bok Chang, Se Hun Kim, **Jeong Yun Kim**, Jae Pil Kim, ‘Synthesis and characterization of bay-substituted perylene dyes for LCD black matrix

of low dielectric constant', J. Incl. Phenom. Macrocycl. Chem., **2015**, 82, 187-194.

4. Se Hun Kim, Jin Woong Namgoong, Sim Bum Yuk, **Jeong Yun Kim**, Woosung Lee, Chun Yoon, Jae Pil Kim, 'Synthesis and characteristics of metal-phthalocyanines tetra-substituted at non-peripheral (α) or peripheral (β) positions, and their applications in LCD color filters', J. Incl. Phenom. Macrocycl. Chem., **2015**, 82, 195-202.

5. **Jeong Yun Kim**, Chun Sakong, Sang-a Choi, Hyeyoun Jang, Se Hun Kim, Kil Seong Chang, Myoung Sic Han, Jeong Su Lee, Jae Pil Kim, 'The effect of fluorescence of perylene red dyes on the contrast ratio of LCD color filters', Dyes Pigm., **2016**, 131, 293-300.

6. **Jeong Yun Kim**, Tae Gyu Hwang, Se Hun Kim, Jin Woong Namgoong, Ji Eon Kim, Chun Sakong, Jun Choi, Woosung Lee, Jae Pil Kim, 'Synthesis of high-soluble and non-fluorescent perylene derivatives and their effect on the contrast ratio of LCD color filters', Dyes Pigm., **2017**, 136, 836-845.

7. **Jeong Yun Kim**, Tae Gye Hwang, Sung Wun Woo, Jae Moon Lee, Jin Woong Namgoong, Sim Bum Yuk, Sei-won Chung, Jae Pil Kim, ‘Simple modification of basic dyes with bulky & symmetric WCAs for improving their solubilities in organic solvents without color change’, Sci. Rep., **2017**, 7, 46178.

8. **Jeong Yun Kim**, Sung Wun Woo, Tae Gyu Hwang, Hong Mo Kim, Ji Eon Kim, Chun Sakong, Jun Choi, Woosung Lee, Jae Pil Kim, ‘A general, easy, rapid, and efficient method for removal of basic dyes from wastewater with bis(trifluoromethanesulfonyl)imide anion’, *submitted*.

9. **Jeong Yun Kim**, Sung Wun Woo, Jin Woong Namgoong, Jae Pil Kim, ‘A study on the fluorescence property of the perylene derivatives with methoxy groups’, *submitted*.